AE5310 Thesis Control and Operations

Master Thesis

Modelling transport pilot control behaviour and the effect of motion during a simulated stall recovery manoeuvre

Martijn Rambonnet **1306677**

Supervisors:
Prof. dr. ir. Max Mulder
Dr. ir. Mark Wentink

2015-06-05

TU Delft

Faculty of Aerospace Engineering

Delft University of Technology

Delft University of Technology

Abstract

Loss Of Control In-flight (LOC-I) is currently the largest cause of accidents for the world wide commercial jet transport fleet. To decrease the occurrence of this type of accident, procedures have been modified and pilot training has been increased. However, current training devices lack the appropriate flight models and motion capabilities to be fully representative of these accidents. With the SUPRA generic transport aircraft model and the Desdemona simulator it is possible to provide a representative flight model and to simulate the positive g-loads experienced during upsets and upset recoveries.

To better understand the pilot response in these manoeuvres a descriptive pilot model was developed in this thesis. This provides insight into which indications are used by the pilot and how they are interpreted. Additionally the effect of three simulated motion conditions was explored; no motion, extended 'hexapod-like' motion and centrifuge motion.

Ten civil transport pilots from several different airlines with varying levels of experience flew two types of stall scenarios in the Desdemona simulator. Both scenarios were repeated 12 times with variations in cockpit indications, control loading and motion condition.
Based on the experiment data and pilot feedback a basic descriptive pilot model was developed. Using an iterative fitting process the pilot model response was matched to the experiment data.

The resulting pilot model provides a reasonable fit for the average pilot response in the no motion condition. The variation between experiment runs can be partially reproduced by varying the pilot model control gains. No accurate representation could be determined for the effect of the speed tape and the pilot model does not fully reproduce the typical discrete control input behaviour.

The experiment also showed a significant effect of the extended 'hexapod-like' motion condition on pilot control behaviour in the unloading phase of the stall recovery. A significant effect of the centrifuge motion condition was found in both the unloading and loading phase of the stall recovery. These effects could not be reproduced by classical negative motion feedback in the pilot model, but were best represented by a small decrease in the pilot model open loop control gain.

Table of Contents

List of Figures

List of Tables

Nomenclature

Greek Symbols

α	Angle of attack
β	Angle of sideslip
γ	Aircraft flight path angle
μ	Mean
μ_c	Friction coefficient
μ_k	Kinetic friction coefficient
μ_s	Static friction coefficient
ϕ	Aircraft roll angle
ψ	Aircraft yaw angle
σ	Standard deviation
θ	Aircraft pitch angle
w_{cy}	Rotational velocity of the central yaw axis (centrifuge)

Latin Symbols

F_n	Normal force
H	Transfer function
m_{cc}	Representative control column mass
n	Load factor
n_z	Vertical load factor
V	Velocity
V_∞	Freestream airflow
v_{CAS}	Calibrated airspeed
v_{margin}	Speed difference between the CAS and stick shaker activation CAS
v_{ss}	Stick shaker activation in CAS

Subscripts

$_c$	Central visual
$_{nm}$	Neuromuscular
$_{oto}$	Otoliths
$_{scc}$	Semicircular canals

Acronyms

AFM	Aircraft Flight Manual

ANOVA	ANalysis Of VAriance
AoA	Angle of Attack
ARX	AutoRegressive with eXternal
CAS	Calibrated Airspeed
CFIT	Controlled Flight into Terrain
DMU	De Montfort University
EICAS	Engine-Indicating and Crew-Alerting System
FP-7	Seventh Framework Programme
FPV	Flight Path Vector
GFRI	Gromov Flight Research Institute
IAS	Indicated Airspeed
LOC-I	Loss Of Control In-flight
LOC	Loss Of Control
MSE	Mean Squared Error
ND	Navigation Display
NLR	Dutch National Aerospace Laboratory
PFD	Primary Flight Display
PLI	Pitch Limit Indicator
SUPRA	Simulation of UPset Recovery in Aviation
TAS	True Airspeed

Introduction

Over the years aviation safety has steadily improved to make it one of the safest types of transport (EASA, 2012). This has been achieved through constant progress in pilot training, procedures and aircraft design. However, these changes over the years have also caused a shift in accident causes. Where in the past Controlled Flight into Terrain (CFIT) was the largest cause of fatalities in aviation accidents (AIRBUS, 2014), this has now shifted to Loss Of Control In-flight (LOC-I) (Boeing, 2011) (see Figure 1).

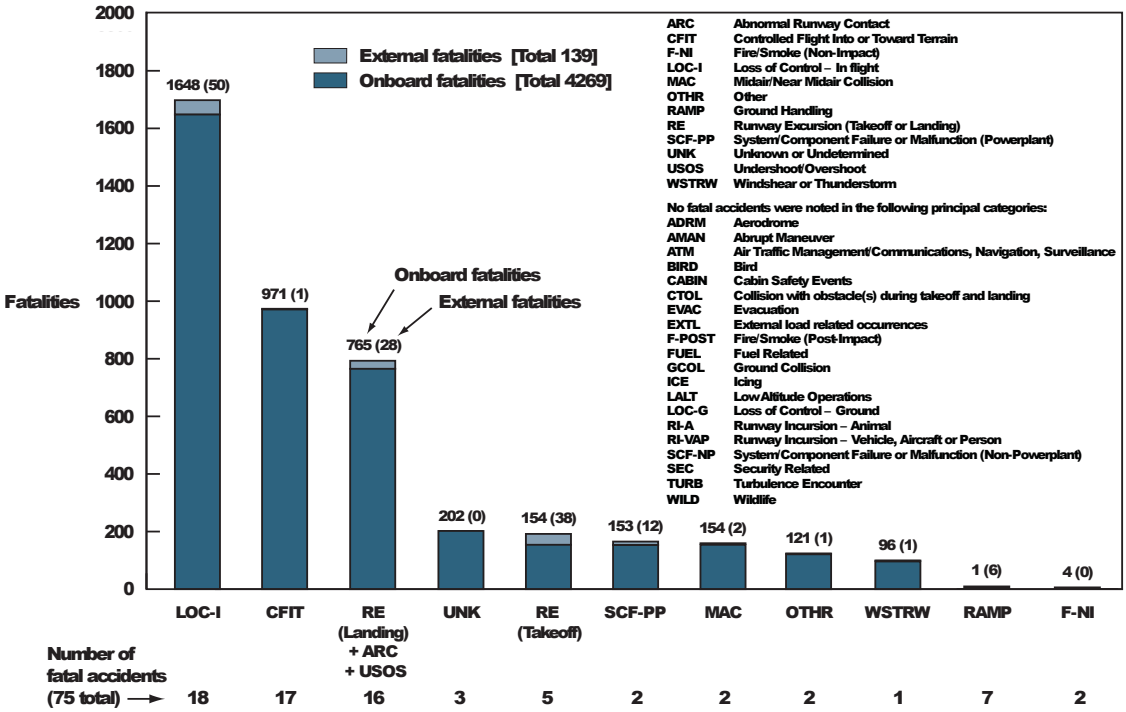

Figure 1: Fatal accidents for the worldwide commercial jet fleet during 2003 through 2012 (Boeing, 2011)

Because of the relative increase in LOC-I, priorities have shifted and the interest in prevention has increased. Upset recovery procedures have been improved and in particular stall recovery procedures have changed to increase the focus on the management of angle of attack instead of minimum loss of altitude. There is however a lack of effective training tools, since training of upset scenarios in real flight is expensive and possibly dangerous. Some airlines attempt to improve the upset recovery skills of their pilots by training on small aerobatic aircraft, but these are not fully representative for the behaviour and response of a large transport aircraft. Another approach is to use existing full flight simulators to train upset recovery procedures, but these flight simulators lack the capability and validation for use outside the normal flight envelope.

Within the EU project Simulation of UPset Recovery in Aviation (SUPRA) this problem was tackled. By developing a generic transport aircraft model valid for flight outside the normal flight envelope, different aircraft responses could be demonstrated and trained. Another goal was to improve simulator motion cueing through improved modelling of human perception and optimization of the use of the motion space. Additionally the use of non-standard simulators, like the Desdemona simulator capable of cueing g-load through the use of a centrifuge, was investigated. The SUPRA aerodynamic model was successfully validated and the usefulness for training was generally affirmed. Also the importance of motion and the added benefit (although with associated false cues and limitations) of g-load through the use of the Desdemona simulator was shown (Fucke et al., 2012).

With the availability of this new aircraft model and its successful implementation on the Desdemona simulator, questions again rise about the precise effects of motion on pilot control behaviour. One of the concerns with training upsets in simulators has been the possibility of negative transfer of training: due to simulator abstractions pilots can learn incorrect behaviour. For this further research is necessary to better understand these effects of motion.
By modelling pilot control behaviour during these manoeuvres in an experiment, the effects of motion might be quantified and the relevant perceptual systems might be identified. This has lead to the proposal of the following research subject:

> *Modelling pilot control behaviour in unusual attitude recovery manoeuvres, and to use this model in the investigation of the effect of motion simulation in (large attitude) manoeuvring.* (Wentink, 2012)

The term unusual attitude recovery manoeuvres covers a wide range of scenarios and aircraft upsets. I am aware that is too much to consider as a whole, and at the same time to perform an in depth analysis, all in one single thesis. For this, my thesis will first describe a general method and then apply this to a single type of upset scenario. A scenario which can be considered as a case study to test the method.
The specific scenario I selected is the quasi-symmetric, fully developed, pitch up stall. This condition was chosen because it is a relevant scenario and has been extensively tested and validated during the SUPRA experiments. Luckily also a data set from a previous experiment, which considered a similar scenario, is available. This dataset is helpful for a preliminary analysis of the scenario before the experiment is set up.
With respect to the modelling of pilot control behaviour I have to consider some limitations. A conventional approach would be to start with idealized and more abstract scenarios. This would then be expanded up till a complete simulation of the manoeuvre. Limited time and resources hamper such an approach, which would require a large experiment and a large number of participants. Instead I choose to use the already available pilot models and research to model a fully realistic stall recovery. If successful this will provide concrete and useful results, without the danger of abstractions.
Inherent to this research subject and approach is the assumption that pilot control behaviour in these kinds of simulated upsets can be modelled using current pilot models. This thesis will test this hypothesis and try to determine the limitations of such an approach.

To reach these conclusions this report has been split up in three major parts. The first part consists of chapters 1 to 3. Chapter 1 contains an analysis of the data from previous experiments that are available and applicable to this work. Chapter 2 considers the available pilot models and their origins and limitations. Finally, based on the initial data and available models, an initial model structure will be considered in Chapter 3.
The data from the preliminary research in part I is not enough to prove my assumption. For this part II describes the collection of additional data through an experiment. In Chapter 4 the hypothesis and requirements for the experiment are defined. Chapter 5 describes the implementation of these requirements and some practical considerations. The results of the experiment are presented in Chapter 6, by means of a short summary and statistical analysis of the relevant data.
Finally, part III, describes the implementation of the experiment results into a pilot model. First the pilot model structure is derived in Chapter 7. Next, the pilot model is fitted to the experiment data in Chapter 8, to test the validity and correctness of the model and to answer the hypotheses. Chapter 9 further investigates the observed variation in pilot control behaviour.

Part I

Preliminary Research

Chapter 1

Preliminary Analysis of Pilot Control Behaviour in Upsets

The first step to modelling pilot control behaviour during a stall recovery is to have a general look at the characteristics of such a manoeuvre. The SUPRA project included two experiments on the Desdemona simulator that provided data that might be relevant to the subject of this thesis (for more information about the SUPRA project itself see Appendix A).
The first SUPRA experiment was conducted in January 2012 with a group of 8 test pilots to assess the validity and usefulness of the SUPRA aerodynamic model and Desdemona motion cueing (Fucke et al., 2012). Pilots were in general positive about the aircraft model and motion cueing improvements. Each pilot was also asked to fill out a short survey about the different information sources during a stall recovery. The second experiment was conducted with a group of 12 line pilots in March 2012, to investigate the awareness of g-load and effects of g-load training in a centrifuge based simulation (Ledegang et al., 2012) (Groen et al., 2012). Again the pilots were asked to fill out a survey about the different information sources during a stall recovery. The scenario that was used in this experiment is similar to the scenario being considered in this thesis and the data will be reviewed to get a basic notion of the control behaviour that is involved.

However, first the general definitions and conventions that are used in this thesis will be discussed. Next some details about the Desdemona simulator are provided to give the reader a general idea of the simulator environment and motion algorithms that are used.

1-1 Definitions

Generally this thesis follows the conventional definitions as used in aerospace engineering. The most important definitions are shortly summarized below.

1-1-1 Coordinate system

The attitude of the aircraft will be described using the Euler angles for pitch (θ), roll (ϕ) and yaw (ψ) in their conventional rotation order ($\psi \rightarrow \theta \rightarrow \phi$). These angles describe the aircraft attitude with respect to a normal earth fixed reference frame (see Figure 1-1(a)). The angle of the actual flight path with respect to the horizon is defined by gamma (γ).

The direction of the free-stream airflow is defined with respect to the body-fixed reference frame by the angles alpha (α) and beta (β) (see Figure 1-1(b)). Alpha, or Angle of Attack (AoA), is the vertical angle between the aircraft reference axis and free-stream airflow. Beta, or sideslip, is defined as the lateral angle between the aircraft reference axis and free-stream airflow.

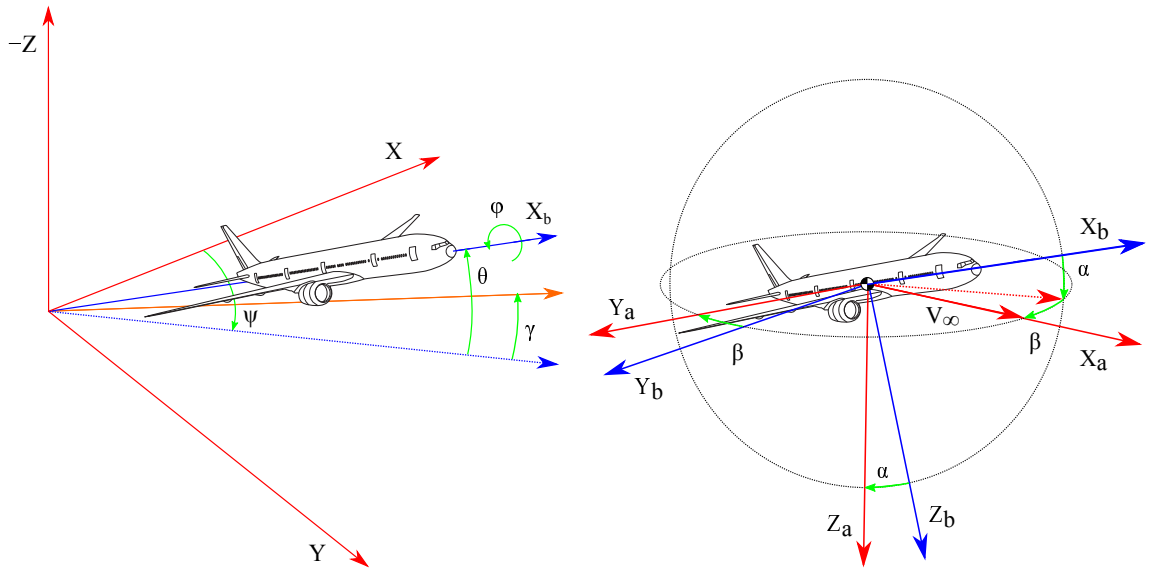

(a) Definition of the aircraft attitude using Euler angles

(b) Definition of the freestream airflow V_∞ with respect to the aircraft (based on Mulder et al. (2007))

Figure 1-1: Aircraft attitude and freestream airflow definitions

1-1-2 Aviation units

In discussing the aircraft velocity this thesis will mainly use the Calibrated Airspeed (CAS). This is the airspeed as measured by the pitot-static tube corrected for measurement and indicator errors. For the SUPRA aircraft model this is the same as the Indicated Airspeed (IAS) since no measurement or indicator errors are modelled. The reason CAS is used is because it better relates to aircraft dynamics at varying altitudes compared to the True Airspeed (TAS).
In some cases the aircraft altitude is referred to as flight levels. Flight levels define a pressure altitude in hundreds of feets assuming a reference pressure of 1013.25 mbar at mean sea level, e.g. 20.000 ft is flight level 200 or FL200.
The Desdemona experiments discussed in this thesis were executed with no wind and a standard atmosphere.

1-1-3 Pilot controls

The aircraft control inputs are expressed as the internal SUPRA model values and are scaled values with respect to the simulator implementation. The control deflections are defined as positive for control column forward (pitch down), control wheel right (roll right) and right rudder (yaw right).

1-2 Desdemona simulator

The Desdemona simulator is a multi-purpose simulator with 6 separate degrees of freedom (see Figure 1-2). The cabin is fully gimbaled providing continuous rotation of up to 180 deg/s in any axis. This gimballed cabin is attached to a 2 meter vertical translation system (heave) which in turn rests on an 8 meter linear track providing lateral (sway) or longitudinal (surge) linear motion depending on the cabin orientation. The linear track is mounted on a central rotation axis capable of providing up to 3 g radial acceleration with the cabin at the 4 m radial limit position. The maximum performance of each degree of freedom is as follows:

Table 1-1: Desdemona maximum performance of each degree of freedom.

Axis	Travel	Maximum velocity	Maximum acceleration
Pitch gimbal	Continuous	3.14 rad/s	3 rad/s^2
Roll gimbal	Continuous	3.14 rad/s	2 rad/s^2
Yaw gimbal	Continuous	3.14 rad/s	3 rad/s^2
Central yaw	Continuous	2.71 rad/s	0.5 rad/s^2
Heave	2.0 m	2 m/s	4.9 m/s^2
Linear	7.4 m	3.2 m/s	4.9 m/s^2

The large motion envelope makes Desdemona suitable for both research and training. Some examples of current applications are: F-16 deep stall training, CH-47 and AH-64 brownout training, off-road driving with military vehicles and upset recovery training for transport aircraft pilots.

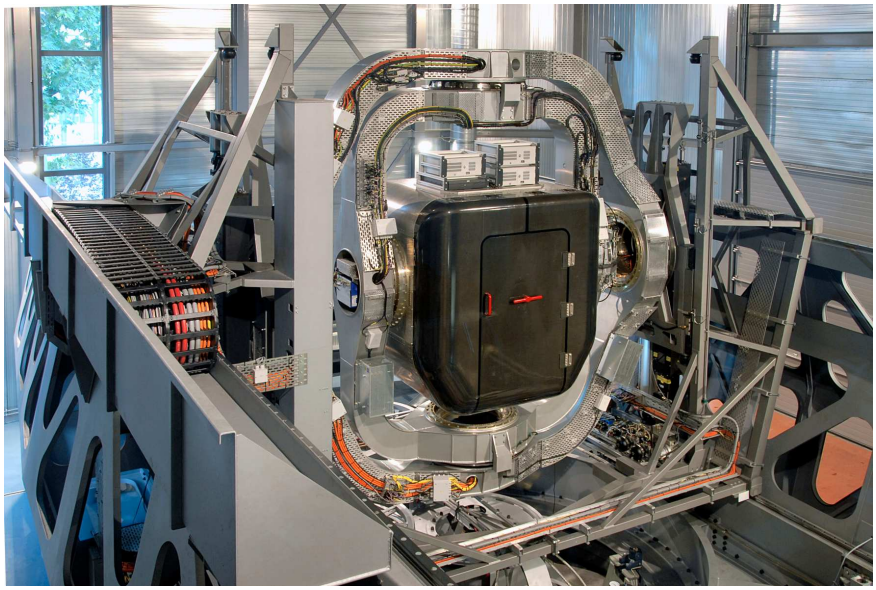

Figure 1-2: Desdemona simulator at the middle of the linear track.

1-2-1 Simulator cockpit

The cabin of the Desdemona simulator features a changeable cockpit. For the SUPRA simulations a Boeing 737NG style cockpit is used. This consists of the captain's side of the cockpit providing the PFD, Navigation Display (ND) and Engine-Indicating and Crew-Alerting System (EICAS) displays. The primary flight controls consist of a Boeing 737NG style control column with computer controlled control loading on the longitudinal axis. The control wheel and rudder pedals have passive control loading and a Boeing 737NG style throttle quadrant is installed. Additionally a partially functional EFIS and MCP panel is provided. The normal PFD shows a typical Boeing style primary flight display. The ND shows a heading indicator and the stabilizer position (the indication on the throttle quadrant is not functional). The EICAS display shows the N1, N2, fuel flow and EGT values for both engines, but other EICAS indications are inoperative. The control wheel has buttons to control the stabilizer trim position and to disconnect the auto-pilot.
The out of the window visual system provides approximately 180 degrees horizontal, and 35 degrees vertical field of view. The visual is not collimated and the cockpit window frames are overlaid on the visual. The cockpit in Desdemona does not include elements like an overhead panel, radios and CDUs since these are not required for the maneuvers flown in the experiments.

1-2-2 Motion cueing

For the SUPRA project two types of motion cueing algorithms were developed. The first is a modified classical washout algorithm aimed at hexapod like motion platforms (from here on referred to as hexapod

motion). The gimbals are used to provide the classical onset cues. By tilting the cabin laterally and longitudinally sustained accelerations are cued. A new addition was the cueing of loading and unloading by tilting the cabin respectively backwards and forwards. The heave axis is used to provide loading and unloading onset cues. In addition specially developed stall and mach buffets are cued using the heave axis. The main rotation axis is used to provide general yaw cues. The linear translation axis is not used.

The second motion cueing algorithm provides sustained g-cues through the use of centrifuge motion (from here on referred to as centrifuge motion). In this motion condition hexapod cueing is provided up to stick shaker activation at which point the centrifuge accelerates to a baseline g level (roughly 1.15 g). This initial spin up is largely masked by the stall buffet and the unloading that occurs during the initial part of the recovery. When the aircraft has regained enough speed, the centrifuge will have reached the baseline rotational velocity and is used to cue the actual aircraft g-loads by further accelerating.
This initial baseline is necessary to be able to provide a large enough g-onset. This can be best understood looking at the equation for the total acceleration felt by a pilot in a centrifuge (neglecting accelerations generated by axes other than the central yaw):

$$a_{total} = \sqrt{((r\omega_{cy}^2)^2 + (r\dot{(\omega)}_{cy})^2 + g^2)} \tag{1-1}$$

In this equation $g = 9.81 m/s$, $r = 4m$ for Desdemona and ω_{cy} is the central yaw velocity. Inspection of this equation shows that the total acceleration is largely determined by the square of the centrifuge velocity and thus at low rotational velocities the increase in g load with increase in w_{cy} is relatively small. Additionally to minimize jerk and false cues the centrifuge is initially not accelerated at its maximum acceleration.

Due to the unique configuration of Desdemona the position of the cabin during centrifuge motion is different from a conventional centrifuge. In most conventional centrifuges the pilot is positioned tangentially to the direction of rotation (see Figure 1-3(a)). Because the direction vector of the total acceleration changes during centrifuge motion the cabin has to roll to coordinate with the resulting acceleration vector. This can be done passively by allowing the cabin to freely rotate around its roll axis or by actively driving the roll axis. In some conventional centrifuges the pitch axis is also controlled to coordinate the cabin with the tangential acceleration. Pitching and rolling the cabin while the centrifuge is rotating results in an uncomfortable tumbling sensation caused by cross-coupled stimulation of the semi-circular canals. This is commonly referred to as the Coriolis effect (Oxford Aviation Academy, 2011).

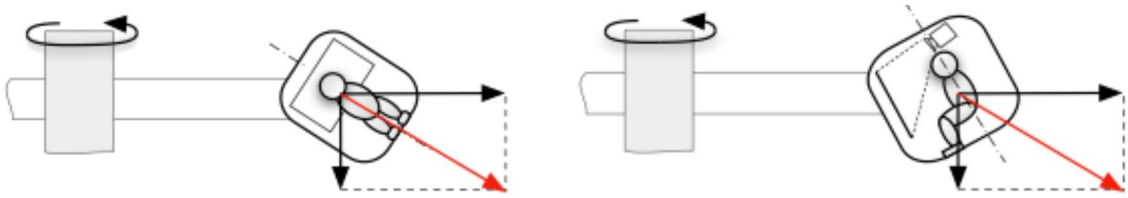

(a) Conventional centrifuge (b) Dedemona solution

Figure 1-3: Cabin orientation in centrifuges (based on Groen et al. (2012))

To minimize the Coriolis effect in Desdemona the cabin is oriented perpendicular to the direction of rotation (see Figure 1-3(b)). By using the same unloading effect as in the hexapod motion the cabin can be partly prepositioned before the simulator reaches large rotation rates. In addition coordination with the g-vector can be slowed down and limited because a longitudinal offset of the g-vector is generally less noticeable than a lateral offset. The disadvantage of this solution is that acceleration of the centrifuge causes a side force although this can be (partly) compensated by yawing the cabin to align it with the resulting total acceleration vector.

1-3 SUPRA experiments pilot surveys

The two surveys (see Appendix B and Appendix C) given to the pilots in the first and second SUPRA experiment were designed to help better understand which information sources the pilots used during the stall upset recoveries. Although the results are subjective it provides a good starting point for a more objective (but more time consuming) analytical analysis.

The recovery from a pitch up stall has been divided in to two parts. The first phase is when the pilot pitches the aircraft down, to a negative pitch angle to decrease the angle of attack and to increase speed. This will be referred to as the *unloading* phase ($n_z < 1$). The second part consists of slowly (as not to exceed the maximum load factor) raising the nose to a normal flying condition, when enough speed has been gained, and will be referred to as the *loading* phase ($n_z \geq 1$).

1-3-1 Indications and motion cues used during the unloading phase

The first question of the surveys asked pilots to rank what they thought were the five most important indications during the unloading phase of the stall recovery. The goal of this question was to get a general idea from the pilots about what indications they are actively using. A simple analysis was done by converting the rank to a score ranging from 5 to 1 and summing the results to determine the 8 highest rated indications and motion cues. In Table 1-2 the results from the two experiments are shown. Surveys not filled out correctly have not been included.

Table 1-2: Eight highest rated indications or cues during the unloading phase

(a) SUPRA experiment 1 with 6 valid surveys

Indication/cue	Total points
Pitch ladder	28
Speed tape	11
Yoke deflection	10
PLI	9
Speed trend	7
G-load (motion)	6
Altimeter	5
Outside view	3

(b) SUPRA experiment 2 with 10 valid surveys

Indication/cue	Total points
Pitch ladder	36
Horizon	32
Pitch rate (motion)	17
Speed tape (incl. speed trend)	15
G-load (motion)	15
Yoke deflection	11
Yoke forces	10
Pitch (motion)	8

Both the test pilots and line pilots rate the pitch ladder as the most important indication during the unloading phase. Another important indication is the speed tape which indicates the airspeed, airspeed trend, reference speeds and limit speeds. The lower speed limit shows the stickshaker activation speed, v_{ss}, and is an important indication in preventing stalls. This limit is commonly referred to as the barber pole.

With respect to motion; pitch rate, g-load and pitch angle were reported as important cues by the pilots. Positive g-loads were cued using centrifuge motion. Sustained $\leq 1\,\mathrm{g}$ g-loads were cued using forward pitch tilt as explained before.

Another important interaction is the control column deflection and force. In the selected scenario the recovery requires almost full deflection forward and the control column forces are very much reduced (compared to normal flight) due to the low speed. As the aircraft increases speed these forces slowly increase again.

In the first experiment the test pilots could also use the Pitch Limit Indicator (PLI) indication on the PFD. The PLI is a proprietary Boeing indication appearing at high angles of attack and near the stick shaker activation speed. It is a graphic representation on the PFD of the maximum pitch angle available at a constant flight path angle, thus indicating the alpha margin to the stick shaker alpha. This provides a quick indication of the possibility to increase aircraft pitch or the need to decrease the aircraft pitch. Depending on the experience of the pilot this information can also be indirectly estimated from the Flight Path Vector (FPV), when the stick shaker activation alpha is known.

1-3-2 Indications and motion cues used during the loading phase

The second survey question considered the indications during the loading phase of the stall recovery, similar to the first question. Table 1-3 again shows the results.

Table 1-3: Eight highest rated indications or motion cues during the loading phase

(a) SUPRA experiment 1 with 6 valid surveys

Indication/cue	Total points
Pitch ladder	19
PLI	13
G-load (motion)	13
Speed tape	12
Speed trend	11
Speed	10
Pitch rate	4
Horizon	2

(b) SUPRA experiment 2 with 10 valid surveys

Indication/cue	Total points
G-load (motion)	36
Pitch ladder	33
Speed tape (incl. speed trend)	23
Horizon	14
Pitch rate (motion)	14
Yoke forces	13
Speed	10
Pitch (motion)	3

The pitch ladder is again considered an important indication together with the g-load. The speed tape which helps to prevent secondary stalls is also rated as being important. Control column forces and deflection seem to be of less importance compared to the unloading phase.

1-3-3 Additional questions

The test pilots were asked two additional questions. The first question was about whether or not the pilot thought he was missing any indications or motion cues in the simulation. Three out of 6 answered with a no. Of the others two remarked that the g-load was different in real life and the third said he expected a different response from the throttles.
The other question was regarding the fact how pilots were able to determine if they would exceed the 2.5 g structural limit. They were asked if they thought they could estimate the 2.5 g limit from seat-of-the-pants. Three out of five answered positively, two others answered negatively.

1-4 Analysis of the logged data from SUPRA experiment 2

In the following analyses the logged data from 7 different pilots flying the same scenario using the centrifuge motion cueing is analyzed. The colour for an individual pilot is the same in each plot.

1-4-1 Scenario overview

The stall scenario, that is analyzed, starts with the aircraft in a pitch up attitude of approximately 35 deg with thrust idle and the aircraft trimmed pitch up. Once the aircraft had fully stalled the pilots are triggered by an audio message to start their recovery. Figure 1-4 shows an 2D altitude profile of such an recovery with the flight path of 7 different pilots. The initial increase in altitude occurs while the pilot starts pitching down but still has a positive flight path angle. He then descends until he has enough speed to safely level off the aircraft. As can be observed there is wide spread in the recovery profiles flown by the pilots.

1-4-2 V-n diagram

Another way of visualizing the recovery is by plotting the time trace in a v-n diagram. This is especially interesting due to the fact that there are large changes in g-load and speed during the manoeuvre. Figure 1-5 shows an approximate v-n diagram with the flight path for the 7 different pilots. As can be seen in the v-n diagram there is a general path everyone follows, but the increase in g during the recovery is not smooth and seems to consist of peaks approaching the stick shaker activation. This most likely due to the fact that the barber pole indication is relatively slow in its response to variations in g-load and some times not in the visible range of the PFD.
From a performance point of view, it is interesting to note that the recovery indicated by the yellow line in the graphs has the minimum altitude loss. This comes at a cost of having to recover close or in the stickshaker, and results in the lowest speed of all at the end of the recovery.

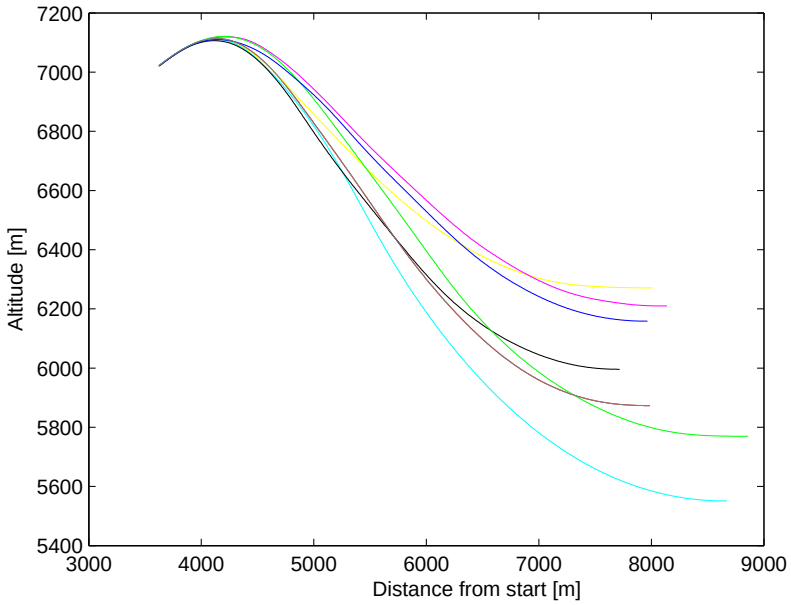

Figure 1-4: 2D spatial profile of the recovery as flown by 7 different pilots

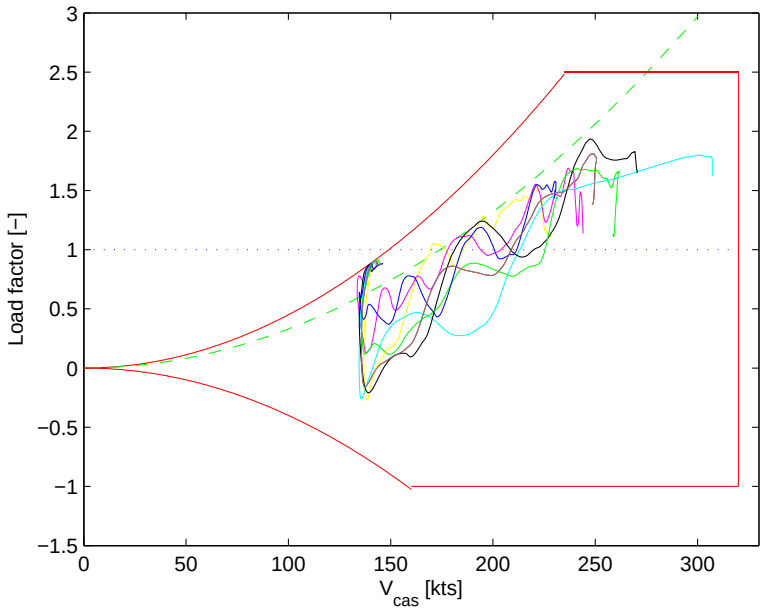

Figure 1-5: V-n trace of the recovery as flown by 7 different line pilots. The dashed green line indicates the approximate stick shaker activation boundary. The red lines indicate the approximate possible flight envelope based on aerodynamic limits and load limits.

1-4-3 Pitch phase plot

A phase plot shows the value and the derivative of a variable over time. An interesting variable in this regard is the pitch angle, which is the variable that is actively controlled and of which its derivative , i.e. the pitch rate, $\dot{\theta}$, has been mentioned in the surveys as one of the indications used by the pilots. Figure 1-6 shows a phase plot of the aircraft pitch. The resulting phase plot gives some interesting information. The stall recovery starts at the top right of the phase plot at an pitch angle of approximately 35 deg. A lot of pilots seem to unload with a negative peak of around -12 deg/s. A possible cause for this could be the fact that this is the resulting pitch rate from full forward control column input.

The pitch rate then gradually seems to decrease when approaching -20 deg pitch and most trajectories show

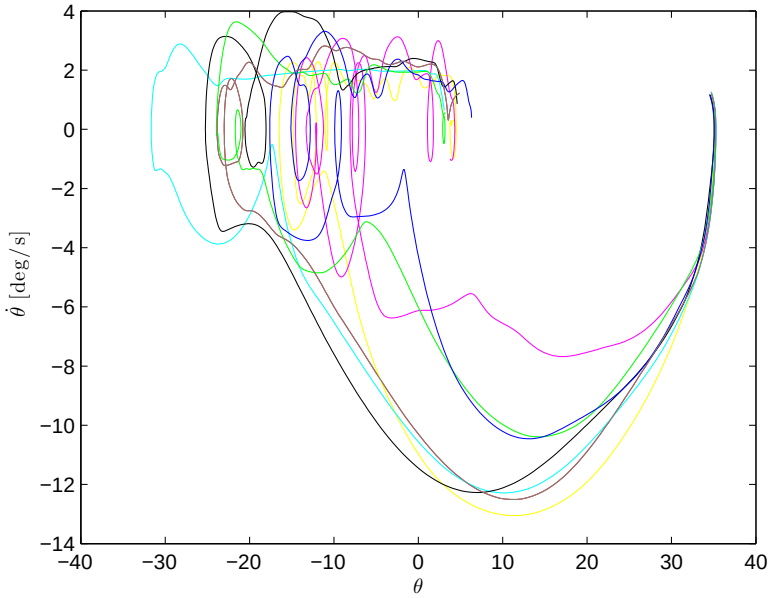

Figure 1-6: Phase plot of the aircraft pitch during the stall recovery of 7 different pilots

an additional correction by a new increase in negative pitch rate. Some of the trajectories form a loop, which is caused by a temporary increase in pitch, followed by a new decrease in pitch. This might be caused by the pilots not fully correcting for the initial trim and subsequent variation as trim as airspeed and control effectiveness increases.

The last interesting observation is the general tendency of pilots to approximate a 2 deg/s pitch rate during the last phase of the recovery. The pitch rate is similar to the 2.5 deg/s commonly used during take-off rotation and was mentioned by some pilots as a guideline for stall recoveries.

1-4-4 Control inputs

Another important part to review is the pilot control inputs, in this case especially the longitudinal control column inputs. Figure 1-7 show the time traces for the longitudinal control inputs of the 7 pilots during a recovery. Again a general trend is noticeable and as was suspected in the previous section, some pilots use the full forward control column deflection during the initial unloading phase. The control behaviour between pilots varies widely. Some pilots exhibit a very undamped behaviour (e.g. the purple and blue time trace), while others show more damped behaviour (e.g. cyan and green time trace).
The high frequency noise at the beginning of the traces is caused by the stickshaker and buffet at high alpha conditions.
A surprising result is the step like shape of the control input. This was also mentioned by Hosman in a recent conversation as something that was observed during the balked landing study (Hosman et al., 2005). Hess also extensively studied pulsed and discrete control behaviour, sometimes observed in pilot performance. This was found to occur with unstable systems or at high workloads, and Hess proposed a dual loop system, which can reproduce this behaviour (Hess, 1979). Another, less likely cause, would be the static friction in the control column, which could also cause discrete inputs.

1-5 Conclusions

From the data and the surveys it can be concluded that the PFD is most likely the main information source. The pitch ladder on the artificial horizon and speed tape contain most of the necessary information. Motion also has been shown to have a significant effect on pilot behaviour in previous research and is listed by the pilots as a source of information. Another possible input or feedback system is the yoke force and deflection. The outside visual was not deemed important, but may have had an effect in the peripheral field of view.
In the unloading phase (almost) full forward control column deflection is used. The negative g-load limit is

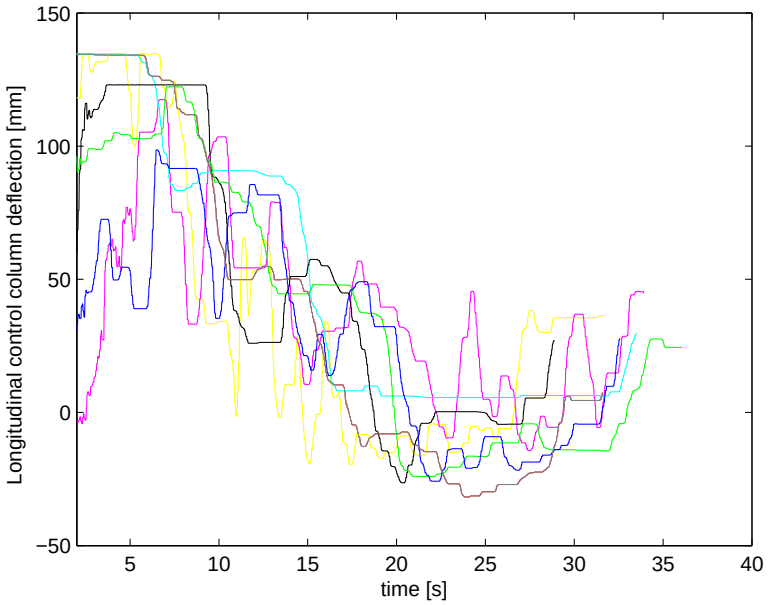

Figure 1-7: Longitudinal control inputs over time of 7 different pilots during a stall recovery

not approached and there is some variation in the largest pitch rate that is reached. Also there is a large variation in the lowest pitch that is reached.
The loading phase seems to consist of approximating a 2 deg/s positive pitch rate, while observing the stick shaker speed limits as seen in the v-n traces.

The most important observation is the large difference between pilots. This could be caused by a difference in training, small differences in initial conditions, and/or variations in recovery procedures.

Chapter 2

Literature Review of Available Pilot Models

The previous chapter has provided a general notion of the type of control behaviour that is under investigation. It is my assumption that this type of behaviour can be modelled using the current models for compensating and tracking tasks, as a basis for a general structure. To get a better idea of the (historical) basis for these models the present chapter provides a short overview of the different pilot models that are relevant to this research subject.

Already early on in aviation it became apparent that a better understanding of the interaction between the pilot and aircraft was needed to get the best performance. With feedback control system theory becoming available in the early twentieth century, work was started on describing human behaviour when controlling a system like an aircraft. Most of this early work started of with the very basic task of compensatory control where a pilot is presented with his current position (which can represent for example pitch or bank angle) and stationary reference position. External disturbances (for example turbulence) will cause changes in his current position, which the pilot has to compensate for by giving opposing inputs to the system.
A basic feedback system is shown in Figure 2-1. The pilot observes the difference between the stationary reference and the current position as an error. The pilot model, Y_p, models his response and provides the output u. The output u goes into the aircraft model, Y_c, which models the aircraft's response and outputs the new state y. This state y is fed back through the model of the aircraft sensor dynamics, Y_s, although they are usually omitted or combined with a separate display block modelling the display delay.

Analysis of such a system can be done in the time domain, but using transfer functions in the frequency domain offers usually a much simpler and easier system description.

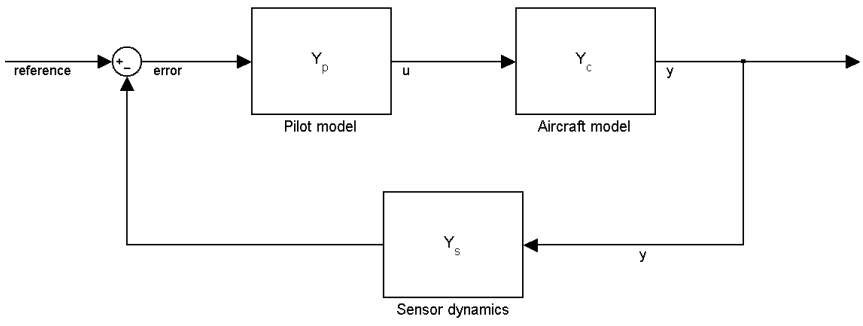

Figure 2-1: Basic pilot feedback model for a compensatory task

2-1 Crossover model

In 1965 McRuer created one of the first successful pilot models using a feedback system model (McRuer et al., 1965). Based on the observed experiment data in the past decades the crossover model was proposed (see Figure 2-2). This system is assumes a linear pilot model and a linear aircraft model. A human controller however also displays non-linear behaviour, which cannot be represented by a linear model. This is called the remnant and is usually added to the pilot model output. In some cases it is left out or is replaced by noise.

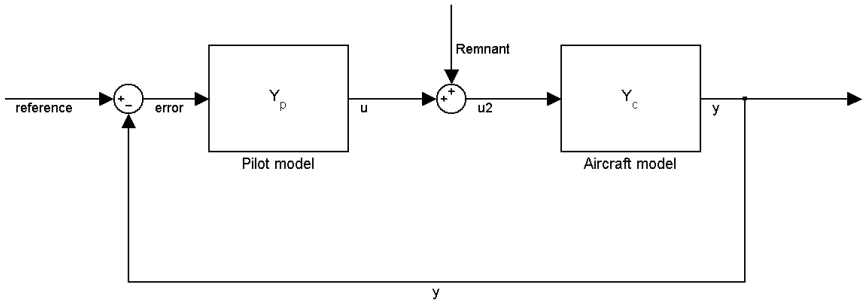

Figure 2-2: Crossover model for a compensatory task

The observations from the experiments concluded that a pilot tends to adapt himself so that the open loop transfer function becomes similar to equation 2-1.

$$Y_p(j\omega)Y_c(j\omega) = \frac{\omega_c e^{-j\omega\tau_e}}{j\omega} \tag{2-1}$$

The variables ω_c and τ_e can be varied to shape the response of the pilot/aircraft model combination. Using several rules and reference values appropriate values are selected. The resulting model was determined to be a reasonable model of pilot behaviour around the crossover region for first and second order controlled systems. The low frequency behaviour proved to be inadequate.
The resulting response is that of an error integrating system, with a limited upper bandwidth caused by the time delay, created by the pilot and aircraft system.

To improve the low frequency modelling, the crossover model was extended to the, so called, extended crossover model, or α model. By adding an additional delay term, which diminishes with frequency, additional lag is introduced near low frequencies. For a first order controlled systems the equation then becomes:

$$Y_p(j\omega)Y_c(j\omega) = \frac{\omega_c e^{-j\left(\omega\tau_e + \frac{\alpha}{\omega}\right)}}{j\omega} \tag{2-2}$$

where now the additionally parameter α can be varied to add additional lag at lower frequencies.

2-2 LQG model

In 1970 Kleinman et al. proposed a different version of the crossover model called the Linear Quadratic Gaussian (LQG) model (Kleinman et al., 1970). It improved upon the crossover model by providing a fully linear model and using optimization to derive the parameters. As shown in Figure 2-3 the LQG model separates the pilot model into a time delay, Kalman estimator, predictor and gain. It features a separate neuromuscular system modelled as a first order lag filter. Also it adds Gaussian observation noise and a Gaussian motor noise to model the inaccuracies in the human systems.
The model parameters are determined by minimizing a cost function appropriate for the situation. An example cost function would be:

$$J(u) = E\{e^2\} + kE\{u^2\} + gE\{\dot{u}^2\} \tag{2-3}$$

By selecting the appropriate values for k and g, the properties of the steering output, u, can be influenced.

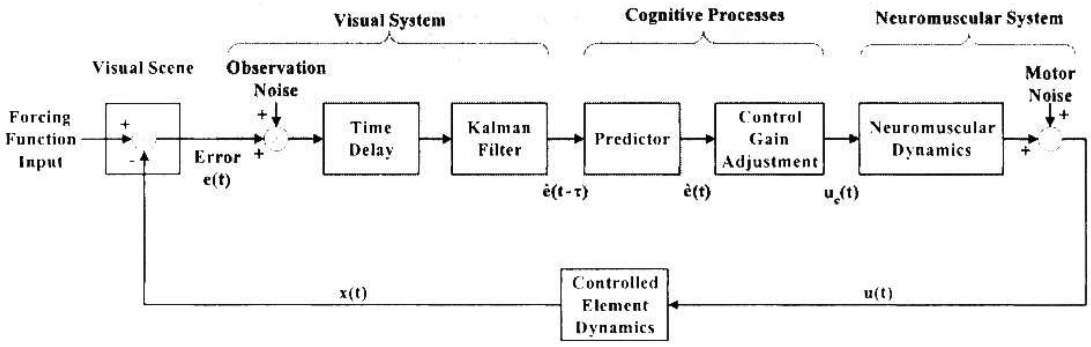

Figure 2-3: LQG model for a compensatory task (Based on Barton (2004))

2-3 Precision model

McRuer and Krendel describe in the 1974 report on pilot models the development of the precision model (McRuer & Krendel, 1974). The precision model was developed to remove the bandwidth limitations of the crossover model, and also to provide a physical interpretation of the different terms, that together with the aircraft dynamics, result in the crossover model. This resulted in the following transfer function for the pilot model, $Y_p(j\omega)$:

$$Y_p(j\omega) = K_p e^{-\tau j\omega} \left(\frac{T_l j\omega + 1}{T_I j\omega + 1}\right) \left(\frac{T_K j\omega + 1}{T_{K'} j\omega + 1}\right) \frac{1}{(T_{N_1} j\omega + 1)\left(\left(\frac{j\omega}{\omega_N}\right)^2 + \frac{2\zeta\omega_N}{\omega_N} j\omega + 1\right)} \tag{2-4}$$

The first two terms are the total delay, τ, (visual, neural, etc.) and open loop gain, K_p. The first set of brackets contains the series equalization to obtain the $-20\,\mathrm{dB}$/decade slope at the crossover frequency. The second set of brackets contains a lag-lead term to compensate the low frequency lag similar to the contribution of α in the α model. The last term is a third order the neuromuscular system model. McRuer et al. note that with the precision model the pure time delay is much smaller and seems to conform more with physiologically predicted values.

2-4 Structural model

In 1981 Hess introduced a new type of pilot model named the structural model (Hess, 1981). Based on his earlier research regarding dual loop behaviour, he attempted to improve the model by adding a second loop to the interceptor (e.g. control column, stick, force stick) control and by including a model of the central nervous system. Hess revised his model in 1997 (Hess, 1997a) which became the revised structural model shown in Figure 2-4.

The dual loop idea stems from his earlier research in 1977 (Hess, 1977) and 1979 (Hess, 1979), which describes the coupling between (not only) the inputs, but also the force from the control manipulator. This could explain the pulsed behaviour that is observed at high workloads and marginally stable aircraft.

2-5 Descriptive model

Another pilot model was proposed by Hosman (1996). This model is called the descriptive model and it separates the human perception system in individual sensors, each modelled by a time delay and transfer function. The contribution of each input is weighted by an individual gain. The output is then modelled by a delay representing the time constant of the cognitive processes and the neuromuscular system. Figure 2-5 shows the descriptive model for a roll task.

The individual sensor gains are determined by optimizing a cost function similar to equation 2-3.

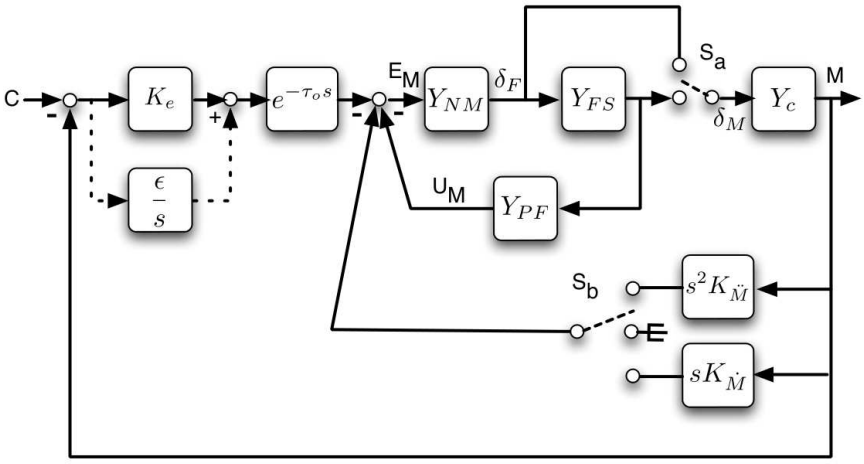

Figure 2-4: Revised structural model for a compensatory task from Grant & Schroeder (2010)

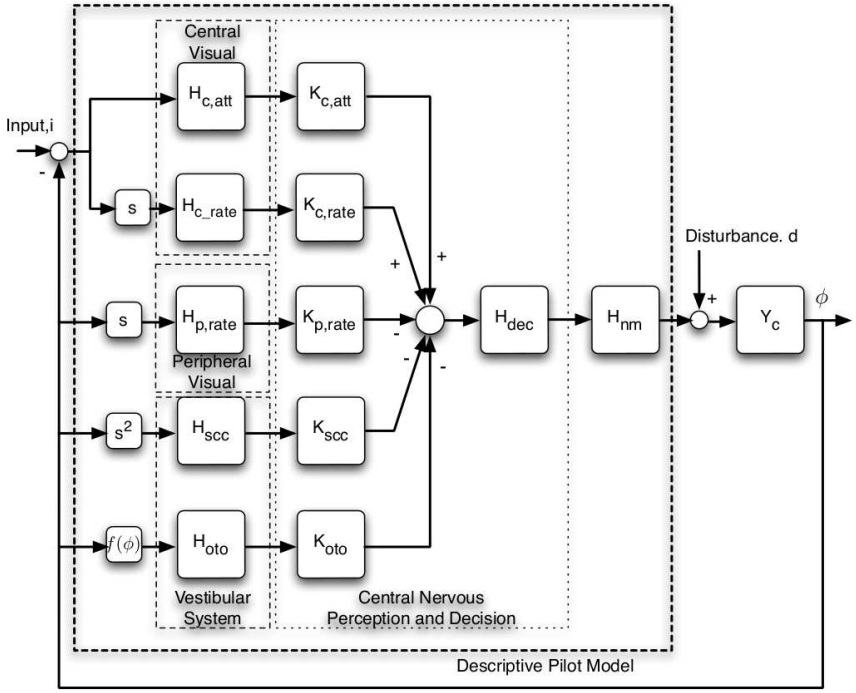

Figure 2-5: Descriptive model for a compensatory roll task from Grant & Schroeder (2010)

2-6 Pilot model identification

A different approach to determine a transfer function for the pilot model is to try to identify the frequency response experimentally. Using two varying disturbance functions and by determining the Fourier coefficients the frequency response can be determined for certain frequencies (van Paassen & Mulder, 1998). The method was improved by using the AutoRegressive with eXternal (ARX) model (Nieuwenhuizen, Zaal, Mulder, & Van Paassen, 2006) which had several advantages regarding the forcing functions and resulting frequency response. This approach has been successfully used to identify different parts of human perception and pilot behaviour, but does require the use of two specified frequency and amplitude disturbance signals (or a disturbance and forcing signal) to be able to identify the transfer function in a reliable way.

Chapter 3

Preliminary Pilot Model

Based on the preliminary analysis and the available pilot models, an initial design can now be considered. This will serve as basis for the final model and should help in determining the main questions and gaps. First the applicable pilot models will be considered, secondly the internal control and feedback structure and finally possible ways of fitting the model.

3-1 Applicable pilot models

The pilot models mentioned in the previous chapter reflect the different variations and approaches that have been used in the past. Depending on the subject, different pilot models have been applied, but starting at the crossover model a general trend can be seen towards more detailed models. The model response is split up and attributed to different parts of the human anatomy.
In a recent paper by Grant & Schroeder (2010) four major pilot models; the crossover, precision, structural and descriptive model, are applied to several tasks and the results are compared to the expected behaviour. It is concluded that the models can be used to analyze pilot behaviour, but that the descriptive model seems most likely to succeed in predicting unusual situations. This is due to its optimization technique compared to the tuning rules of the other situations which are more aimed at typical situations.
The structural model is the only model that, by default, takes into account control forces and the interaction between the pilot and the controls.

For the research subject of this thesis the logical step is to apply a model similar to the descriptive model. This provides a basis for the different inputs into the control part and has been successfully applied to manoeuvres like a balked landing (Hosman, Schuring, & van der Geest, 2005). It does however not include the possible interaction between the control column and pilot, as Hess's structural model does.

3-2 Preliminary pilot model structure

The analyzed control task consists mainly of a pitch task where the pilot has to pitch the aircraft according to the (general) recovery procedures. This can be incorporated as a skill based tracking task where the tracking target is determined by the recovery procedure.

3-2-1 Rule based and skill based control

It is obvious that the complete recovery, as executed by the pilots, cannot be encompassed by a single linear model. The recovery as flown in the second SUPRA experiment had in general two main phases; pitching down to rapidly exchange altitude for speed, and then pitching up to return to a normal flying condition. The surveys have shown that different sources of information were used in these scenarios and it is expected that the pilot response adjusts to the changes in aircraft response. This change in aircraft

response is especially large due to the large changes in aircraft speed and angle of attack.
This prescribed procedure of first pitching down and, when enough speed is gained, pitching up again can be seen as rule based control behaviour. The rule based behaviour determines the parameters, for example the target pitch, which a skill based part of the pilot model tries to control.

3-2-2 Pilot model inputs

The results from the preliminary analysis suggests that the following inputs are most relevant to the pilot model:

- Pitch (rate)
- Speed (trend)
- G-load [motion]
- Pitch (rate) [motion]
- Yoke position and forces

The exact relation and effects of these inputs requires further analysis.

3-2-3 Pilot model closed loops

Another question is whether or not the pilot control behaviour in the upset is closed loop behaviour. The behaviour in the loading phase shows a relatively constant pitch rate while the control input is changing. This suggests a closed loop for pitch control.
The unloading phase is less clear and while some pilots give a simple full nose down input, other pilots show less simple steering behaviour. It is not expected that a simple pitch control loop will provide the necessary smooth intercepts and it does not explain the undershooting visible in Figure 1-6. A pitch control loop with an inner pitch rate control loop might explain this behaviour (Chapter 7 will further extend on this). This dual-loop structure has also been used in past experiments by for example Hess (Hess, 1977).

3-2-4 Structure

Taking all the current considerations into account a pilot model shown in Figure 3-1 should roughly describe the observed behaviour. It uses a structure similar to the descriptive model, adds a second pitch loop and a possible control column-neuromuscular interaction.

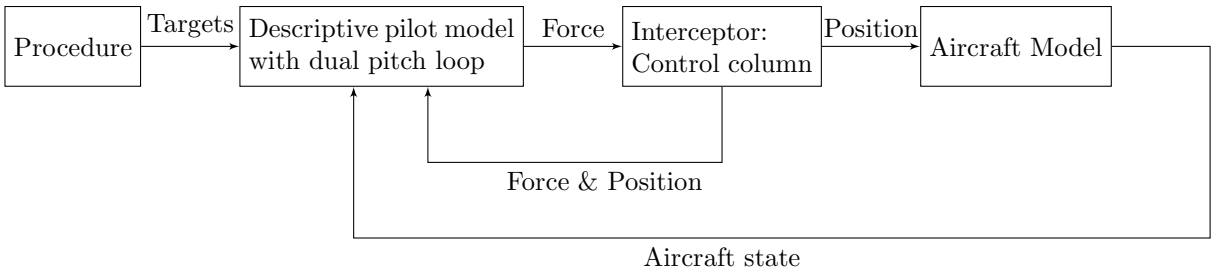

Figure 3-1: Preliminary pilot model

3-3 Pilot model fitting

To tune or fit the model to the specific scenario ideally a cost function should be used to fit the model to the prescribed behaviour. This would make it possible to predict behaviour in other (similar) applications. The lack of a linear(ized) aircraft model and the complexity of the scenario complicates this.
Another approach would be to fit the model gains to the logged data using an iterative optimization. It will provide a more straightforward path to a good fit of the model, and while the predictive capability is lost the resulting model will still help in better understanding pilot behaviour in these types of scenarios.

Part II

Data Collection

Chapter 4

Experiment Hypotheses and Requirements

The preliminary research from the previous part has shown that a somewhat common behaviour is observed during the considered upset recoveries. A rough structure for a pilot model has been proposed, but more information and a better dataset is required to confirm and fit the pilot model. Based on this the hypotheses and requirements for the new experiment will be determined.

4-1 Experiment hypotheses

The introduction provided the main hypothesis of this thesis; that current pilot models can be used to model pilot control behaviour in quasi-symmetric pitch up stalls. Based on the results from the preliminary research this hypothesis has been refined and subdivided as follows:

1. The pilot control behaviour in the recovery can be modelled using current pilot models
   (a) The recovery can be modelled as a primarily closed loop pitch control task
   (b) The control behaviour can be generalized for different pilots
   (c) The pilot behaviour can be modelled as quasi-linear control behaviour
2. The effect of simulated motion can be modelled using current pilot models
   (a) Simulated motion has an effect on pilot control behaviour in a stall recovery
   (b) The effect of simulated motion can be generalized for different pilots
   (c) The effect of simulated motion can be modelled using quasi-linear models

The first hypothesis has been split up in three sub-hypotheses based on the observations from the preliminary research. The first step is to determine if the pilot control behaviour can be represented by a closed loop pitch control system. The data suggests several possible inputs that are used by the pilots to track certain reference values, but the precise (closed loop) control structure is unclear.
Another observation was the relatively large spread in pilot control behaviour. This has several causes and also some individual variation between humans is to be expected. However, most pilot models only provide a single specific response and the validity of this has to be determined.
The third sub-hypothesis concerns the fact whether or not the selected quasi-linear pilot model can be used to accurately model the pilot response. Abstractions in the model, simplifications of the control structure, and limitations of the quasi-linear form, will limit the accuracy of the model. Part of this difference will be the remnant representing the non-linear properties of human behaviour.

Past experiments have also shown that motion has a measurable effect on pilot control behaviour and their perception of the simulation. Because the main part of the pilot model is not expected to depend on the simulated motion, the added effect of motion is considered separately. The first step is to determine which parts of the simulated motion affect pilot behaviour. For these motion inputs the generalized effect and variation on pilot control behaviour has to be determined. Again the last sub-hypotheses is concerned with the applicability of the quasi-linear model and resulting differences.

4-2 Experiment requirements

To test the hypotheses an experiment is necessary. However, not all hypotheses can be tested in a direct way and some can only be evaluated when the complete pilot model has been constructed and fitted. During the preliminary research also several specific requirements for the new experiment were identified.
In line with the chosen approach to attempt to model a fully realistic stall recovery, the requirements determined in the preliminary research, and the selected hypotheses, the requirements for the experiment have been determined.

4-2-1 Recovery procedure

The SUPRA experiment data showed a large spread in pilot behaviour. Possible explanations (and probably a combination of these) are differences in pilot training, company procedures, familiar aircraft and flying experience. Since it is not yet possible to model all these variables in a pilot model, and because the main interest is the effect of motion on pilot behaviour, this effect should be minimized.
By providing the pilots with a strict, but realistic, recovery procedure, the differences due to aircraft and company specific procedures should be minimal. Ideally only the skill based control behaviour should remain. By using the experience from previous experiments, and recommended procedures (FAA, 2012), a realistic recovery procedure can be created.
Another necessary improvement, with respect to the preliminary data set, is a better controlled aircraft state at the entry of the stall. Small differences in the aircraft state caused by the time dependence of the model can cause some variation between the different experiment runs. This should be minimized in the new experiment.

4-2-2 Control structure

To test sub-hypothesis 1a more detail is required on the (closed loop) structure. This extends into whether or not a dual-loop control model is representative of the pilot control behaviour. However, it is difficult to separate the pitch and pitch rate inputs.
While it would be possible to use a disturbance signal to identify the effect of the pitch information, the dynamic situation caused by a low airspeed (decreased aircraft responsiveness) and/or high alpha (decreasing stability) makes this very difficult. Instead all pitch information will be removed from the PFD, forcing the pilot to use the outside visual to estimate the aircraft attitude. This will most likely change the perceptual noise and also introduce an offset in the perceived pitch. This should give some idea of the effect of the pitch input on pilot behaviour.
Another unknown is the precise effect of the barber pole and speed trend vector, which were mentioned in the initial surveys, on the pitch control loop. By hiding the speed tape this input can be removed and the effect of this input in the different recovery phases can be determined.
These two specific scenarios have been chosen because both situations are representative of possible instrument failures and do not directly introduce any disturbances.

4-2-3 Control loading

Another possibly important interaction found in the preliminary research was the control column position and force. This has given rise to several questions, the first being whether or not the control is pure position control, force control or both. The second question is whether or not the control force has an effect on the discrete steering behaviour observed in the preliminary analysis. To determine the effects of the control loading, but without making significant changes to the actual scenario, the control loading force will be made independent from airspeed. For this the control loading force will be representative to the average

airspeed during the scenario. This will remove the changing spring force and will cause the control loading spring force to be relatively higher in the initial part of the recovery and to be relatively lower in the second part of the recovery.

4-2-4 Motion

To measure the possible effects of simulated motion (sub-hypothesis 2a) and to determine the variation between pilots (sub-hypothesis 2b), ideally the different relevant motion inputs like pitch, pitch rate and g-load should be isolated. Physically this is of course almost impossible, nor could the resulting simulation be considered realistic. The best approach to this is to use three different motion conditions; a no motion condition, a condition with basic hexapod motion, providing pitch and pitch rate, and a centrifuge based motion condition providing g-load feedback.

4-2-5 Model fitting

The three different motion conditions will provide the necessary data to be able to fit the resulting model. To be able to asses the general validity of the fit, the results should be compared for at least two different scenarios which are similar in procedure, but not exactly the same. It is expected that the skill based control gains are the same, since the aircraft response does not significantly change and thus the pilot adaptation will be the same (based on the crossover model theory).
The resulting pilot model and differences with the experiment data should provide an answer to the two final sub-hypotheses.

Chapter 5

Experiment Setup

Based on the requirements the experiment can now be designed. First the practical implementation of the required scenarios and conditions is considered, next the required participant group and experiment structure is discussed. Finally the data collection through surveys and data logging is explained.

5-1 Experiment conditions

Theoretically a large number of participants and minimal repetition would be ideal, the latter to eliminate the learning effect. However the number of available pilots is limited. For this an optimal use of the experiment time and runs has to be made to get best possible results from the experiment.

5-1-1 Scenarios

For the requirements listed in the previous chapter, four different cockpit configurations were designed, from here on referred to as scenario 1, 2, 3 and 4.
In the first scenario, the cockpit indications and flight controls are configured as validated during the SUPRA project. An example of the PFD configuration is shown in Figure 5-1(a), displaying the situation just after a stall recovery is started.
In scenario 2 the speed tape is hidden and the amber failure indication `SPD` is displayed to notify the pilot of this condition. An example of the PFD configuration under this condition can be seen in Figure 5-1(b).
The third scenario does not provide pitch information on the PFD, but instead of hiding the complete artificial horizon and also removing any roll information, the displayed pitch has been fixed to an angle of zero. The pitch ladder has also been removed as an additional reminder, and the amber failure indication `pitch` is shown (see Figure 5-1(c)).
In the last scenario, scenario 4, the control loading spring force is fixed to a value representative of a CAS of 200 kt. This is approximately the average speed during a normal stall recovery. The PFD configuration in this scenario is the same as in scenario 1.

5-1-2 Motion conditions

The motion conditions are *no motion*, *classical washout hexapod motion* and *centrifuge motion*, from here on referred to as respectively motion condition 1, 2 and 3. The no motion condition is a reference condition without any motion input at all. The addition of buffet motion was considered since this should not affect any of the common pilot model motion inputs, but because of the possible interference with the controls, a completely clean scenario was decided to be more useful.
In general the motion cueing solution will be the same as in the SUPRA experiments as described in Section 1-2-2. In motion condition 2, the improved hexapod cueing will provide pitch, roll, yaw and heave onsets, including sustained side force by using roll tilt. The improved unloading and loading through pitch,

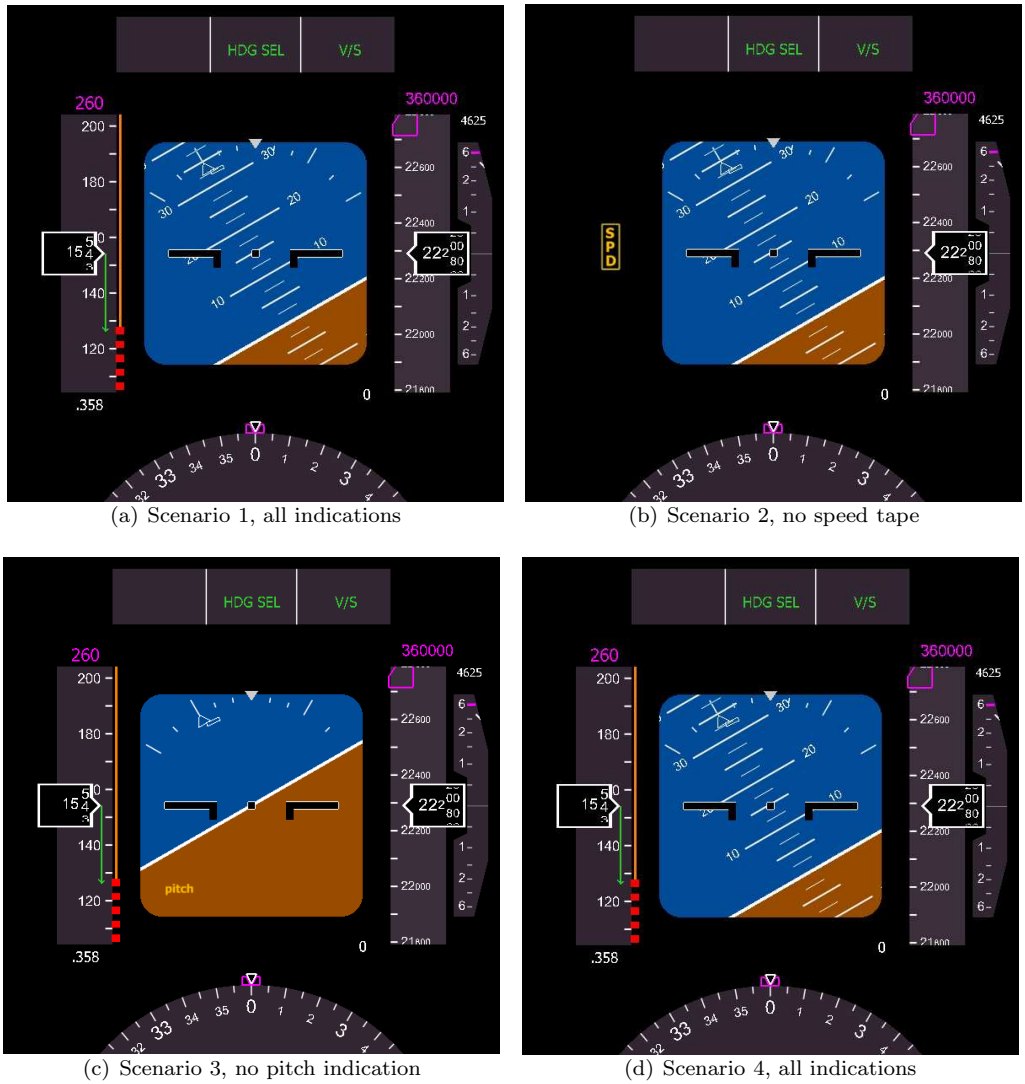

(a) Scenario 1, all indications

(b) Scenario 2, no speed tape

(c) Scenario 3, no pitch indication

(d) Scenario 4, all indications

Figure 5-1: Different PFD configurations just after starting the stall recovery (FL200 condition)

used in the SUPRA experiments, will not be enabled, to disconnect sustained g-loads from the possible pilot motion inputs in this condition.

In the third motion condition, the hybrid Dedemona g-cueing solution will be used. Up until stickshaker activation the motion cueing algorithm is the same as in motion condition 2. However, on stickshaker activation the centrifuge component of the simulator will start accelerating to a slow baseline rotation. This event is partially masked by the stall buffet and aircraft roll-off, but some false cues are possible in this stage. The pitch down during the unloading phase is partially matched with the simulator cabin repositioning, which is necessary for the centrifuge solution. This makes it possible for the simulator to follow the aircraft g-load during the loading phase. This g-load is not exactly matched due to the offset caused by the baseline rotation. Upon reaching the recovery attitude of zero degrees pitch and unloading of the aircraft to normal flight conditions, the centrifuge will slow down to a complete stand still. Because the perceived motion during this deceleration can be associated with a right turn the autopilot will be automatically engaged and a right level turn is automatically initiated.

5-1-3 Stall conditions

Two different, but similar, fully developed quasi-symmetric pitch up stall conditions are required. Not only is this necessary for the fitting of the pilot model, it might also decrease the training effect during the experiment. Two scenarios were designed, the first is a stall at approximately flight level 200 (FL200), with an approximate pitch up entry of 30 degrees and a very small roll-off. The second scenario is a high altitude stall at approximately flight level 350 (FL350), with a 20 degrees pitch up entry and a slightly larger roll-off

component than during the first scenario.
Both scenarios are based on previous experiences during the SUPRA project and are considered realistic upsets. Although the entry is clearly different, the recovery procedure for both scenarios is the same. Based on previous experiences and regulations, the recovery procedure for these scenarios has been specified as follows:

- Pitch down to −20 degrees
- Add thrust
- Wait for the speed to increase to the top of the amber band on the speed tape
- Pitch up for level flight again at approximately 2 deg/s

5-2 Participants

Since the pilot model depends on skill based behaviour the participants should have had the relevant flight training to be able to execute this experiment as intended. Also to get a representative sample of the airline transport pilot community care has to be taken that most of the participants represent daily airline pilots, without special training in for example upset recoveries or with ratings like flight instructor.

5-3 Experiment structure

Based on the scenarios and motion conditions the next step is to determine the order and grouping. Because fully randomizing the motion conditions might be too disruptive it was decided to group each set of scenarios per motion condition. This means that during every motion condition each of the 4 different scenarios are completed. This yields $3 \times 4 = 12$ sets. To get more data a repeated measurement is done by repeating the whole set once more but with a different stall condition for each respective scenario/motion condition combination, providing a total of 24 experiment runs per participant. In between the two sets of 12 runs, a break is mandated. The order of the motion conditions, scenarios and stall conditions is randomly distributed. An example experiment structure is shown in Table 5-1.

Table 5-1: Example experiment structure

Motion condition	Scenario	Stall scenario
3	3	FL200
3	2	FL350
3	4	FL200
3	1	FL350
1	2	FL350
1	1	FL200
1	4	FL200
1	3	FL350
2	2	FL350
2	4	FL200
2	3	FL350
2	1	FL200
Mandatory break		
1	3	FL200
1	1	FL350
1	4	FL350
1	2	FL200
2	3	FL350
2	4	FL200
2	1	FL350
2	2	FL200
3	1	FL200
3	4	FL350
3	2	FL200
3	3	FL350

5-3-1 Participant briefing and familiarization

The participants are provided with a short document (see Appendix D) shortly before the experiment date, explaining the experiment setup and recovery procedure, to make sure the level of preparation is the same

for everyone. On the day itself any remaining questions by the participants were answered and the properties of the simulator are briefly discussed. After showing them the simulator, cockpit indications and controls, they were seated in the simulator for the first 12 experiment runs.
Before starting the experiment they are given the chance to familiarize themselves with the aircraft response, performance and controls. During the familiarization hexapod motion is enabled with g-load on pitch enabled (to slightly differentiate it from the experiment motion condition 2). They are requested to perform some climbs, descents, turns and other basic flying manoeuvres, to experience the aircraft response and control feel. When they are satisfied they are requested to approach the stall up to stickshaker, to familiarize themselves with the red barber pole indicating the stick shaker activation and the feel of the stick shaker. This also gave them a chance to experience the initial stall buffet.
The entry to each scenario is flown automatically by an autopilot and at a fixed point in time, the pilot is triggered to start the recovery by an audio message saying 'recover now'. The pilot then has to disconnect the autopilot and can start controlling the aircraft.
After 12 recoveries there is a mandatory break. Once back in the simulator they are again given a short period to get used to the controls again.
The first centrifuge run is preceded by a stall recovery with centrifuge motion where the participant is talked through the simulation to make them aware of the difference with a normal hexapod simulation, and the major false cues when stopping the centrifuge.

5-3-2 Survey

During the experiment the pilots are given two surveys, one during the experiment runs and one at the end of the experiment. Although their answers to these surveys give subjective indications they can prove useful in getting a global idea of possible inputs and trends.
During the experiment the pilot is asked after each scenario to rate the following three questions with a number between 0 and 10:

- How high was the workload? (0 very low - 10 very high)
- How precisely could you follow the recovery procedure? (0 very imprecise - 10 very precise)
- How accurately could you control the aircraft? (0 very inaccurate - 10 very accurate)

These questions are designed to get an idea of the change in workload over time due to the learning effect, the effect of motion on handling and workload, and the effect of missing indications. The results might also prove useful in identifying outliers in the data.

After the experiment the participants are given a survey with several questions (see Appendix E). The first set of questions asks them about their total flight hours and type rating to get a general idea of their experience with respect to large, control column controlled, transport aircraft. The second set of questions asks them to rate the realism of the recovery procedure, and possible problems or false cues affecting their behaviour. The next set of questions asks them to list the indications and motion cues they used in the three recovery phases and how that changed in the other scenarios. The final question is not specifically related to the experiment, but asks them their opinion regarding the usefulness of these types of simulations to pilot training.

5-4 Data collection

To be able to compare the experiment runs it is necessary to log the required data. Based on experiences from previous experiments, it has been decided to log the following main data sources at a rate of 200 Hz (the same time step as used for the aircraft model and motion cueing):

- Aircraft model state variables and some derived values
- Control loading inputs
- Pilot inputs
- Simulator cabin gyroscopes and accelerometers

- Commanded simulator motion state (Position/Velocity/Acceleration for each degree of freedom)
- Experiment condition settings

This will make it possible to calculate any derived value of the aircraft or simulator state at a later time.

Chapter 6

Experiment Results

The experiment proposed in the previous chapter was successfully conducted in January 2013 with a total of 10 pilots. First, the experiment execution will be summarized. Next, the logged data from the experiment and the pilot surveys will be analyzed. An ANalysis Of VAriance (ANOVA) will be used to determine the effects of the different scenarios, motion conditions and repetition, on pilot behaviour. Finally, the other (in)direct pitch inputs like, for example, trim and rudder will be considered.

6-1 Experiment execution and participants

With the help of contacts from the SUPRA experiments and Desdemona B.V., several pilots were asked if they would like to participate in the experiment. In total 10 pilots volunteered. Most of these pilots were active airline pilots, with no or limited experience with aerobatics or test flying. Exceptions were two pilots who had experience with test flights and/or aerobatics, and a recently retired airline pilot.

Over a time period of two weeks in January 2013 all 10 pilots were able to participate in the experiment. Depending on the planning this ranged from 1 to 3 participants per day. When possible the participants switched during the break in the middle of the experiment.

During the experiment it became clear that some subjects experienced nausea due to the centrifuge in motion condition 3. At their discretion the centrifuge conditions were either completely skipped (1 out of the 10 pilots) or limited to one set instead of two (4 out of the 10 pilots). Due to varying reasons the order of some experiment conditions for some participants was slightly altered. Also some experiment runs had to be repeated due to reasons like errors, miscommunications and software failures.

6-2 Data analysis

A statistical analysis was performed on specific logged parameters, as well as on the data gathered using the surveys. For this purpose several MATLAB scripts were developed to automate most parts of the analysis and graphing.
The first step was to extract and identify the experiment runs from the raw data files. The start of the experiment run was determined by the auto pilot disconnect event which is triggered by the pilot, when he is told to initiate the recovery. The end of the stall recovery was marked by a positive pitch angle, which also triggered the centrifuge slow down and associated automatic turn in motion condition 3.
A second set of MATLAB scripts was developed to automatically gather specific data points from a selected set of experiment runs. These data points are then processed using the specified functions and plotted in a graph for comparison.

For the statistical analysis of the parameters an (unbalanced) one way (repeated measures) ANOVA was used for a comparison with a control or baseline situation. This was done for the 4 scenarios where the first (normal conditions) scenario was the control, and for the three motion conditions where the first condition

(no motion) was the control. This makes it possible to determine the changes caused by the variations in scenarios and motion condition. A two way analysis, where the effects of motion during specific scenarios is analyzed, might be useful, but due to the limited amount of data this analysis was not expected to provide any significant (or useful) results. In Section 6-2-1 more detail about the statistical method is provided.

While normally the complete data set should provide the most significant results, the large number of experiment runs (24) per participant probably also caused a learning effect and adaptation during the experiment to occur. Because of this, the analysis is done for data sets consisting of the first 4, 8, 12 and 24 experiment runs of all participants. Thus the first data set only consists of the first 4 experiment runs done by all participants, the second data set consists the first 8 experiment runs done by all participants and so on. Although the results from the smaller data sets are less likely to be significant, they can give insights into possible effects that disappear due to learning or adaption in the larger data sets.

The analysis of the results is split into the 3 basic maneuver phases of the recovery. The procedure gives clear boundaries between the three control phases, but because not every pilot reached the target pitch of -20 degrees an alternative boundary had to be chosen. Using Figure 6-1, which shows a phase plot of the pitch and pitch rate, a new transition boundary was selected. This results in the following three recovery phases:

- **Phase A:** Starts at auto pilot disconnect
- **Phase B:** Starts when pitch below -13 degrees and pitch rate smaller than $-2\,\mathrm{deg/s}$
- **Phase C:** Starts when speed above amber band

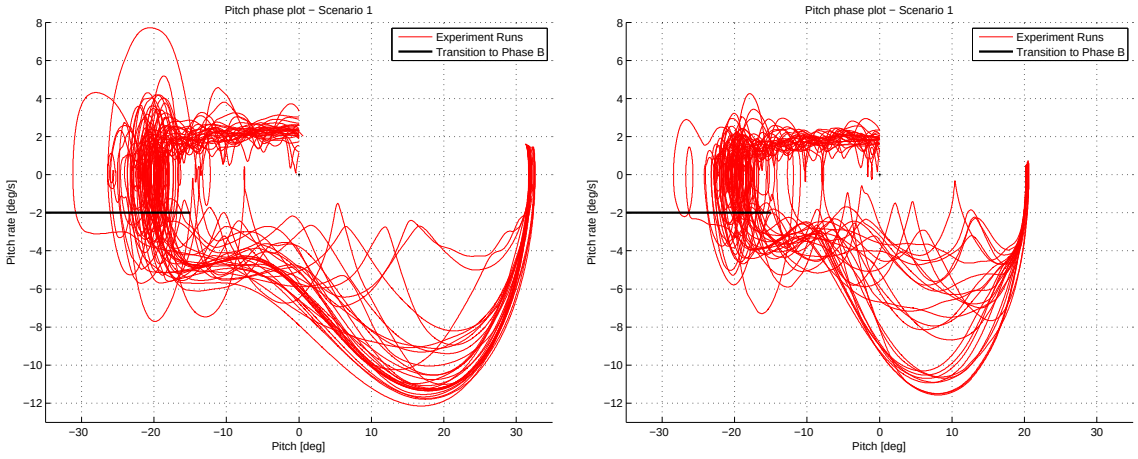

(a) FL200 (b) FL350

Figure 6-1: Phase plot of the pitch angle for the recoveries in scenario 1

Each phase will be considered individually. First, the results from the post-experiment survey will be reviewed to get some idea about possible inputs for the pilot model for that specific phase. Next, several parameters will be analyzed to investigate the effects of the different scenarios, motion conditions and repetition on the pilot control behaviour.

6-2-1 Statistical method and validity

Two different ANOVAs are used in the statistical analysis. The first ANOVA is a simple, between group, comparison where the data is independent from the test subject. These results can be recognized by the single degree of freedom F-factors and blue colour p values in the plots. A more statistically powerful test is a within subject comparison. This compares the changes per subject, and can be recognized by the multiple degrees of freedom F-factors and red p values in the plots. Although the within subject comparison is usually more significant not always enough data is available. For example after 4 experiment runs non of the test subjects will have executed more than 1 motion condition. In other cases the repeated measures from the between group ANOVA gives more robust results. The reported p values are the most significant value from either of these two tests.
Both ANOVAs can be unbalanced and can incorporate repeated measures depending on the available data.

As a threshold for significance the general value of $p < 0.05$ is used, but it should be kept in mind that the large number of reported statistical tests increases the possibility of a type I error (incorrect rejection of the null hypothesis).

6-2-2 Validity of the ANOVA

The ANOVA has three basic assumption; independence of observations, normality and equality. The dependence of samples from the same test subject is prevented by the repeated measures implementation. There could be other dependant factors, but the experiment was designed to prevent this as much as possible. Test subjects were not allowed to watch experiment runs of others or discuss the experiment with the others until all their experiment runs were completed.
The spread of the data is difficult to test, especially because of the small amount of samples in some cases. An obvious case where this assumption would be violated is the maximum control deflection (which is almost at the limit position). Although the results from this are not used, they might also cause non-normal distributions in the other parameters.
The equality is another difficult to assess property with a small number of available samples, but visual inspection of the variances should give some idea of this property.
Although there are mathematical tests available to help assessing the validity of these three assumptions, these have not been used. The limited amount of available data points make this extremely difficult and the ANOVA is usually robust enough for small data sets. Where necessary an inspection of the variances and means should confirm the results and assumptions of the ANOVA.

6-2-3 Implementation of the statistical method

The two different ANOVAs have been implemented in MATLAB to provide maximum flexibility for the analysis of the experiment data. The `anovan` function was used for both types. Although the analysis is only one-way the more obvious `anova1` function could not be used because of its lack of support for repeated measurements.

6-3 General analysis of longitudinal control inputs

To get some insight into the control inputs that the pilots made, the longitudinal control inputs for 10 randomly selected experiment runs are shown in Figure 6-2. The average input is an initial full forward deflection and then a slow return to neutral or slightly aft control deflection. There are large differences in control stability, and most inputs show a step like profile. In the preliminary analysis (Section 1-4-4) this behaviour was also observed and discussed.

A statistical analysis of the effects of a change in control loading on the stepped control characteristic is included in Appendix F. The effect of a change in control loading force, on the step like control inputs, was small and no significant effects were found.

6-4 Analysis of recovery phase A

The first recovery phase consists of the control task to level the wings and reduce pitch to -20 degrees. As described in Section 6-2 this part is considered finished when the aircraft pitch is below -13 degrees and the pitch rate less than 2 deg/s.

When the pilot is triggered to initiate the recovery, and after disconnecting the autopilot, the general response is to immediately provide up to full forward control column deflection (see Figure 6-2), even though there still is a roll component. The negative load limit of -1 g was never reached, because in both the FL200 and FL350 stalls conditions the control effectiveness is not high enough. For example instantaneous and full forward deflection in the FL200 condition gives a maximum unloading of -0.15 g.

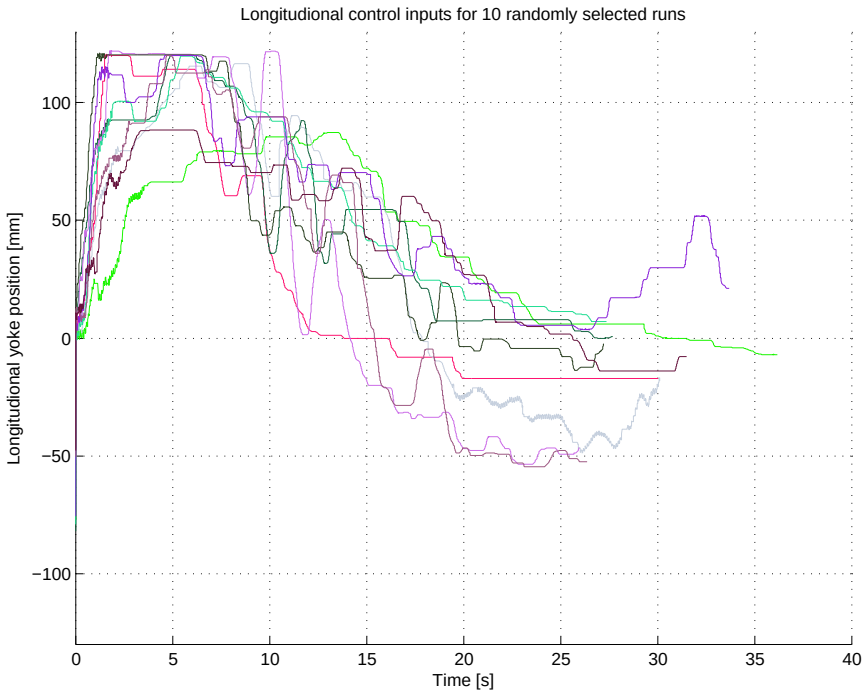

Figure 6-2: Longitudinal control column inputs for 10 randomly selected experiment runs

6-4-1 Post-experiment survey on possible inputs

In the post-experiment survey pilots were asked what information sources they used to complete the recovery task. They were asked to list the cockpit indications and motion cues they thought they used in scenario 1 and if and how that changed in the other scenarios. The results are listed in Table 6-1, but have been limited to indications and cues that were mentioned by at least two out of the ten pilots. Also similar cues or indications (e.g. speed, speed tape, speed trend, barber pole) have been grouped together.

The pitch ladder is the main indication used in this flight phase, followed by the motion pitch cue. Another,

Table 6-1: Indications or cues mentioned by more than one pilot on the survey for recovery phase A

(a) Scenario 1 baseline indications/cues

Indication/cue	Score
Pitch ladder	9
Pitch cue	3
Yoke force	2
Speed (tape)	2
Altimeter	2

(b) Scenario 2 additional indications/cues

Indication/cue	Score
None	None

(c) Scenario 3 additional indications/cues

Indication/cue	Score
Outside visual	5
Speed (tape)	3
Pitch cue	2
Yoke deflection	2

(d) Scenario 4 additional indications/cues

Indication/cue	Score
Speed (tape)	3

less often mentioned input, is the speed(tape). Also listed is the altimeter, which provides information about the flight path of the aircraft, and yoke force which can give some feedback about the speed and change in speed.

Scenario 2, where the speed information is hidden, lists no additional indications or cues (although speed has been mentioned as a possible input in scenario 1). Analysis of the logged data might provide an insight whether or not the control behaviour is different, as to determine if speed is a relevant information source for this part of the recovery.

The third scenario hides the pitch information on the PFD from the pilot, which triggers a change to the outside visual as mentioned by 5 of the pilots. Also additional use was made of the speed (tape) indication, yoke deflection and the pitch cue to control the aircraft. The outside visual will of course provide a direct source of pitch information, although less precise. The speed tape gives some idea of the aircraft pitch through the speed trend vector, and the yoke deflection provides a good baseline input.

In the final scenario, where the yoke force is slightly altered, some pilots list speed as an additional cue although pilots frequently commented not to be aware of any change in yoke force.

6-4-2 Statistical analysis of the changes in pilot control behaviour

To objectively investigate the effects of cockpit indications and motion on the resulting pilot behaviour, several key values of the resulting recoveries are analyzed. In Figure 6-3 a statistical analysis of the minimum pitch rate reached during this recovery phase is presented. This pitch rate is typically attained early in the recovery, as seen in Figure 6-1. Scenario 1, 2 and 3 show little variation which would suggest that neither speed indications, nor pitch indications have any influence in this part. Scenario 4 shows a significantly ($F(1,9) = 4.2$, $p = 0.043$) smaller pitch rate ($\mu = -8.67$, $\sigma = 2.34$) with respect to scenario 1 ($\mu = -9.37$, $\sigma = 2.24$) which can be explained by the higher control loading force decreasing control column deflection (since the speed is < 200kt).
Motion condition 2 does not show a clear effect except for the initial set of 4 repetitions. The third motion condition ($\mu = -8.78$, $\sigma = 2.36$) shows a significantly ($F(1) = 4.2$, $p = 0.043$) smaller maximum pitch rate than motion condition 1 ($\mu = -9.57$, $\sigma = 2.17$).

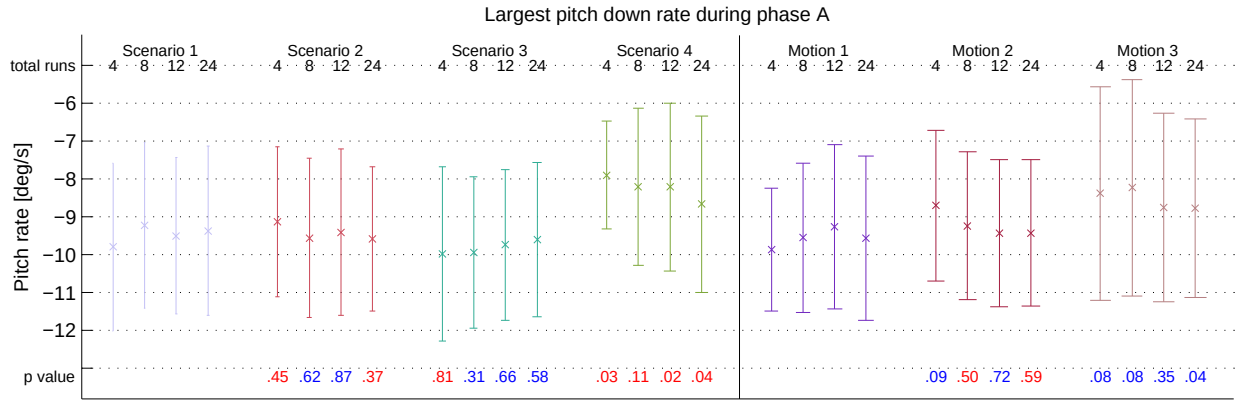

Figure 6-3: Mean and variance plot with ANOVA of the maximum pitch rate during phase A

Figure 6-4 show the minimum g-load that is reached during phase A. This is of course coupled to the pitch rate and similar results are expected. Again scenario 2 and 3 do not show significant differences but scenario 4 ($\mu = -0.0147$, $\sigma = 0.124$) is significantly ($F(1,9) = 9.6$, $p = 0.003$) different from scenario 1 ($\mu = -0.06$, $\sigma = 0.11$). Motion condition 3 ($\mu = -0.0104$, $\sigma = 0.126$) shows a consistent significant ($F(1) = 12$, $p = 0.001$) change from the baseline motion condition 1 ($\mu = -0.0795$, $\sigma = 0.11$). Motion condition 2 ($\mu = -0.0118$, $\sigma = 0.0964$) shows a significant ($F(1) = 5.3$, $p = 0.029$) difference for only the initial 4 experiment runs ($\mu = -0.0984$, $\sigma = 0.103$), but the mean is consistently smaller than the baseline means.

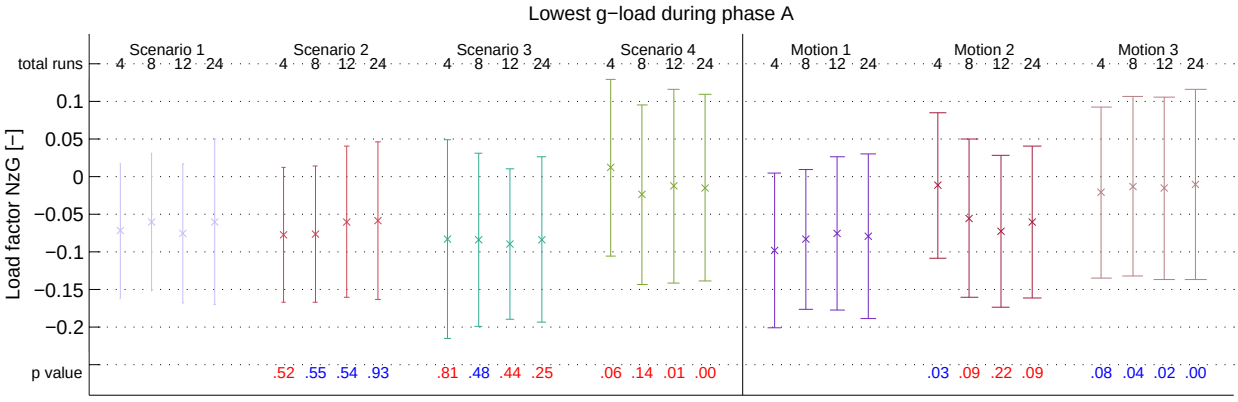

Figure 6-4: Mean and variance plot with ANOVA of the lowest g-load during phase A

6-4-3 Conclusions

For phase A the main controlling input seems to be the pitch ladder although changing this to the outside visual does not cause a significant change in observed control behaviour. Both motion conditions cause an average decrease in pitch rate and minimum g-load. Also the increased control loading force causes a significant decrease in the absolute value of the observed parameters.

6-5 Analysis of recovery phase B

In phase B of the stall recovery the pilot has to intercept the -20 degrees pitch attitude and keep the attitude constant by slowly decreasing the forward yoke deflection to compensate for the shift in trim as airspeed increases.

6-5-1 Post-experiment survey on possible inputs

The results of the survey for the second recovery phase are shown in Table 6-2. Again only indications which were mentioned at least twice were listed. In the baseline for the indications and cues (Table 6-2(a)), the speed tape is shown to be the most important indication. This is of course due to the fact that the procedure explicitly states to monitor the speed for the top of the amber band speed. Also the speed tape shows the approaching barber pole, for which the pilot has to compensate in this phase. Meanwhile, pilots have to keep the pitch attitude at -20 degrees, for which they can continue to use the pitch ladder. Other indications mentioned are the yoke force and g-load. The yoke force will increase as speed increases. The g-load is only cued in the centrifuge, and at low g values this is experienced as a shift of the 1.2 g baseline g-vector from forward to more vertical.
In the second scenario (Table 6-2(b)) pilots report replacing the missing speed tape with timing and g-load to decide when to transition to the pitch up part of the recovery.
In scenario 3 (Table 6-2(c)) the lack of the pitch ladder has to be compensated by other indications such as the outside visual, pitch rate motion cue and speed tape. The pitch cue can help stabilizing the aircraft without the pitch ladder and the speed tape can provide some reference as to the current flight path angle via the speed trend vector.
In scenario 4 (Table 6-2(d)) no difference with respect to the baseline scenario was reported.

Table 6-2: Indications or cues mentioned by more than one pilot on the survey for recovery phase B

(a) Scenario 1 baseline indications/cues

Indication/cue	Score
Speed (tape)	10
Pitch ladder	4
Yoke force	2
G-Load	2

(b) Scenario 2 additional indications/cues

Indication/cue	Score
Timing	6
G-load	3

(c) Scenario 3 additional indications/cues

Indication/cue	Score
Outside visual	2
Speed (tape)	2
Pitch rate cue	2

(d) Scenario 4 additional indications/cues

Indication/cue	Score
None	None

6-5-2 Statistical analysis of the changes in pilot control behaviour

As in the previous section several parameters from the experiment runs will be examined to compare the effects of the different scenarios and motion conditions. Because the starting point of this phase depends on phase A it should be taken into account that certain variations in phase B might be due to changes in control behaviour in phase A.
The first value to be considered is the minimum pitch reached during phase B. This should be indicative of the pilots' performance to level off the aircraft at the specified attitude. Figure 6-5 shows the statistical analysis. The change in yoke force or missing the speed tape does not seem to have significant effect. Missing the pitch ladder causes a large change in the lowest pitch attitude ($\mu = -25.4$, $\sigma = 6.39$) with respect to the baseline scenario 1 ($\mu = -22.5$, $\sigma = 2.28$), but the equality assumption for the ANOVA is probably not valid. This change could be either an offset caused by the outside visual or an intentional choice by the pilots. The motion conditions do not seem to have a significant effect on this parameter.

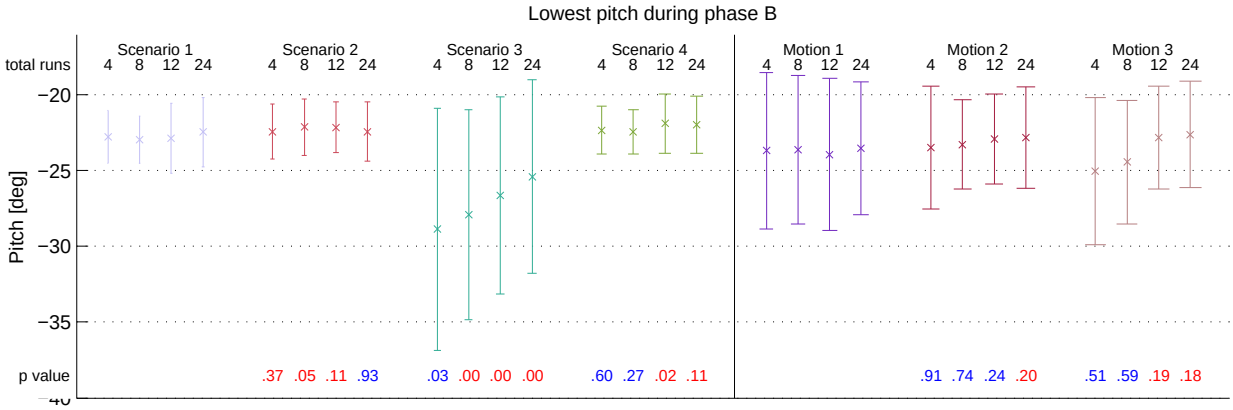

Figure 6-5: Mean and variance plot with ANOVA of the lowest pitch during phase B

In an attempt to quantify the stability of the aircraft attitude during phase B the following equation was used:

$$value = avg\left(\|x\|\right) - avg(x) \tag{6-1}$$

It gives the average absolute value of for example the pitch rate with a compensation for a non zero average pitch rate. Although crude this should give some insight into the general control characteristic in this phase. A spectral analysis would be required for more detail.
Figure 6-6 shows the statistical analysis of the average absolute pitch rate with compensation for an offset. The scenarios do not show any significant changes, but motion has a significant effect on the stability. Motion condition 2 yields a significant ($F(1) = 13$, $p = 0.0013$) change for the first set of runs but motion condition 3 is significantly ($F(1) = 6.6$, $p = 0.011$) different with respect to the baseline motion. Another

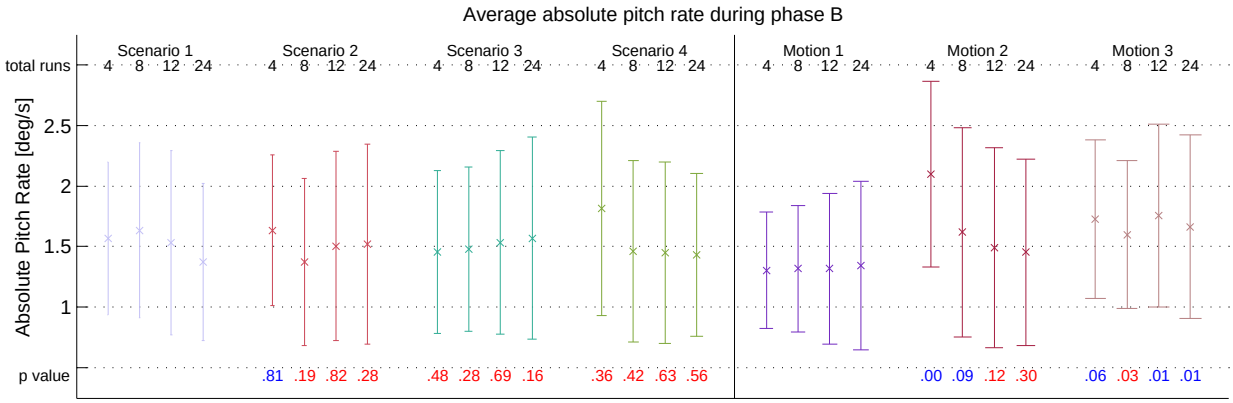

Figure 6-6: Mean and variance plot with ANOVA of the average absolute pitch rate during phase B

value that could be of interest is the effect of the barber pole which starts to appear at some point during phase B. The margin of speed with respect to the top of the barber pole is shown in Figure 6-7. Surprisingly scenario 2 does not yield a significant difference although the margin is on average smaller than the baseline. One possibility could be the fact that when approaching the barber pole the stall induced roll-off or buffet can also be noticed. Also the actual margin to the stall is smaller due to the sometimes rapid increase of alpha and the low-pass filtered response of the barber pole. Scenario 3 does yield a larger margin, but this is most likely due to the lower pitch attitude observed in Figure 6-5. Motion does not seem to have any significant effect.

6-5-3 Conclusions

For phase B the main input still is the pitch ladder and changing this to the outside visual causes a decreased accuracy. The lack of a speed tape does not shows any significant effects although a slight, consistent,

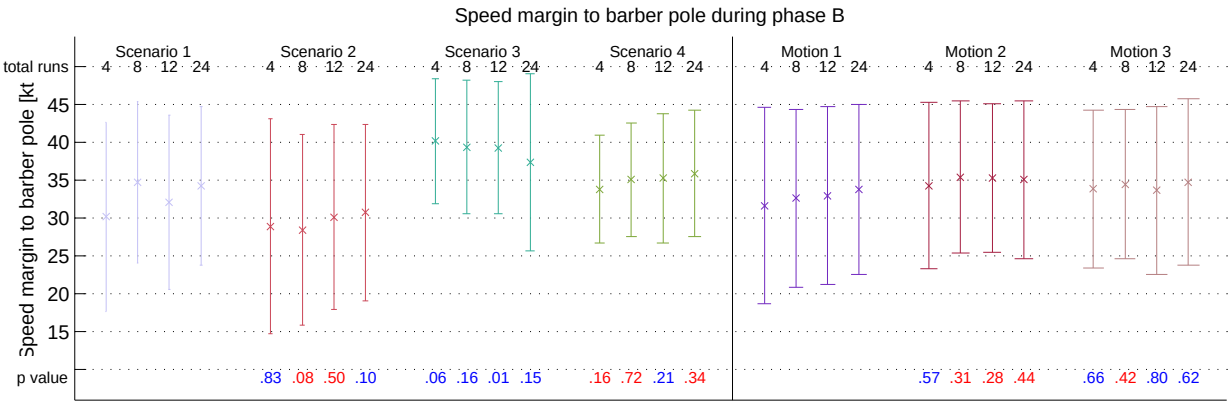

Figure 6-7: Mean and variance plot with ANOVA of the speed margin to the top of the barber pole during phase B

decrease in the speed margin to the stickshaker is observed. Motion does not have a direct effect on the analyzed parameters, but it does cause a decrease in pitch stability.

6-6 Analysis of recovery phase C

In phase C of the recovery the pilots have to pitch up with a pitch rate of 2 deg/s without overstressing the aircraft or entering a secondary stall. Pilots have to smoothly attain the specified pitch rate (as not to cause a dynamic stall) and monitor the barber pole and g-load.

6-6-1 Post-experiment survey on possible inputs

Table 6-3 shows as before the results from the pilot surveys. Again the results can be influenced by the previous recovery phases.
For this phase the g-load was mentioned as an important motion cue by almost all pilots, followed by the speed tape and pitch ladder (Table 6-3(a)). The g-load is of course considered the main limiting factor during this part of the manoeuvre, and the speed tape indicates possible approaches to a secondary stall. The pitch ladder is required to verify the pitch rate of approximately 2 deg/s.
Scenario 2 does not yield any specific replacements for the missing speed tape, except for possibly the pitch motion cue providing information about approaching stalls.
In scenario 3 the pitch ladder is said to be replaced by the outside visual and pitch rate motion cue. Scenario 4 does not yield any interesting results.

Table 6-3: Indications or cues mentioned by more than one pilot on the survey for recovery phase C

(a) Scenario 1 baseline indications/cues

Indication/cue	Score
G-Load	9
Speed (tape)	8
Pitch ladder	7
Stickshaker	2
Altimeter	2
Pitch cue	2

(b) Scenario 2 additional indications/cues

Indication/cue	Score
Pitch cue	4
Timing	2
Altimeter	2
G-load	2

(c) Scenario 3 additional indications/cues

Indication/cue	Score
Outside visual	3
Pitch rate cue	3
VSI	2
Altimeter	2

(d) Scenario 4 additional indications/cues

Indication/cue	Score
Pitch cue	2

6-6-2 Statistical analysis of the changes in pilot control behaviour

Figure 6-8 shows the statistical analysis of the average pitch rate during phase C. Surprisingly scenario 2 has a significantly ($F(1) = 7.3$, $p = 0.0082$) lower average pitch rate ($\mu = 1.48$, $\sigma = 0.341$) than the baseline scenario ($\mu = 1.65$, $\sigma = 0.291$). This could be due to a different starting time of the recovery (since the

exact speed is no longer known) or an intentionally lower pitch rate to prevent secondary stalls.
For the motion conditions, condition 3 yields a significantly ($F(1,9) = 5.7$, $p = 0.018$) lower pitch rate ($\mu = 1.5$, $\sigma = 0.375$) for the largest set of runs with respect to the baseline value ($\mu = 1.63$, $\sigma = 0.412$). Figure 6-9 shows the maximum g-load during phase C and shows only a consistent significant ($F(1,9) = 4.9$

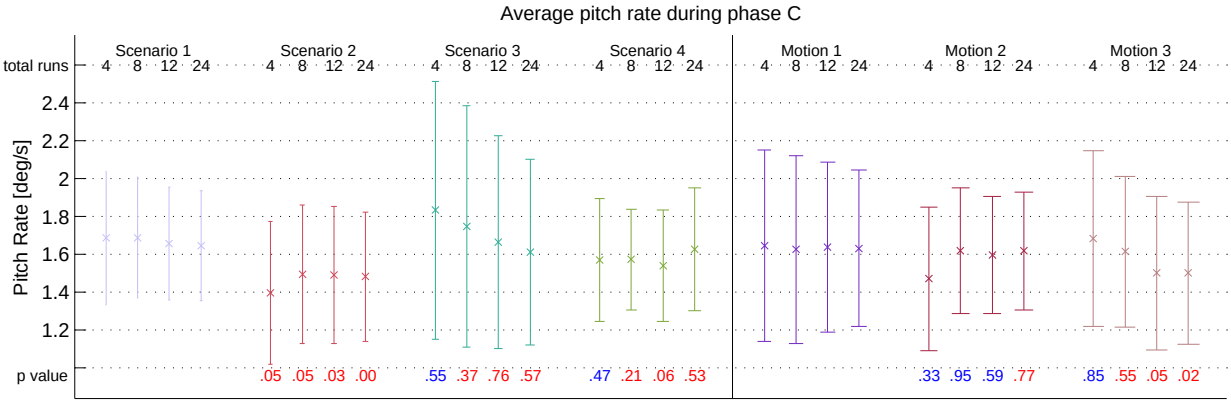

Figure 6-8: Mean and variance plot with ANOVA of the average pitch rate during phase C

$p = 0.03$) difference in scenario 3 with respect to the baseline. This increased maximum g-load is most likely caused by the lack of a precise pitch rate feedback.
Motion condition 2 shows a significantly ($F(1) = 5.1$ $p = 0.032$) higher value ($\mu = 1.88$, $\sigma = 0.157$) for the initial set of 4 stalls while motion condition 3 shows a significantly ($F(1,9) = 5.4$, $p = 0.022$) smaller value ($\mu = 1.73$, $\sigma = 0.12$) for the complete set of stalls with respect to the baseline ($\mu = 1.77$, $\sigma = 0.143$).

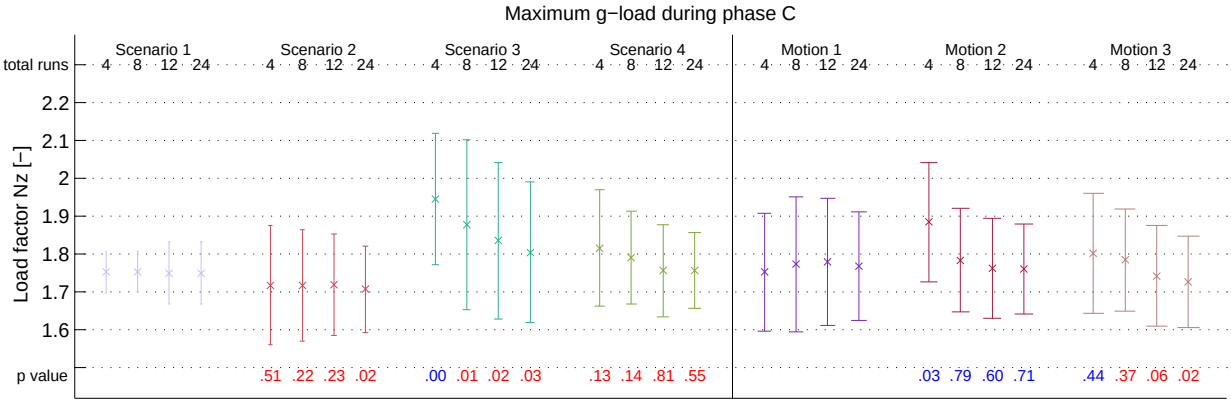

Figure 6-9: Mean and variance plot with ANOVA of the maximum g-load during phase C

6-6-3 Conclusions

In phase C the pitch ladder, but also the speed tape, appear to be an important input for the pilot. Motion condition 2 seems to have less influence, but motion condition 3 has a significant effect on the pitch rate and maximum g-load. From an operational point of view however, the actual difference in maximum load factor is very small.

6-7 Other inputs

Along with longitudinal control column input the pilots also had other control inputs like pitch trim, rudder, throttle and roll control at their disposal. The electric pitch trim switches were only used in 34% of the experiment runs and primarily used during the initial unloading phase where the deflection and thus the control force is large (see Figure 6-10). Some of the pilots, who use the trim, only make a single change in

trim position while others seemed to make constant changes.

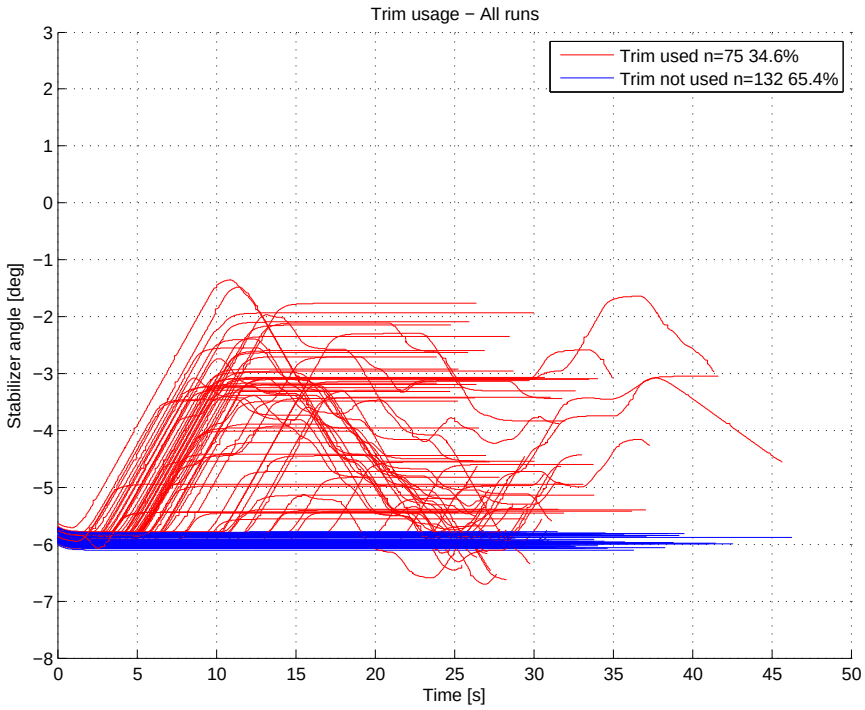

Figure 6-10: Stabilizer trim inputs through the electric pitch trim switches during all runs

As can be seen in Figure 6-11 no significant rudder inputs were given by the pilots in 99% of the experiment runs as also specified in the experiment briefing (see Appendix D).

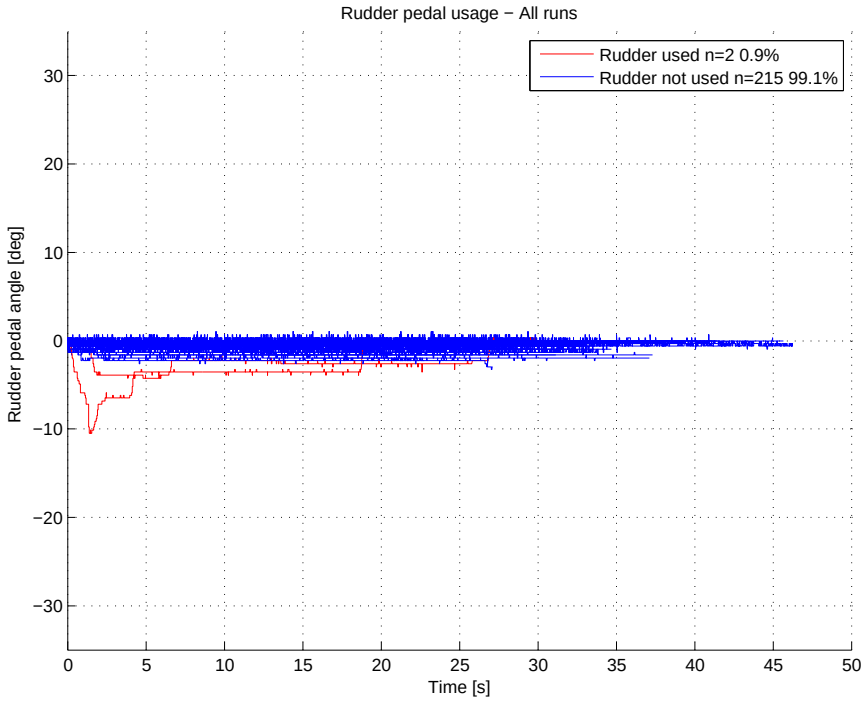

Figure 6-11: Pedals inputs during all runs

The briefing, in which it was specified to add thrust after pitching down to −20 deg, was not sufficiently clear enough and a large number of pilots added thrust too early or too late. Figure 6-12 shows the throttle

inputs for scenario 1 and the resulting average throttle input. This average of course complete neglects the rapid throttle increases by the individual pilots.

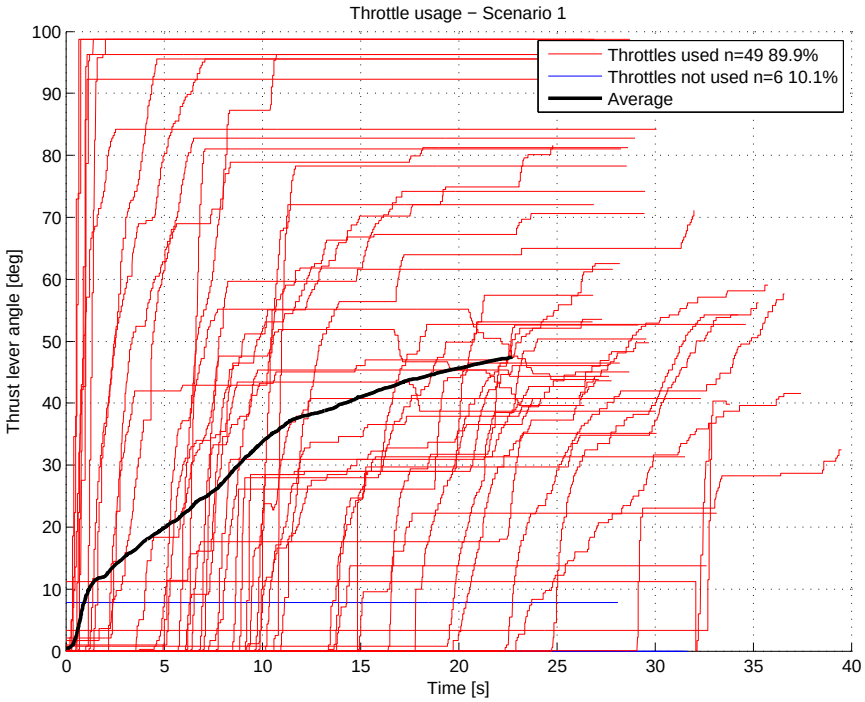

Figure 6-12: Throttle inputs during scenario 1 FL200/FL350

Roll inputs also have to be given to compensate for the roll-off component and decreased roll stability. These were largest in the FL200 condition for which the control inputs have been plotted in Figure 6-13. As can be observed, the pilot in the loop causes a underdamped response with significant control inputs.

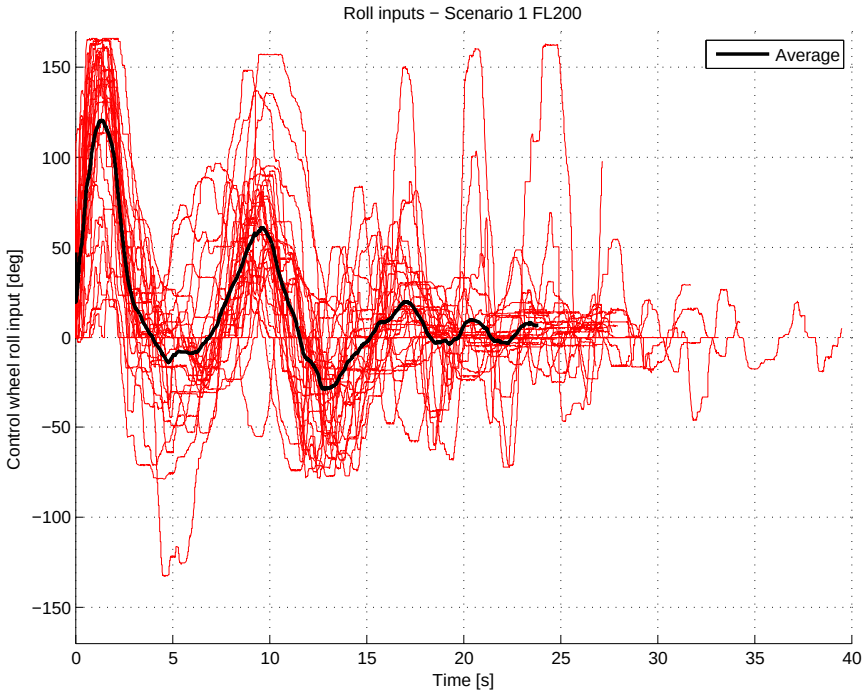

Figure 6-13: Roll inputs during scenario 1 FL200

6-8 Subjective performance scores

Besides the survey questions related to the indications and cues, the pilots were also asked during the experiment to estimate their workload, procedural conformity and accuracy. The results of this have been plotted for the different scenarios and motion conditions

6-8-1 Workload

Probably the most meaningful rating was the workload. As can be seen in Figure 6-14 for most scenarios generally a stable or slightly decreasing trend over time can be seen. Scenario 2 and scenario 3 show a slightly increased workload, but the largest difference can be seen in motion condition 3.

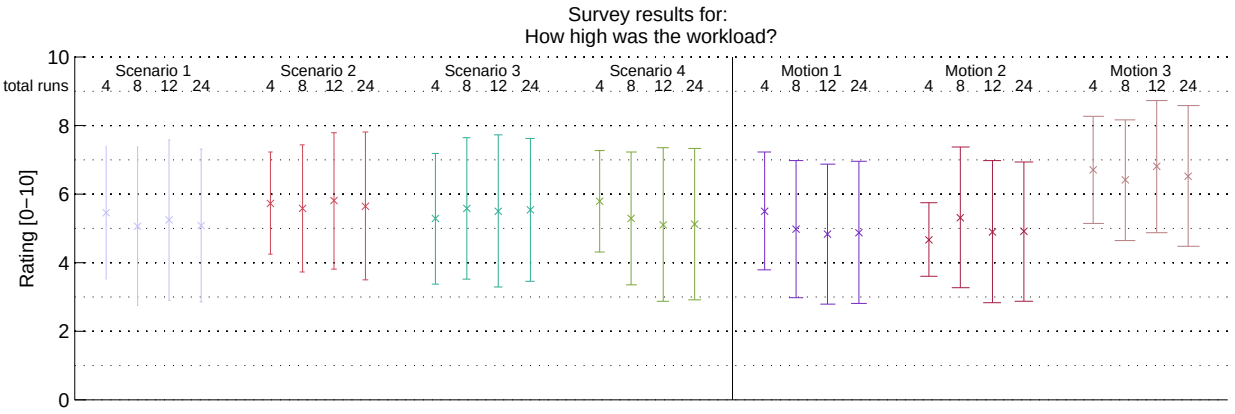

Figure 6-14: Survey results for pilot workload

6-8-2 Procedural conformity

In Figure 6-15 the subjective ratings of the pilot's adherence to the procedure is given. Scenario 2 and 3 show a distinct decrease, which follows logically from the fact the essential indications are missing. For the motion conditions only condition 3 shows a consistent difference.

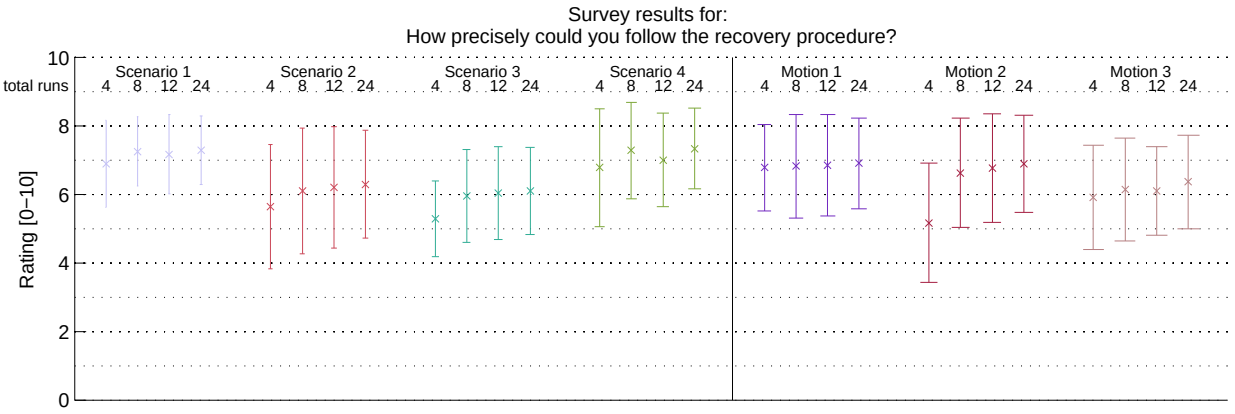

Figure 6-15: Survey results for conformity to the recovery procedure

6-8-3 Accuracy

The subjective accuracy ratings in Figure 6-16 show that the lack of a speed tape only had a relatively small effect. The lack of the pitch indication was experienced as much more obstructing. In motion condition 3 also a consistently lower rating for accuracy can be seen.

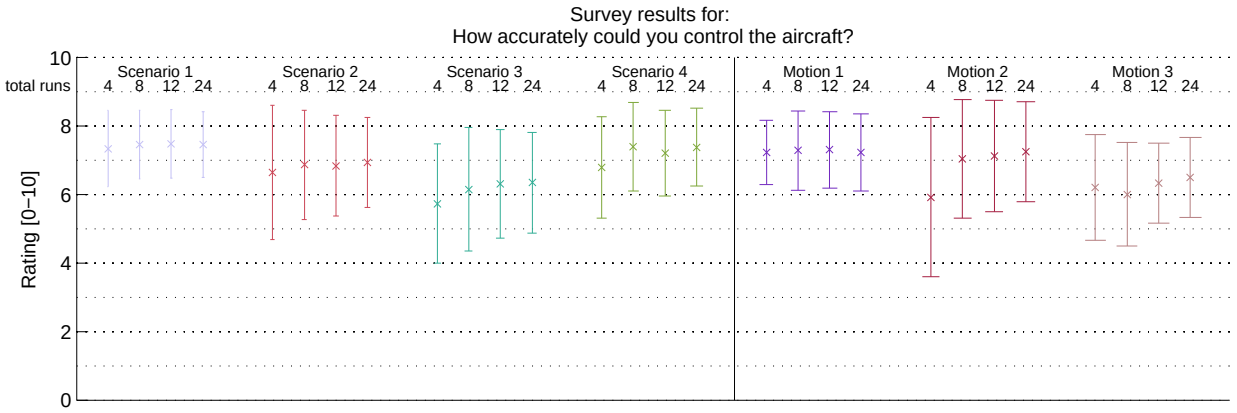

Figure 6-16: Survey results for accuracy

6-9 Realism of the simulation

To make sure that the procedure and simulation was representative of a real life scenario, the pilots were asked to name any deficiencies they experienced. The procedure was in general considered to be realistic and appropriate for the conditions.
Almost all comments were related to the false cues during motion condition 3. The centrifuge start and acceleration to the baseline g was in some cases a cause for nausea. The centrifuge slow down after the recovery with the autopiloted turn was also experienced as unpleasant by several pilots.

Finally the pilots were asked to rate the usefulness of these simulations for pilot training. This scored an average of 7.9 ($\sigma = 1.7$) out of 10.

Part III

Pilot Model

Chapter 7

Pilot Model Structure and Implementation

Based on the results from the statistical analysis of the experiment data and surveys, the preliminary pilot model (see Chapter 3) can be further refined.
First the general structure of the pilot model and the implementation is shown. This shows the majopr parts of the pilot model, which are then discussed one by one. The last section presents the Simulink implementation.

7-1 General structure

The general structure and implementation is similar to the preliminary pilot model and is shown in Figure 7-1.
The recovery procedure is contained in the *rule based control* part which provides the appropriate target values (e.g. target pitch) based on the current phase of the recovery. The *skill based control* part tries to follow these target values using the appropriate control mechanism based on the input from the *perception* part. The output from the skill based control is transmitted via the *central nervous system*, which represents any cognitive and nervous system delays, to the *neuromuscular system*. The neuromuscular system is a model of the muscle response to the target force and control column interaction from the *simulator*.

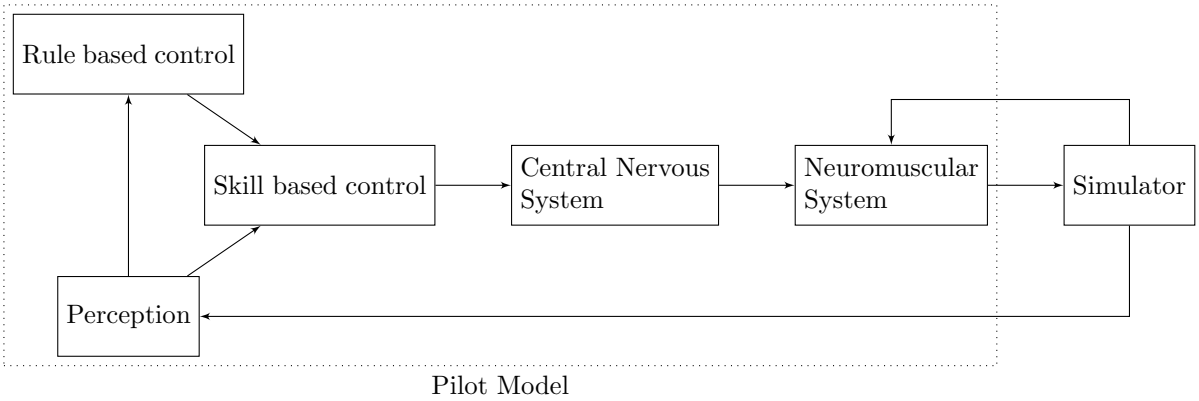

Figure 7-1: Pilot model structure and implementation

7-2 Perception and skill based control models

The perception and skill based control models are closely linked and will be considered together. The next two subsections discuss the models of these two parts for recovery phase A & B and C. Recovery phase A

and B have been combined together because of the relatively similar control task.

7-2-1 Recovery phase A & B

In control phase A and B the pilot has to do a pitching manoeuvre to −20 deg pitch attitude and track this attitude until sufficient speed is gained. The experiment results show that the pitch ladder, motion and control loading force have an effect on pilot behaviour. Thus they should be inputs for the pilot model.

The first step is to determine the basic control structure. Sub-hypothesis 1a concerns the fact whether or not this is a closed loop control task. However, it is difficult to characterize the first part of phase A because the experiment shows no significant differences for scenario 2 and 3. This is partly because the control input is saturated during a large part of this recovery phase, hiding any closed loop behaviour. It can be expected that part of the pilot response is not closed loop, especially after a large number of repetitions. In these cases a 'blind' forward control column deflection can explain the observed behaviour. However, as will be shown in the next chapter, a closed loop model can explain some of the outliers in the phase plot (Figure 6-1), by slight changes of the control gains (which can vary between people).
Using a closed loop pitch control system, the most basic model would be a simple pitch control loop. However, a single pitch control loop cannot smoothly intercept the target pitch in this model.
Another common control model is a dual-loop pitch control with pitch rate as an inner loop (Hess, 1977). Such a model can explain the observed smooth interception of the target pitch attitude and the observed variations. Figure 7-2 shows the implementation of this control model for recovery phase A and B. Steering gains K_p and K_v, respectively the pitch position and velocity gain, determine the individual behaviour of a pilot.

The selected pitch control system has two feedback values; the pitch angle and pitch rate, which are primarily observed from the PFD. These observed values are subjected to the properties of the human perceptual system which has been modelled by the central visual perception transfer functions $H_{c,att}$ and $H_{c,rate}$. The transfer functions used for this are:

$$H_{c,att} = e^{-\tau+j\omega} \tag{7-1}$$

$$H_{c,rate} = e^{-(\tau+\tau_c)+j\omega} \tag{7-2}$$

where $\tau = 0.05\,\text{s}$ and $\tau_c = 0.1\,\text{s}$ (Hosman, 1996). The outside view, and related peripheral vision is not included in the pilot model. None of the pilots listed the outside view as an indication they used during the experiment. Also observation of the pilots during the experiment showed them to be only looking at the PFD. Any peripheral input from the outside visual is most likely minimal in this situation.

The experiment results show that motion condition 2 causes small differences in pilot behaviour, and motion condition 3 causes larger differences in pilot behaviour. The most likely source of this is vestibular feedback through either the otoliths or the semi-circular canals. The otoliths can (indirectly) provide information about linear acceleration, linear velocity through internal integration, or the direction of the specific force. There is no large sustained linear acceleration cue or sustained linear velocity cue in phase A and B. There is a change in specific force direction, especially in the third motion condition, which should be included.
The semi-circular canals will provide feedback on the change in pitch rate through their sensitivity for rotational acceleration. The transfer functions used for the otoliths and semi-circular canals are:

$$H_{scc} = \frac{(1+j\omega\tau_L)}{(1+j\omega\tau_1)(1+j\omega\tau_2)} \tag{7-3}$$

$$H_{oto} = \frac{1+\tau_n s}{1+\tau_{o1} s} \tag{7-4}$$

where $\tau_1 = 5.9\,\text{s}$, $\tau_2 = 0.005\,\text{s}$ (Hosman, 1996), $\tau_n = 0.3\,\text{s}$ and $\tau_{o1} = 0.12\,\text{s}$ (Grant & Schroeder, 2010). The adaptation term for the semi-circular canals $((\tau_a s)\,(\tau_a s+1)^{-1}$, $\tau_a = 30\,\text{s})$ has not been included because the pitch accelerations are of a relatively high frequency (Grant & Schroeder, 2010). The resulting outputs are added directly to the compensation output, similar to the structural and descriptive pilot models.

Another possible input for the pitch control is the speed tape and more specifically the top of the barber pole. The barber pole (v_{ss}) is a highly dynamic quantity and a strong indication to decrease the pitch or pitch rate. The available speed margin to the top of the barber pole has been defined as $v_{margin} = v_{CAS} - v_{ss}$.

It has a range from −45 kt to 45 kt since this is the visible range on the speed tape.

In phase A the barber pole is not visible, but it will come back into view during phase B. Generally pilots kept a certain margin from the barber pole, defined as C_{spd}. A possible feedback loop to take this into account has been added and is visible at the top in Figure 7-2. Using a saturation this loop is only active when the v_{margin} drops below C_{spd}.

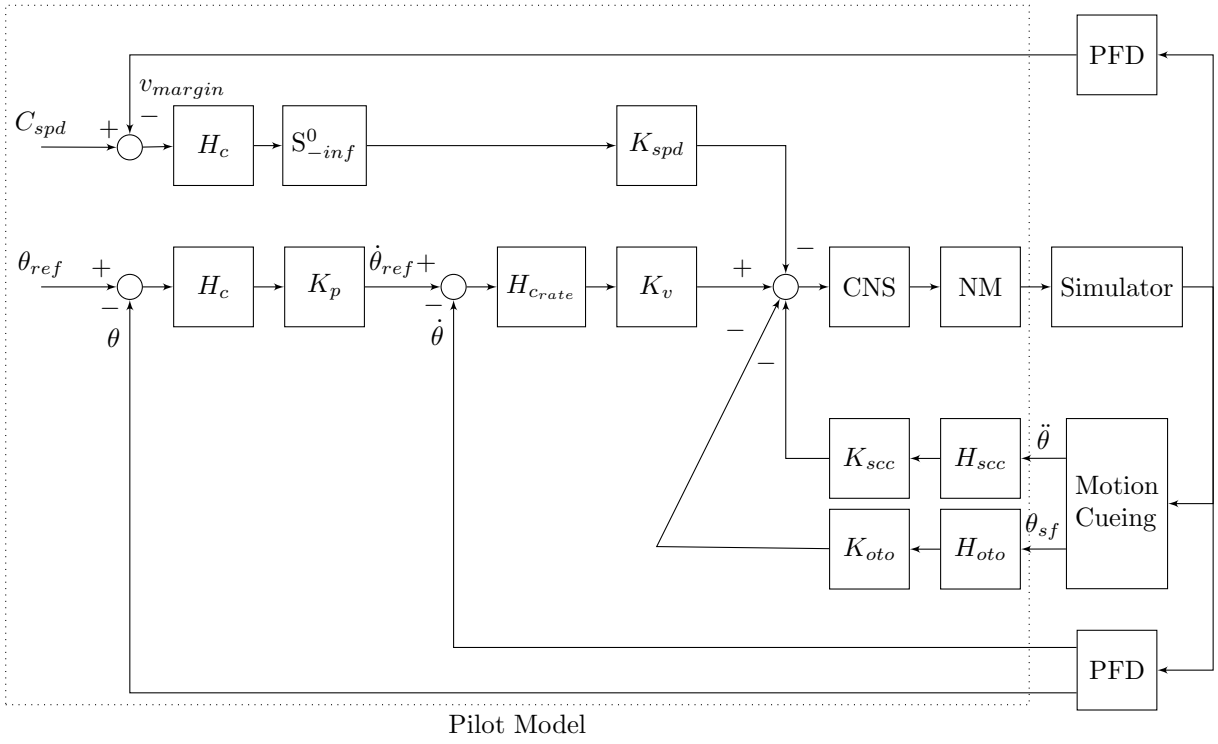

Figure 7-2: Simplified control structure during phase A & B (CNS = Central Nervous System, NM = Neuro-muscular System)

7-2-2 Recovery phase C

The control task in phase C is different from the previous two phases and requires pilots to maintain a pitch rate of approximately 2 deg/s, without exceeding the maximum load factor or causing a secondary stall. The relatively constant pitch rate seen in the phase plot and the changing control inputs suggest a closed loop control mechanism. Since the pilot only has to control pitch rate and is not concerned with the pitch angle, the control structure from the previous control phases is slightly modified (see Figure 7-3).

From the experiment results it was concluded that the speed tape has a significant effect on the control behaviour. This is again most likely caused by the barber pole represented by the feedback from v_{margin}.

The experiment results also showed a significant change in phase C for motion condition 2, most likely similar to phase A & B. Additionally the g-load has also become an important input. It has not been modelled as a boundary condition, because the 2.5 g limit was not approached by the pilots. The observed average maximum g-load of $\sim$ 1.8 g is more likely a results of the airspeeds and specified pitch rate for the recovery. Instead it is modelled as a negative feedback, similar to the other motion inputs. Since g-load is mainly sensed by the otoliths the transfer function for the otoliths, H_{oto}, is used.

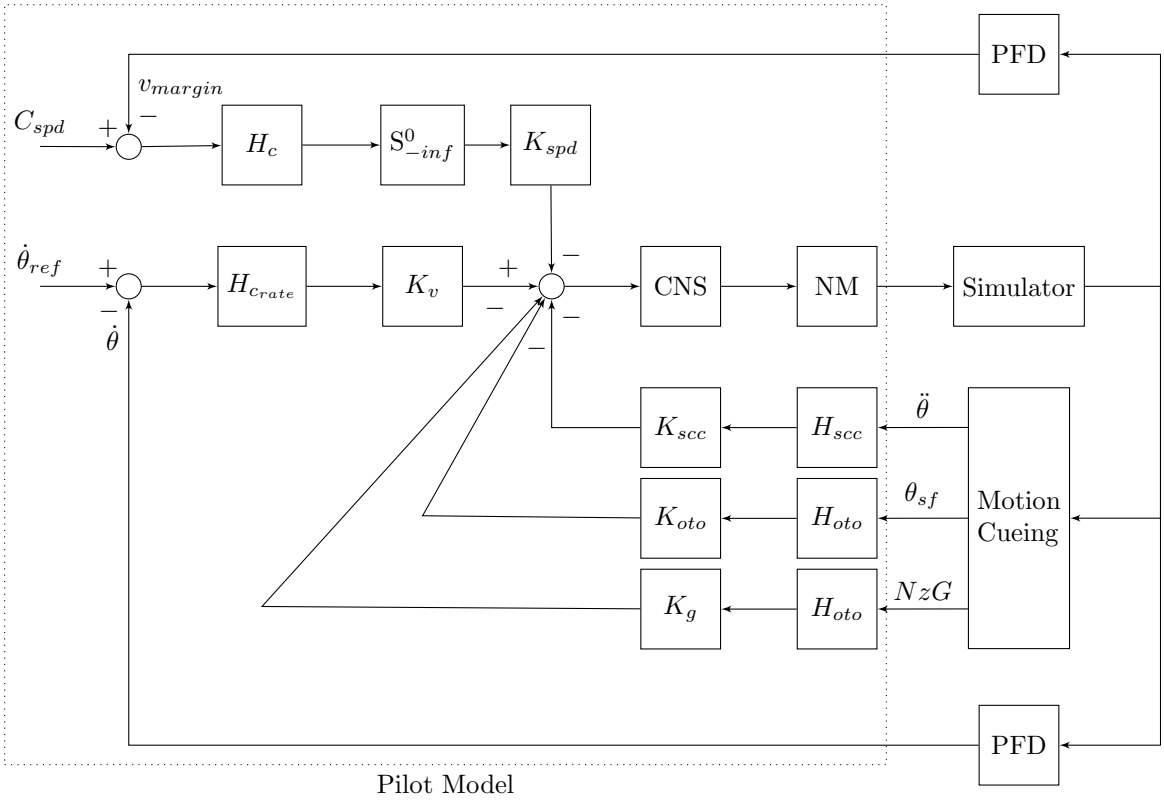

Figure 7-3: Simplified control structure during phase C (CNS = Central Nervous System, NM = Neuromuscular System)

7-3 Central nervous system

The central nervous system part of the model contains a time delay as a representation of the cognitive decision delays and nervous system delays. The transfer function used for this is:

$$H_{c,att} = e^{-\tau_{CNS}s} \tag{7-5}$$

and τ_{cns} was selected to be 0.08 s based on the work by Hosman (Grant & Schroeder, 2010).

7-4 Neuromuscular system

The output from the skill based control part has to be translated into a change in arm position or muscle force. This can be modelled as either position based control with force feedback, or force based control with position feedback. Because the results from Chapter 6 show a clear difference when the control force is slightly changed, a force based interaction was chosen. The position feedback is ignored (except for the range limits), because the change in force over time is relatively small and the pitch control is sufficiently dampened.

An important property of the stall scenarios is that the aircraft is not trimmed and that the trim position is constantly changing as there are large changes in airspeed, loading, thrust, and pitch. This means that the pilots have to steer by smoothly changing the input and verifying the effect. This is best represented in a linear model by an integrator where the input is a change in force and the output is the steady muscle force. Figure 7-4 shows the implementation of this.

The input to the integrator is limited when the control column reaches the end of the range (which is easily noticed by the pilots). This also prevents any unrealistic integrator wind up and associated issues.

The neuromuscular dynamics have been modelled as:

$$H_{nm} = \frac{\omega_{nm}^2}{s^2 + 2\zeta_{nm}\omega_{nm}s + \omega_{nm}^2} \tag{7-6}$$

which is a second order low pass filter where $\zeta_{nm} = 0.7$ and $\omega_{nm} = 10\,\text{rad/s}$ (Hess, 1997b).

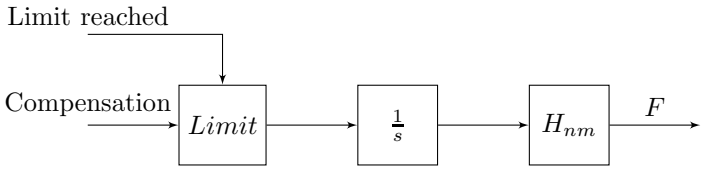

Figure 7-4: Neuromuscular part of the pilot model containing a force integrator and limit

7-5 Implementation

To evaluate and fit the proposed pilot model an accurate implementation of the other parts of the simulation is required. The most important interaction between the software and the pilot is the control column which will first be discussed. Other inputs like roll, rudder and throttles also have to be modelled since they will directly and indirectly affect pitch behaviour. Finally this all is combined into a single Simulink computer simulation.

7-5-1 Control column model

The control column is modelled as a point mass with 1 degree of freedom. It is assumed to have a linear displacement and a static and kinetic friction. The general structure of the control column model is shown in Figure 7-5. The total representative point mass of the control column at actuator level, m_{cc}, is estimated to be 12kg based on some rough measurements. The output is limited between -0.1m and 0.1m, approximately the linear range of the actuator. When these hard limits are reached, the velocity is forced to zero. The friction is modelled as a static and kinetic friction using the following equation:

$$F = \mu_c F_n = \mu_c m|n| \tag{7-7}$$

and is assumed to come only from the actuator. The static break out force (stiction) was measured to range between 10 N and 15 N. Based on the measured actuator weight of 6.0 kg this corresponds to a static friction coefficient, μ_s, of 0.17 to 0.25. This is within the expected range for the dry steel on plastic sliding surface of the actuator (Beardmore, 2013). For the model a static friction of 0.25 and a kinetic friction, μ_k, of 0.15 will be used.
In motion condition 3 the friction force will vary since the actual g-load is no longer constant. This is implemented as a scaling of the friction force with the g-load from the motion cueing (for this the cabin pitch is assumed to be perpendicular to the direction of the N_zG component).

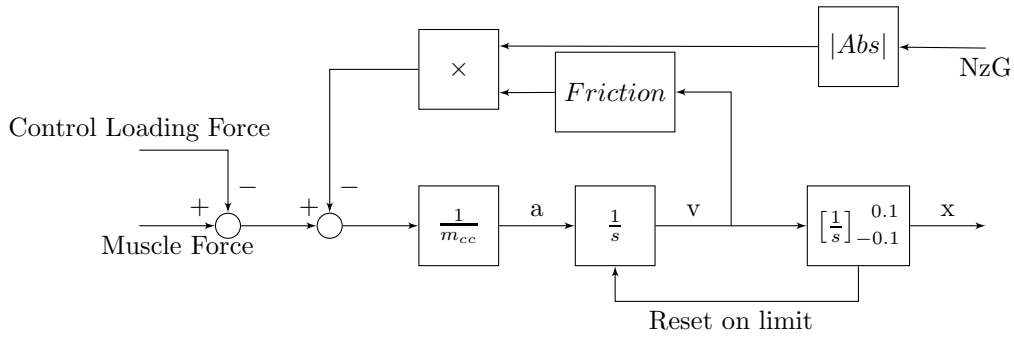

Figure 7-5: Control column model as a mass with 1 degree of freedom and a static and kinetic friction depending NzG

7-5-2 Other control inputs

Besides the longitudinal control column movement, the pilot has other controls at his disposal during the experiment. Although these are not of primary interest, they have to be modelled to compare the simulation results.

The pilot model assumes that trim is not used since the experiment results show that only 34% used the trim buttons to change the stabilizer position during the recovery.

The experiment results showed a wide variation in throttle application rate and timing. It is not possible to include this variation in a linear model. To include the average effect of the pitch up moment the throttles have been modelled as a linearly increasing throttle lever position based on the average value from Figure 6-12. Chapter 9 will further explore the effect of a variation in throttle application on the resulting pilot control behaviour.

To accurately simulate the moment of disconnecting the autopilot the average delay between the start of the sound message and disengagement of the autopilot was determined to have a mean of 0.74s ($\sigma = 0.19$ s), and is implemented as such.

Roll

Although the roll component for the selected stalls is relatively small, it requires large control inputs (see Figure 6-13) due to the low aileron effectiveness in the recovery. It was also noticed that the resulting behaviour was poorly damped.
A comparison of the average roll angle and the average roll control inputs shows limited correlation. This shows that a simple roll angle control loop can not be sufficient for explaining the roll behaviour. A more likely control structure would be a dual-loop roll control structure with roll rate as the inner loop. This structure has also been used in other pilot models for roll control.
The implementation for the control of the roll axis is basically similar to the pitch axis but with some simplifications. Roll rate and roll angle perception through motion is ignored for the sake of simplicity and because no roll cues are available in motion condition 1 and 3 (except during the initial stall entry). The control wheel is modelled as a mass with 1 degree-of-freedom at the rotation axis. The friction was too low to be accurately measured with the available tools, but the friction coefficient has been matched to provide a similar (underdamped) response to step torque inputs. The simplified structure of the resulting model for the roll control axis is shown in Figure 7-6.

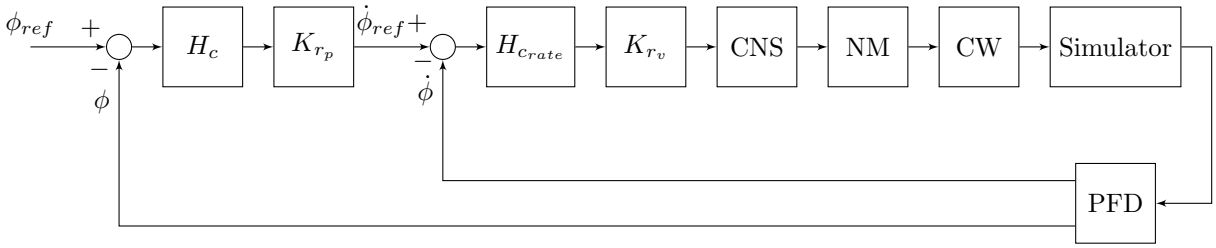

Figure 7-6: Simplified control structure for the roll control axis (CNS = Central Nervous System, NM = Neuromuscular System, CW = Control Wheel)

7-5-3 Simulator delays

As in every simulation there is a delay between the pilot inputs and the simulator outputs (e.g. motion system, displays, sound, control loading). The main sources of delay are the displays, motion system, model time step size and network connections.
The network round trip time was measured to be in the order of milliseconds and is not a significant source of delay. The display refresh rate for the visuals is 60 hz. The motion delay was estimated at roughly 100 ms based on accelerometer data.
Based on these measurements a time delay of 20 ms has been selected for the visual systems and 100 ms for the motion system. The delay in the sound system was not measured, but the total pilot model response delay was matched to the measured mean total delay.

7-5-4 Simulink model

To apply and fit this pilot model to the experiment runs it has been implemented in a Simulink model. This model contains the complete pilot model as well as a simulation of the control column, control loading,

aircraft model, motion cueing, and delays. For the aircraft model, control loading and motion cueing, the original Simulink models have been used.
The general structure of the Simulink model is shown in Figure 7-7 and is similar to the structure originally shown in 7-1. An image of the top level Simulink model is included in Appendix G.

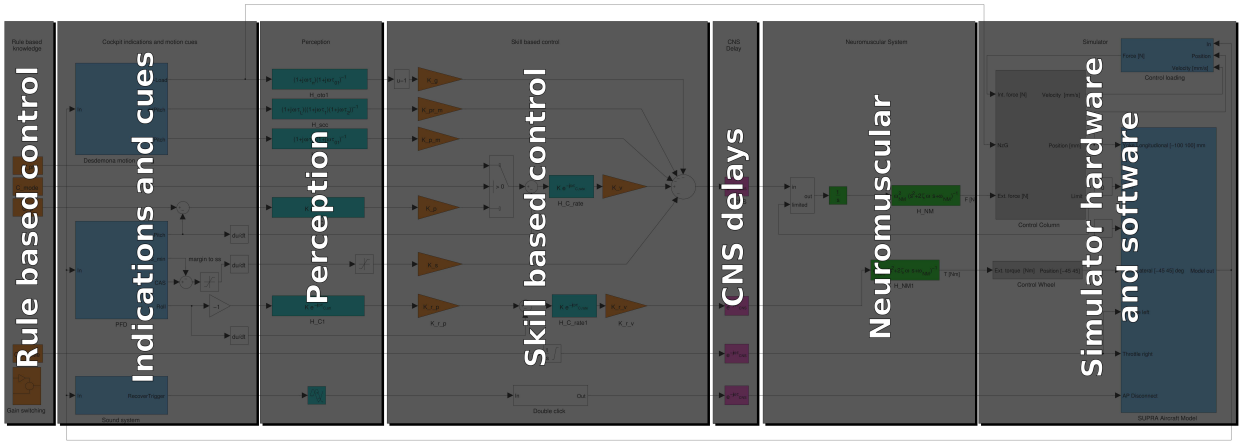

Figure 7-7: Overview of the Simulink pilot model implementation structure

During the experiment a first order Euler solver with a step size of 0.005 s was used for both the aircraft model and motion cueing. For the control loading and physical models of the control column ideally a smaller step size and higher order solver should be used (because of the relatively stiff equations). However Simulink did not allow mixing sample times, because of the hybrid states in the model. In addition this would have increased the execution time too much. Therefor the models of the control column, control loading and control wheel have been manually checked for stability in combination with the selected solver and time step.

Chapter 8

Pilot Model Fitting

Now that the structure of the pilot model has been selected, the appropriate control gains can be determined. These variable gains represent the adaptation of the human controller to the specific control task. The exact values for the gains depend on the specific performance objective the pilot is attempting to fulfill. This can range from for example minimizing control inputs (changes) to minimizing the control target error.
As discussed in Section 3-3 the selection of the representative control gains is done using an iterative fitting process attempting to fit the pilot model output on the experiment data. First the fitting method, its properties and assumptions will be described. Next, the model will be fitted for the different recovery phases of the no motion condition. The results are then used to consider the effects of the simulated motion conditions in the pilot model.

8-1 Fitting procedure

The fitting of the model is based on a generic procedure to provide objective and reproducible results.

8-1-1 Quality of the fit

To assess the quality of the model fit, the results from the pilot model and the experiment runs have to be compared. The focus will be on the time domain responses of the main control variables. However, the experiment data shows noticeable differences between experiment runs (of the same pilot and between the pilots). Also there is no indication that the control behaviour after the multiple repetitions converges to a single representative control strategy. This consistent difference is most likely caused by differences between individuals, perceptual noise, neuromuscular noise, and variations in cognitive processes. These influences are not modelled and because of this the average of the experiment responses will be used for the comparison. The downside of this approach is that the resulting average time response is excessively smooth and possibly not fully reproducible.

For the actual comparison three specific variables seem most relevant: control inputs, pitch angle and pitch rate. The control inputs are not very ideal due to the fact that they are highly correlated with time-local and individual disturbances. In contrast, the pitch and pitch rate can be considered a filtered result of the model input and should converge back to specific values as specified by the recovery procedure. For phase A & B the control task specifies the pitch angle as the controlled variable. In phase C this is primarily the pitch rate. Since pitch is the integral of the pitch rate it is the best parameter to compare the complete recovery.
For the average of the experiment runs all relevant runs will be used. The average will be compared with the pilot model output using the Mean Squared Error (MSE) of the pitch angle. Since the roll channel is only lightly coupled with the pitch channel, the roll behaviour will be independently optimized with respect to the average roll angle.
The lengths of the recovery phases are not fixed in time but are different between the experiment runs. Because of this the experiment average (and the comparison) is limited to the shortest experiment run.

8-1-2 Iterative fitting method

To optimize the model for a minimal MSE a method for optimizing the gains has to be selected. Since the properties of the recovery manoeuvre and the aircraft model make an analytical solution of this problem impractical, a nonlinear unconstrained optimization of the gains is done. This is performed using the MATLAB `fminsearch` function. This function attempts to optimize a function output by non-linearly varying the input variable(s). It starts at specified initial value(s) and will vary the input variables in small steps (increasing and decreasing the step size as appropriate) as to minimize the output. This method of course assumes a smooth variable space with no local minimums.
However, there is no guarantee that the output of the pilot model optimization complies with these assumptions. To make sure the true minimum is found several precautions have been taken: logical initial values will be used, the actual MSE will be checked to ensure a good fit and a surface plot of the MSE for the relevant gain space will be shown. For use with the `fminsearch` function the gains will be normalized to a value with a zero order of magnitude, because `fminsearch` uses absolute values. The optimization limits are set to a minimum function value and minimum stepsize of 0.1.

The pilot model is fitted for the two different stall conditions, FL200 and FL350. As hypothesized in Section 4-2-5 the control gains are expected to be similar, since the control task and conditions are the same. This will serve as an additional verification that the fit is not dependant on a coincidental fit.

The complete model fit is done in two steps. First the pilot model for phase A & B will be fitted to determine pitch and roll gains during these recovery phases. Because phase C has a different control strategy it is analyzed independently.
Although `fminsearch` can be used to optimize functions with multiple inputs a large number of inputs severely limits the performance and increases the likelihood of ending up in a local minimum. Therefore the optimization has been split up in several steps optimizing at most two different control gains at the same time (see Figure 8-1). The first step is to determine the initial values for the gains to make sure that the model is somewhat stable. Next the pitch and roll channels are independently optimized for a best fit. Depending on the control phase the appropriate gain for the speed tape effect is also determined. Finally, when relevant, the motion channels can be optimized for a best fit. Because these different sets of gains are (lightly) coupled these optimizations have to be repeated until the pitch angle and roll angle MSEs have become stable.

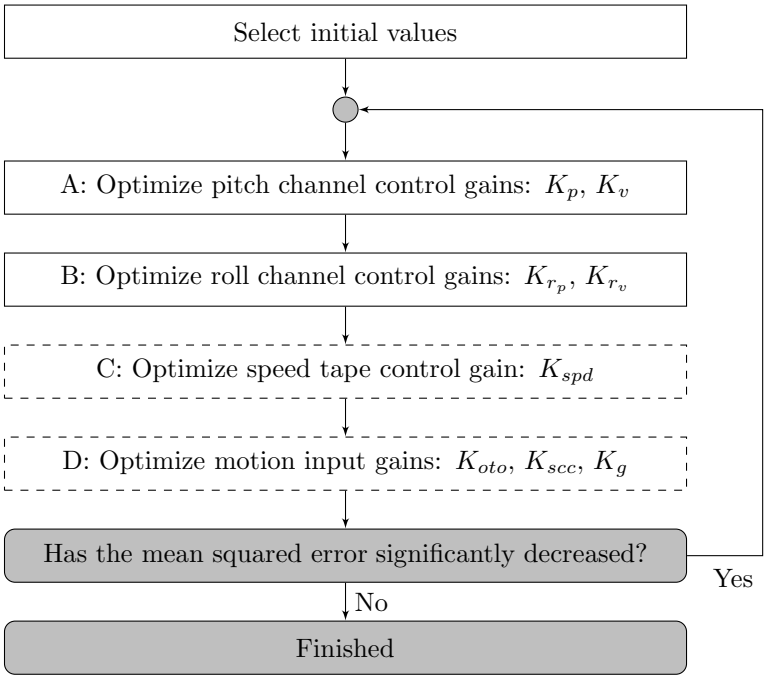

Figure 8-1: Iterative fitting procedure for the different sets of control gains

8-1-3 Initial values

Selecting good initial values will decrease the computation time necessary for the optimization of the gains and decrease the chance of hitting a local minimum. By visual inspection of the experiment data for the pitch and roll axes, with respect to the control inputs, a rough estimate of the pitch and roll channel control gains can be made.

The pitch channel shows a pitch rate of $\sim 12\,\text{deg/s}$ when the pitch error is $\sim 40\,\text{deg}$ suggesting $K_p = 0.3$ (stall condition FL200). Based on the required control loading force and average initial control position ramp up, K_v was selected to be 500.
Similarly for the roll channel the initial values were selected to be $K_{r_p} = 0.6$ and $K_{r_v} = 15$.

8-2 Pitch control channel

The control gains for the pitch channel will first be fitted for recovery phase A & B. The resulting K_v gain will be used as an initial value for recovery phase C.

8-2-1 Recovery phase A & B

The fit for recovery phase A & B was first done for the FL200 stall condition. The speed tape, or more precisely the barber pole control gain, has not been fitted because it is not visible during (most of) this recovery phase. This leaves only the roll and pitch control gains which gave a stable minimum after two iterations (see Table 8-1(a)) with a MSE of $2.13\,\text{deg}^2$.
The resulting pitch manoeuvre has been plotted in Figure 8-2(a) showing a good fit between the average of the experiment runs, the individual experiment runs and the pilot model. The largest error is around 12 s where most pilots seem to overshoot the target pitch. A surface plot of the pitch gains (see Figure 8-3(a)) shows the effects of a -50% +100% variation in the gains to verify that the result is indeed the true optimum.

For the second stall condition, FL350, it was expected that the control gains would be similar. Therefore the gains found in the FL200 condition were used as an initial value (see Table 8-1(b)). This gives a good initial match with a MSE of $3.03\,\text{deg}^2$. After two iterations this error has decreased to $1.30\,\text{deg}^2$ by a small change largely in K_v. The resulting pitch output of the pilot model is shown in Figure 8-2(b) and the effect of variations in the pitch gains is shown in the surface plot in Figure 8-3(b).

Table 8-1: Iterative fitting results for the control gains of phase AB in motion condition 1. Actively optimized values are underlined.

(a) FL200, scenario 1, motion condition 1

	Gains					MSE	
Iteration	$K_p[-]$	$K_v[-]$	$K_{r_p}[-]$	$K_{r_v}[-]$	**Func. Eval.**	**Pitch** $[deg^2]$	**Roll** $[deg^2]$
Initial	0.3	500	0.6	15	-	14.7	48.7
I-A	<u>0.255</u>	<u>887</u>	0.6	15	42	<u>2.42</u>	50.2
I-B	0.255	887	<u>0.281</u>	<u>33.3</u>	48	2.15	<u>3.10</u>
II-A	<u>0.253</u>	<u>905</u>	0.281	33.3	19	<u>2.13</u>	3.11
II-B	0.253	905	<u>0.281</u>	<u>33.3</u>	10	2.13	<u>3.11</u>

(b) FL350, scenario 1, motion condition 1

	Gains					MSE	
Iteration	$K_p[-]$	$K_v[-]$	$K_{r_p}[-]$	$K_{r_v}[-]$	**Func. Eval.**	**Pitch** $[deg^2]$	**Roll** $[deg^2]$
Initial	0.253	905	0.281	33.3	-	3.04	3.53
I-A	<u>0.255</u>	<u>1100</u>	0.281	33.3	32	<u>1.31</u>	3.74
I-B	0.255	1100	<u>0.434</u>	<u>25.3</u>	33	1.31	<u>1.59</u>
II-A	<u>0.255</u>	<u>1100</u>	0.434	25.3	8	<u>1.30</u>	1.57
II-B	0.255	1100	<u>0.434</u>	<u>25.3</u>	12	1.30	<u>1.57</u>

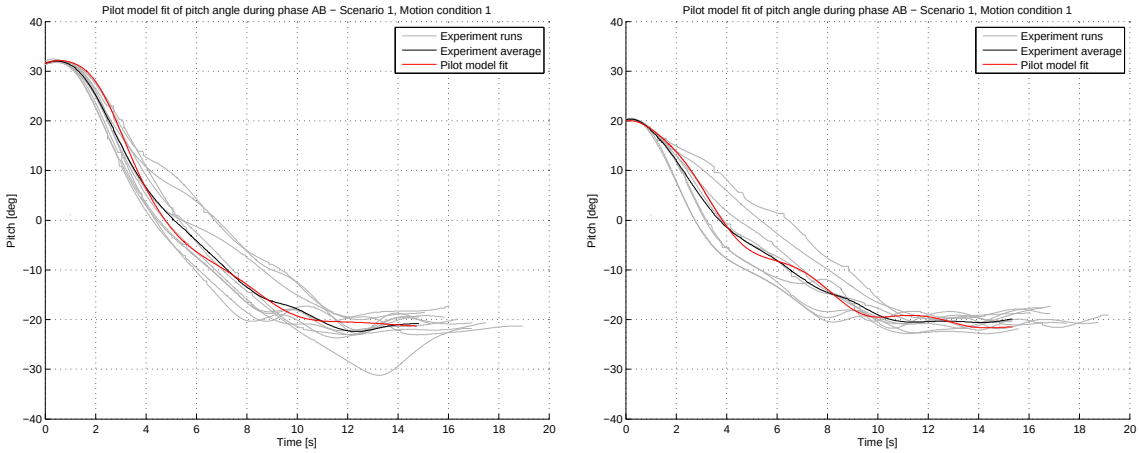

(a) FL200 (b) FL350

Figure 8-2: Pitch angle plot with final pilot model fit, no motion

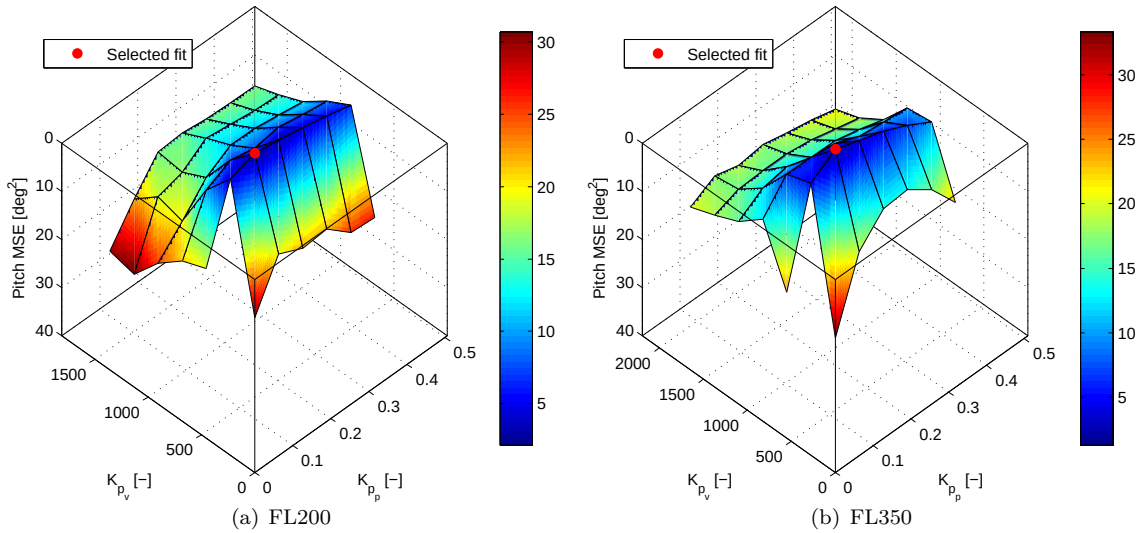

(a) FL200 (b) FL350

Figure 8-3: Surface plot of the MSE with -50% +100% variation in pitch channel control gains

8-2-2 Recovery phase C

For phase C only the speed tape and pitch rate control gains have to be fitted. Assuming that the pitch rate control gain does not change an initial comparison of the stall scenarios has been done. This gives a MSE of 4.62 deg^2 and 1.50 deg^2 for respectively the FL200 and FL350 stall condition (see Table 8-2). This is already a reasonably good fit and the resulting pitch plot is shown in Figure 8-4(a)). Visual inspection learns that the error is mainly caused by an offset in time.

This offset in time can have multiple causes. The average speed of the experiment data is slightly higher causing an earlier recovery. Also some pilots started the recovery earlier than the recovery procedure specified. Another factor might be pilots anticipating the top of the amber band, which is not modelled by the pilot model.

Attempting to improve the fit by optimizing the control gains would most likely result in incorrect results. It is reasonable to expect the control gains in phase A & B to be similar to phase C and the time difference can most likely be explained by other causes.

Table 8-2: Iterative fitting results for the control gains of phase C in motion condition 1. Actively optimized values are underlined.

(a) FL200, scenario 1, motion condition 1

	Gains					MSE	
Iteration	$K_p[-]$	$K_v[-]$	$K_{r_p}[-]$	$K_{r_v}[-]$	**Func. Eval.**	**Pitch** $[deg^2]$	**Roll** $[deg^2]$
Initial	0.253	905	0.281	33.3	-	4.63	2.81

(b) FL350, scenario 1, motion condition 1

	Gains					MSE	
Iteration	$K_p[-]$	$K_v[-]$	$K_{r_p}[-]$	$K_{r_v}[-]$	**Func. Eval.**	**Pitch** $[deg^2]$	**Roll** $[deg^2]$
Initial	0.255	1100	0.434	25.3	-	1.50	1.20

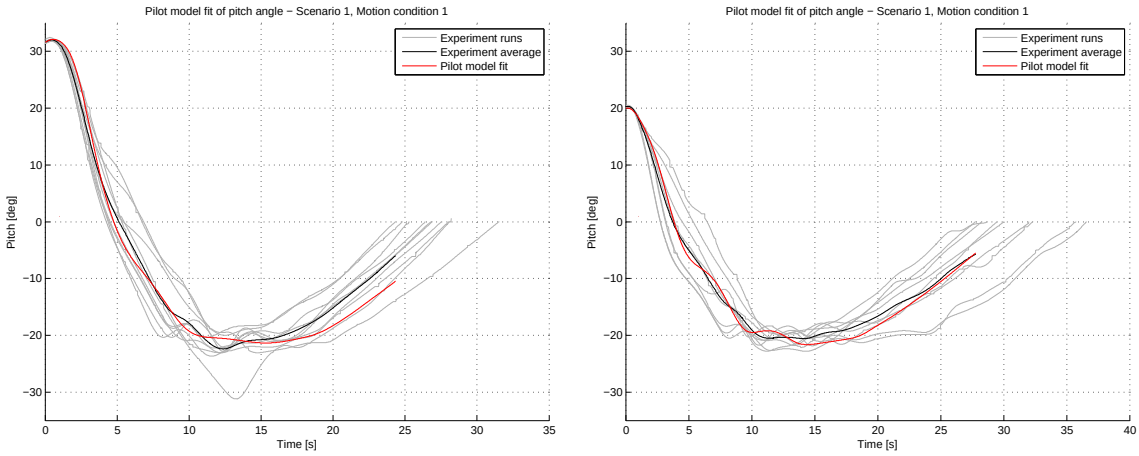

(a) FL200 (b) FL350

Figure 8-4: Pitch angle plot with final pilot model fit, no motion

Speed tape

In the pilot surveys the speed tape was found to be an important indication during the last phase of the recovery. In Figure 8-5 the visible margin between the CAS and stickshaker speed is shown. The experiment data shows that this margin is highly dynamic. This is because it is very sensitive to variations in g-load caused by small changes in pitch rate.
Without using the speed tape as an additional input the speed margin in the pilot model is already within the observed range from the experiment data. Unfortunately the experiment data does not suggest a generic minimal margin all pilots are maintaining, although an overall minimum of 10 kt can be observed. This is however not enough information for a successful optimization of the pilot model input. When the procedure is followed this limit is never reached during the recovery.

8-2-3 Effect of control loading

To test the effect and implementation of the control loading in the pilot model, scenario 4 is used. It is assumed that the change in control forces is small enough that no significant adaptation occurs and that the pilot control gains are constant. Based on this assumption the effect on the pilot model should be the same as has been recorded in the experiment data. To verify this the pilot model and experiment data for scenario 1 and 4 have been plotted in Figure 8-2-3. As observed in the statistical analysis, the decreased control loading force during phase A in scenario 4 diminishes the unloading slightly. A consistent larger difference is visible around the intercept of the target attitude of −20 deg pitch. The difference in phase B and C is relatively small.
The pilot model shows a similar change in phase A but lacks the distinct change at the intercept of 20 deg. Also there is a consistent offset during phase B which is not visible in the experiment data. This could suggest that the pilot adapts his internal control gains to compensate for the change in control force.

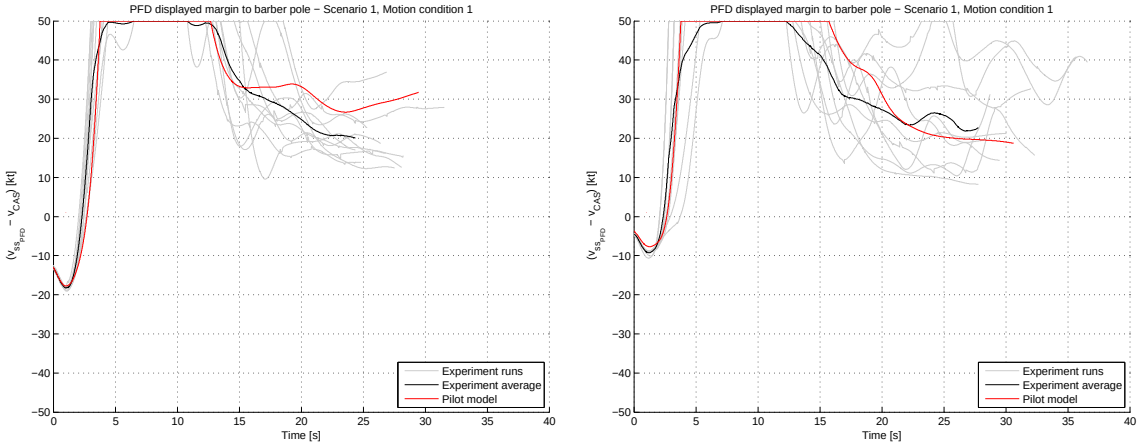

(a) FL200 (b) FL350

Figure 8-5: Speed margin to the barber pole as displayed on the PFD

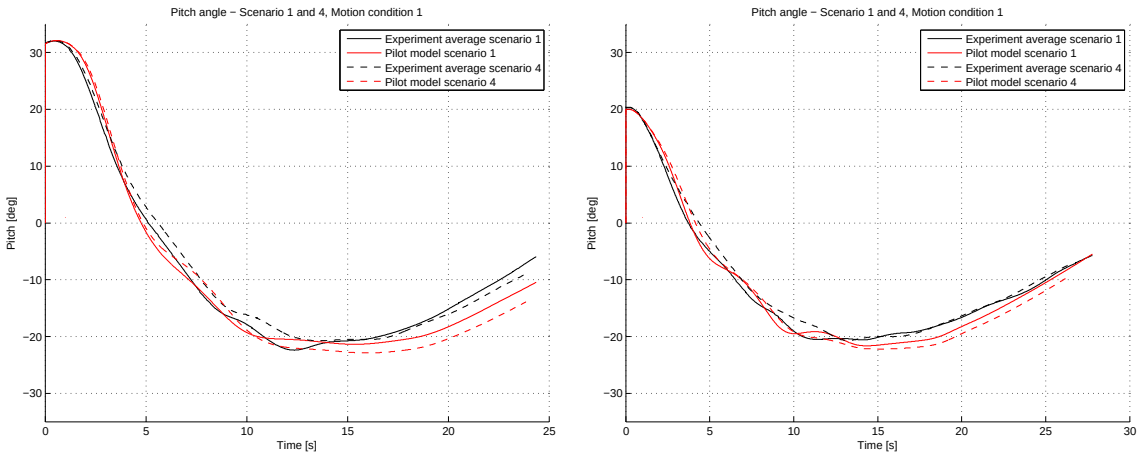

(a) FL200 (b) FL350

Figure 8-6: Pitch angle plot comparing scenario 1 and 4

8-2-4 Control inputs

The resulting control inputs from the control gain optimization are shown in Figure 8-7. In general the pilot model control inputs are similar to the experiment data but much more stable. Additionally the pilot model control input is generally a smooth variation in position, whereas the experiment data shows a step like profile.
The increased stability can be partially explained by the use of the more smooth experiment average for the model fit. The static friction in the control column can apparently not explain the discrete (stepped) behaviour and the pilot model has no other non-linear parts. An explanation would be the QINETIQ model as used by Hosman et al. (2009).

8-3 Roll control channel

The control gains for the roll channel were optimized simultaneously with the pitch channel. The resulting gains and MSE of the roll angle are provided in Tables 8-1 and 8-2.
The resulting roll angle during phase A & B is shown in Figure 8-8. In the FL350 stall condition almost all participants immediately compensate for the roll offset, but in general start a roll oscillation. In the FL200 stall condition a similar response from the participants can be observed, but 3 outliers show a delayed reaction in rolling the aircraft level. A possible explanation is that the participants waited until the stall was completely broken. It is even possible that the bank angle was kept in on purpose as to assist in the

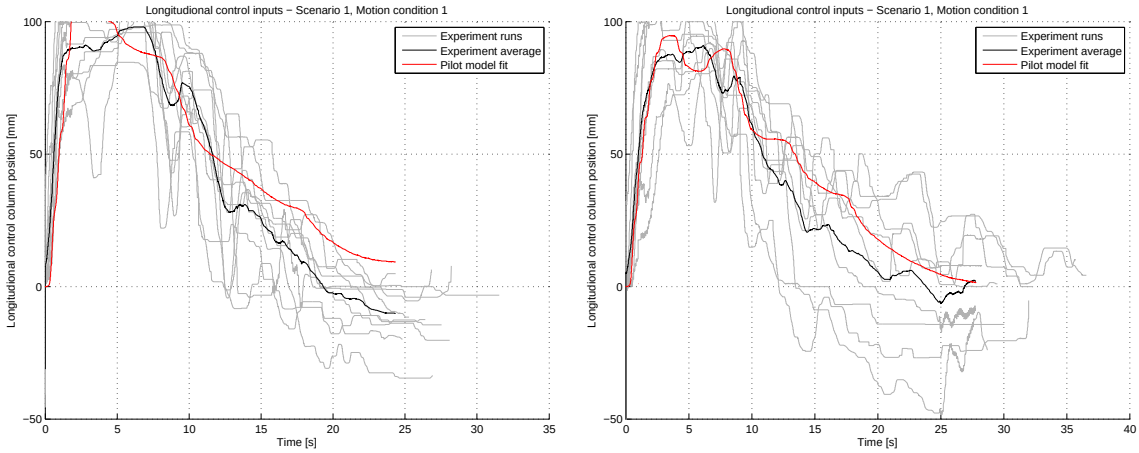

(a) FL200 (b) FL350

Figure 8-7: Longitudinal control column inputs

pitch down maneuver as described in some recovery techniques (Boeing Company, 1998). The experiment procedure did not specify the method of levelling the wings and thus allowed for this difference in recovery.

The pilot model fit for the FL350 stall condition was a relatively good with a MSE of 1.57 deg^2, although the response in roll angle is slightly delayed. The pilot model fit for the FL200 stall condition has a slightly worse fit with a MSE of 3.11 deg^2 with very different gains. This can be explained by the fact that a different roll recovery strategy seemed to be used for the three outliers. Applying the FL350 gains in the FL200 stall condition shows a relatively close fit with respect the the common roll recovery strategy (see the blue line in Figure 8-8(a)).

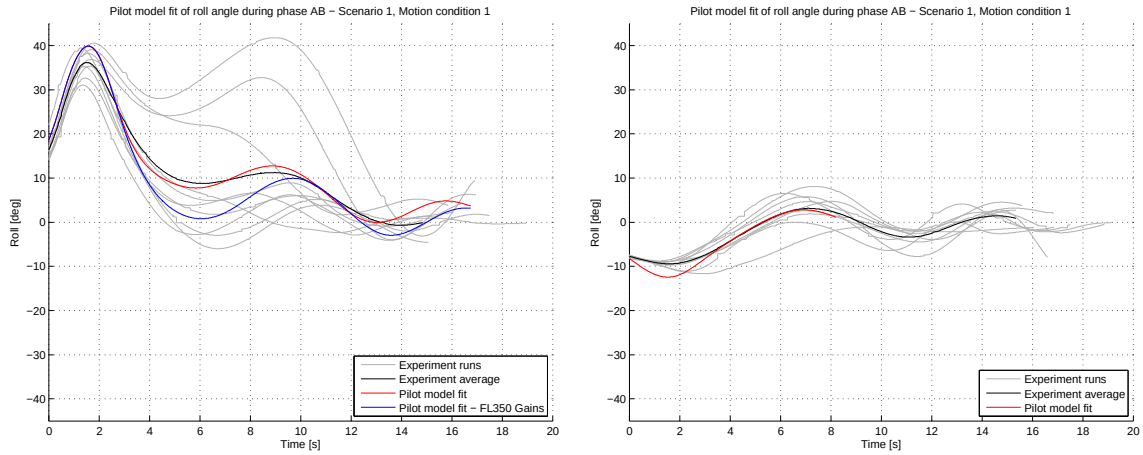

(a) FL200 (b) FL350

Figure 8-8: Roll angle plot with final pilot model fit

8-3-1 Control inputs

The resulting control inputs from the pilot model are shown in Figure 8-9. The result is generally similar to the experiment data. There are instabilities visible at the initial fast and large control deflections. This is caused by the underdamped kinematic representation of the control wheel and the assumption that the neuromuscular interaction is pure force-based and open loop. The actual pilots generally show well dampened inputs suggesting that position feedback and/or the additional arm/muscle dynamics can sufficiently improve the response.
The resulting high frequency oscillations do not significantly affect the simulation and analysis. The aircraft roll inputs are damped and the coupling with pitch is very small.

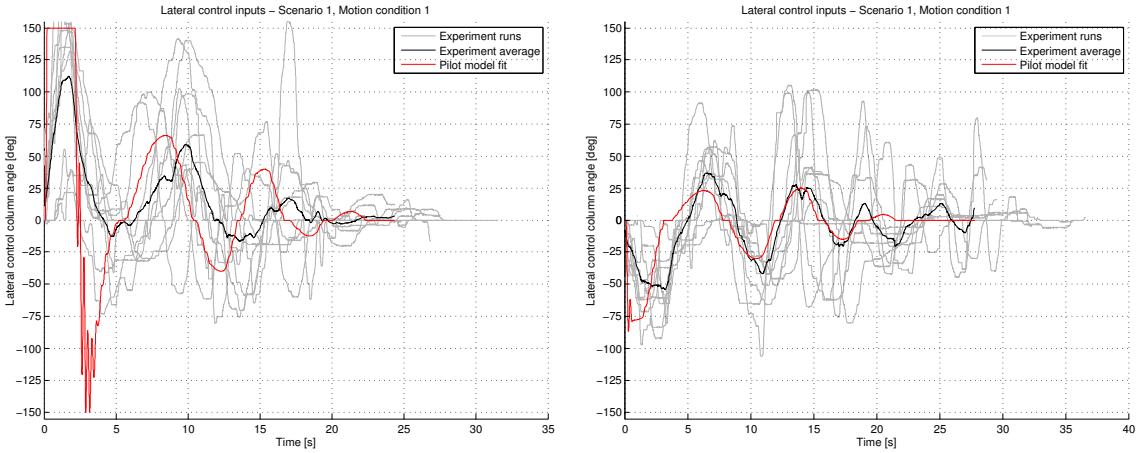

(a) FL200 (b) FL350

Figure 8-9: Lateral control column inputs

8-4 Simulated motion

The previous sections have shown that a reasonable fit of the pilot model was attained for motion condition 1, where no motion was offered to the participants. The analysis of the experiment data showed that motion condition 2 had a minor effect on the control behaviour. Motion condition 3 had a significantly larger effect.

8-4-1 Motion condition 2: Hexapod

In the hexapod motion condition only relatively small motion cues were available. As can be seen in Figure 8-10 the resulting difference with motion condition 1 is small. In recovery phase C the effect is opposite between the FL200 and FL350 stall condition suggesting that this is a statistical variation. Because the difference between motion condition 1 and motion condition 2 is only $0.980\,\mathrm{deg}^2$ (FL200), $1.65\,\mathrm{deg}^2$ (FL350) it would be incorrect to attempt to fit the motion channel gains. The difference is within the optimization error that was reached in the optimizations before. Any new result would most likely be incorrect.

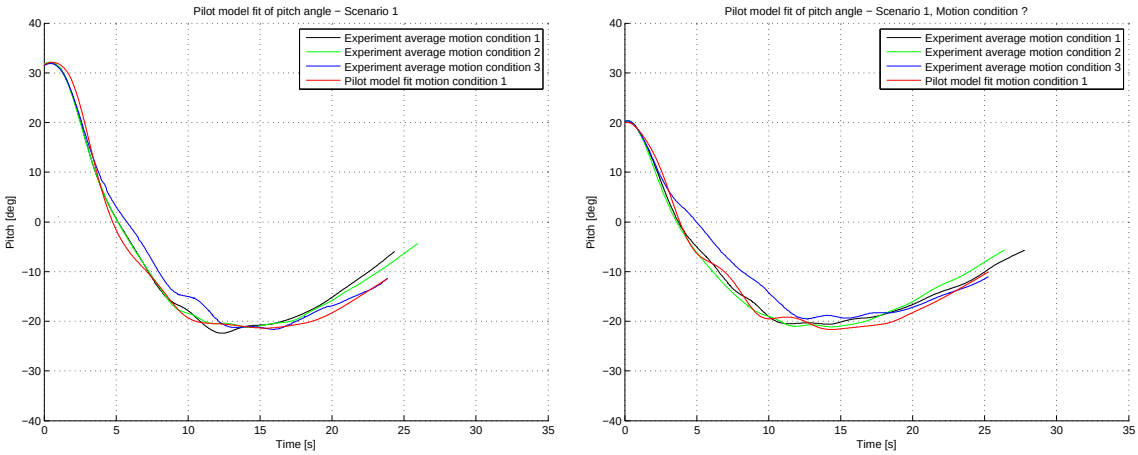

(a) FL200 (b) FL350

Figure 8-10: Pitch angle plot comparing the three different motion conditions

8-4-2 Motion condition 3: Centrifuge

The effect of the centrifuge motion condition on the control behaviour was found to be larger than the hexapod motion condition. Looking at Figure 8-10 an effect can be seen during phase A & B and a slight

decrease in pitch rate during phase C.
It should be noted that the dataset for motion condition 3 is smaller than motion condition 1 and 2, because not all participants completed the full set of centrifuge runs. This causes the average to have more noise and possibly a bias compared to the data for the other two motion conditions.

The optimization of the motion channel feedback gains did not result in a consistent and improved fit of the pilot model. A large variety of motion feedback inputs was tested including the direction of the specific force, strength of the longitudinal acceleration, pitch rate and even the false cue due to the centrifuge motion. Also the feedback from motion was introduced at various locations in the pilot model including as a direct feedback on the neuromuscular system. In none of these cases a clear optimum of the MSE was found, which gave similar results for both the FL200 and FL350 scenario.
Ultimately the best fit was found by repeating the optimization of the pitch control gains (see Table 8-3). The result was an average reduction of 10% of the total open loop gain, which resulted in a decrease of the MSE of roughly 50% and 80%.

Table 8-3: Iterative fitting results for the control gains of phase AB in motion condition 3. Actively optimized values are underlined.

(a) FL200, scenario 1, motion condition 3

	Gains					**MSE**	
Iteration	$K_p[-]$	$K_v[-]$	$K_{r_p}[-]$	$K_{r_v}[-]$	**Func. Eval.**	**Pitch** $[deg^2]$	**Roll** $[deg^2]$
Initial	0.253	905	0.281	33.3	-	7.70	4.94
I-A	<u>0.221</u>	<u>950</u>	0.281	33.3	20	<u>3.92</u>	5.73
I-B	0.221	950	<u>0.310</u>	<u>33.3</u>	11	3.93	<u>5.25</u>

(b) FL350, scenario 1, motion condition 3

	Gains					**MSE**	
Iteration	$K_p[-]$	$K_v[-]$	$K_{r_p}[-]$	$K_{r_v}[-]$	**Func. Eval.**	**Pitch** $[deg^2]$	**Roll** $[deg^2]$
Initial	0.255	1100	0.434	25.3	-	12.3	2.57
I-A	<u>0.201</u>	<u>1180</u>	0.434	25.3	15	<u>1.95</u>	2.47
I-B	0.201	1180	<u>0.390</u>	<u>25.9</u>	21	1.88	<u>2.39</u>

Chapter 9

Variation in control behaviour

The pilot model presented in the previous chapter gives a single response for a scenario. However, the experiment data shows significant variation between experiment runs of the same scenario. To further investigate the possible causes of this variation, this chapter considers the possible effects of the control gains, assumed control inputs and other sources which may explain the variation.

9-1 Variation in control gains

The gains determined for the pitch axis were based on the average of different time responses. Assuming that each pilot was steering with equal "aggressiveness" and equally adapted to the control tasks. In reality this will of course be different between pilots and even within individuals. To better understand the effect of this parameter and to see how this can differences between recoveries a phase plot of the pitch angle is shown in Figure 9-1. This plot shows the effect of a 50% change in gains on the pitch behaviour. A variety of

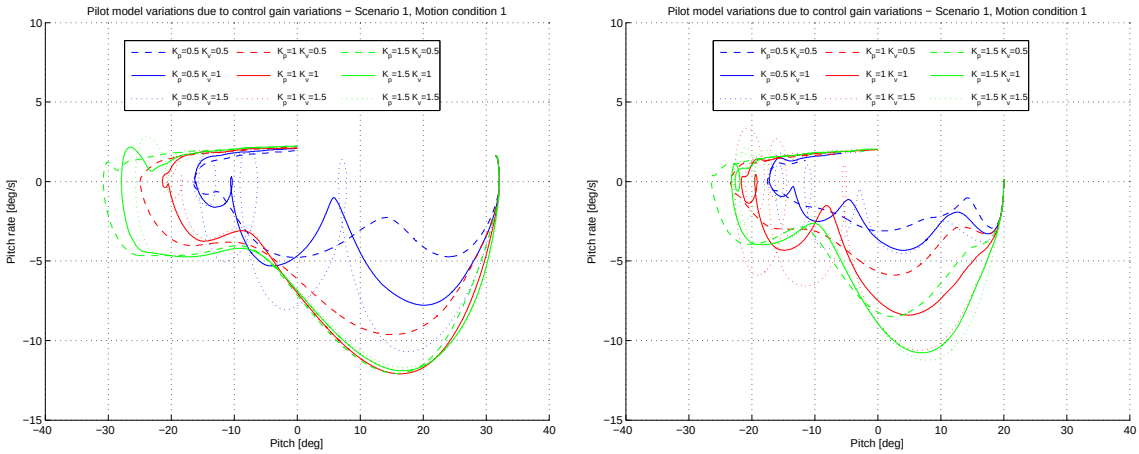

(a) FL200 (b) FL350

Figure 9-1: Pitch angle phase plot variation due to control gain variation

effects is visible including undershooting and overshooting the −20 deg pitch down attitude and oscillations near it. Very similar behaviour can be seen in Figure 6-1.
Variation in the roll behaviour had only a small effect on the pitch behaviour and is most likely not a major contributor to the variation in the pitch axis.

9-2 Variation in other control inputs

Other control inputs include trim, throttles and rudder. The trim inputs are directly coupled to the pitch axis and are usually congruent to pitch inputs. The effect of this will thus be similar to an increase in the pitch control gain.
The assumed input for the throttle is much more different from the observed throttle inputs and was expected to have a more significant contribution to the variation. To test this effect the raw throttle inputs from the different experiment runs have been combined with the fitted pilot model (plotted in Figure 9-2). As can be concluded from the figure, most of the pitch up moment, resulting from the throttle inputs, is accurately compensated. The exception is phase A, where the control authority is limited and the throttle inputs decrease the peak pitch down rate.

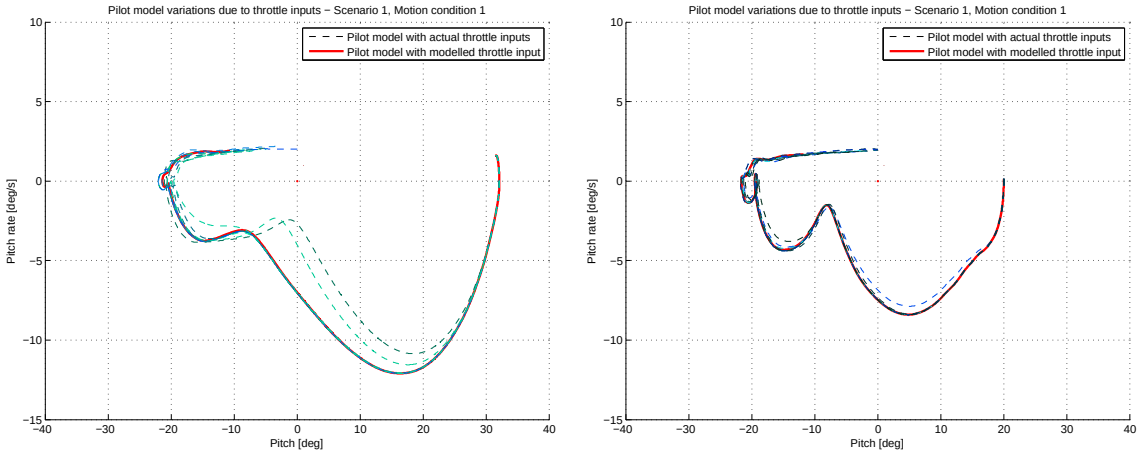

(a) FL200 (b) FL350

Figure 9-2: Pitch angle phase plot variation due to throttle input variation

The rudder pedals were generally not used as specified in the recovery procedures and thus were not an important contributor to the variation.

9-3 Other sources of variation

There are also other obvious sources of variation. The recovery procedure was not always exactly followed and especially the start of phase C was often too early or too late. The perception, cognitive and neuromuscular models used are highly idealized and lack any form of noise. These models also do not model variation between individuals nor the effect of workload and disturbances on perception.

Chapter 10

Discussion and Conclusions

This thesis investigated the possibility of modelling pilot behaviour during a quasi-symmetric stall recovery in a large transport aircraft. Using the SUPRA aircraft model, 10 volunteer civil transport pilots, and the Desdemona simulator, the necessary data was collected to build a basic descriptive pilot model representative of the simulated manoeuvre.

10-1 Experiment

The experiment provided a well defined data set for the derivation and testing of the pilot model. The goal of minimizing simplifications was fulfilled as good as possible. Besides the generic aircraft model and simulated motion, the only other major abstraction was a fixed recovery procedure. This fixed recovery procedure is based on current practices and observed behaviour from the preliminary experiments. The surveys confirmed that the stall recoveries were nevertheless considered to be realistic by the pilots (only 1 pilot had a remark with respect to the recovery procedure).
The ten participants were pilots from several airlines, varying aircraft types and with different levels of experience. This is a reasonable representation of average civil transport aircraft pilots. The sample size is however very limited with ten pilots.
Not all pilots were able to complete the centrifuge motion scenario due to the motion sickness that can be caused by a centrifuge in combination with head movements. It is possible that effect of motion sickness has also influenced the other pilots. However, this was generally not mentioned in the surveys as a disturbing factor, nor does the data show any obvious artifacts.

The statistical analysis of the experiment data using an ANOVA showed significant differences for several key parameters during the stall recovery between the scenarios and motion conditions. The pitch ladder was confirmed to be the most important input for the pilot, with in addition the speed tape during the loading phase of the recovery (phase C). Also the effect of changes in control loading were visible in the analysis. Unfortunately it was not possible to accurately asses the changes in pilot behaviour over time.
The experiment surveys confirmed these results for the normal scenario (scenario 1). Only two pilots mentioned additional inputs like the stickshaker and the altimeter. The subjective performance ratings from the pilots also showed a consistently higher workload for the centrifuge motion condition compared to the other motion conditions.

10-2 Pilot model

Based on the experiment data analysis, a dual loop pitch control structure for the unloading phase was selected. This controller consists of a pitch control loop with an inner pitch rate loop responding to the pitch ladder displayed on the PFD. For the loading phase a single loop pitch rate controller, with an additional input for the barber pole, was chosen. This structure for the human controller is based on the pilot models evaluated in the literature review, the experiment data and aircraft model behaviour.

The fitting of the pilot model was performed using an iterative fitting method. For a more analytical analysis the aircraft model would have to be linearised, but this proofed to be unpractical and unsuitable due to the non-linear behaviour of the aircraft in the selected type of manoeuvre.
The fit of the pilot model aircraft pitch for the initial unloading phase of the recovery (phase AB) was relatively good (MSE of 2.13 $\deg^2$ and 1.30 $\deg^2$) for the stalls at both FL200 and FL350. The correctness of this optimum was checked by a visual inspection of the surface plots of the MSE values. In addition, the gains for both stall scenarios are very similar, as was expected beforehand.
For the loading phase (phase C) the pitch rate control gain from the unloading phase (phase AB) was used and this resulted in a response close to the experiment data, but offset in time. This offset in time is primarily caused by differences in altitude, thrust setting and pilots not fully complying to the recovery procedure. It was not possible to reliably correct for this offset in the experiment data, which limited further fitting of the pilot model in the loading phase (phase C). The results do however show that the selected pitch and pitch rate control gain give results similar to the experiment data.
It was not possible to significantly improve the fit by adding the speed tape as an additional input. This is due to the fact that the output from the pilot model with only the pitch ladder is already very similar to the experiment data. When the recovery procedure is accurately followed it provides an inherent speed margin to the barber pole. Only when starting the recovery too early or when recovering too aggressively the barber pole becomes a significant limitation. Additionally the experiment data did not show a clear generic behaviour of the pilots with respect to the speed margin to the top of the barber pole.

The resulting pilot model control inputs are similar to the experiment data, but much more damped. This is most likely caused by the use of averaging the experiment data, resulting in increased damping for the pitch controller. The control inputs from the pilot model also lack the distinct discrete behaviour observed in the experiment data. The hypothesis that this could be explained purely by friction was not proven and suggests that discretization at the cognitive level is more likely.
The control inputs are modelled as pure force control to incorporate the effect of control loading. Using the modified control loading scenario (scenario 4) this assumption was tested. The results show that the pilot model overestimates the effect of a change in control loading. This suggests a position feedback is necessary in the neuromuscular system and control column interaction.

In a similar way the roll input was also fitted as a dual loop control system, based on the displayed roll angle and roll rate on the PFD. This resulted in a good fit (MSE of 1.57 $\deg^2$ and 3.11 $\deg^2$). The slightly worse fit for the FL350 scenario can be explained by three outliers who show a different control strategy. The simplification of the roll axis as a pure force control resulted in some high frequency oscillations during the initial inputs, but this had no significant effect on the pitch control.
The variation due to differences in throttle input are shown to have a relatively small effect on the pilot model results. The exceptions are the cases where throttle inputs are made during the initial unloading phase (phase A) of the recovery, where control authority is insufficient.

The experiment data also showed that there was significant variation between the experiment runs. One of the most likely sources for this is a difference in the control gains. These gains represent differences between the individual pilots, like control aggressiveness, experience, adaptation and muscle memory. By varying the pitch control gains by 50% and plotting the result in a phase plot of the pitch angle the same undershooting, overshooting and underdamped control behaviour, as observed in the experiment data, is visible.

10-3 Motion channels

The effect of motion could not be accurately modelled by the use of basic motion feedback channels, as proposed in the pilot model. The effect of the extended hexapod motion was too small, compared to the original fitting error, to be accurately considered.
For the centrifuge condition the best fit was obtained by decreasing the open loop gain of the pitch controller in the unloading phase (phase AB), and a decrease of the pitch rate in the loading phase (phase C). This suggests that the low frequency contribution of motion to a manoeuvre like this is an indirect effect, through cognitive adaptation, as opposed to the more traditional direct negative motion feedback mechanisms (as discussed in Chapter 2). This is in part supported by the statistical analysis of the loading phase (phase C) experiment data, which suggests an increased effect of motion condition 3 over time. Another indication is the high workload reported by the pilots in this condition.
The question remains to what extend false cues from the centrifuge motion contributed to these effects. However, generally the reported false cues by pilots occurred during the initial spin up or during the slow down of the centrifuge after the recovery and not during the recovery itself.

10-4 Hypotheses

It is now possible to consider the hypotheses that were defined before the experiment (see Section 4-1):

1. *The pilot control behaviour in the recovery can be modelled using current pilot models*
   A pilot model was developed based on current descriptive pilot models and principles, which was partly able to produce representative behaviour. The average pitch control action is reproduced, but the modelled pilot interaction with the control column is too simple. It also was not able to provide a correct model for the feedback from the speed tape, although the large variation makes it questionable whether this feedback can be generalized.

   (a) *The recovery can be modelled as a primarily closed loop pitch control task*
   The proposed closed loop models for the pitch and roll axis result in representative behaviour for the experiment stall scenarios. Nonetheless it can not be excluded that, for example, the initial forward control column deflection, is an open loop control input.

   (b) *The control behaviour can be generalized for different pilots* The experiment has shown that there is significant variation between the individual experiment runs. The control behaviour can be generalized to some extend to an average behaviour. The variation does not only occur between pilots, but also between individual runs of the same pilot. This limits the value of a pilot model, since it does not model this spread in behaviour. One possible model, explaining this variation, is based on the assumption that the control gains can vary.

   (c) *The pilot behaviour can be modelled as quasi-linear control behaviour*
   The quasi-linear pitch, roll and throttle controllers can in general be matched to the experiment data. They do, however, not reproduce the discrete control inputs observed in the experiment data.

2. *The effect of simulated motion can be modelled using current pilot models*
   The results from this thesis suggest that the low frequency effects of motion, in a manoeuvre like a stall recovery, cannot solely be represented in the pilot model by the classical negative motion feedback.

   (a) *Simulated motion has an effect on pilot control behaviour in a stall recovery*
   The simulated motion had a statistically significant effect on the pilot control behaviour. In the hexapod motion condition a statistically significant reduction in unloading is observed.
   In the centrifuge motion condition there is an even larger reduction in loading. The centrifuge also causes a small, but statistically significant, decrease in loading during the loading phase. However, the largest effect can be seen in the reported workload.

   (b) *The effect of simulated motion can be generalized for different pilots*
   The effect of motion can be generalized for different pilots, but again a large variation between experiment runs is observed.

   (c) *The effect of simulated motion can be modelled using quasi-linear models*
   The quasi linear pilot model of this thesis was not able to reproduce the effect of simulated motion using the classical motion feedback, but did result in an improved fit by changing the pitch control gains. The effect of the classical motion feedback could be too small or have been averaged out.

Chapter 11

General Conclusions

This thesis has explored the applicability of a descriptive pilot model in the modelling of a quasi-symmetric stall recovery manoeuvre. Several conclusions can be drawn from the results:

- The proposed descriptive quasi-linear model can predict and describe basic representative control behaviour for both stall scenarios. For the pitch down and hold task, a dual loop pitch/pitch rate controller can be used and for the pitch up task, a single loop pitch rate controller proved to be sufficient.
- A significant part of the variation between recoveries can be reproduced by a variation of the pitch control gains.
- The pitch control through the control column is not a pure force based interaction, but should include a position feedback.
- Discrete behaviour of the pilot control inputs cannot be reproduced with the common pilot models or by adding a control friction model, and suggests discretization at the cognitive level.

By using the results of the pilot model for the no motion condition as a reference, the effects of the two motion scenarios were considered.

- The effects of the hexapod motion were found to be statistically significant for the unloading phase of the recovery, resulting in less unloading compared to the no motion condition. No statistically significant effect was found for the loading phase.
- The centrifuge motion had a statistically significant effect on the unloading and loading phase of the recovery, resulting in reduced pitch rates and g-loads compared to the other (no) motion conditions. Additionally a significantly higher workload was reported by the pilots.
- The effect of centrifuge motion is best modelled in the pilot model by a decrease of the open loop gain in the unloading phase, and a decrease in desired pitch rate during the loading phase. This suggests a cognitive process, as opposed to the classical direct negative motion feedback.

Current descriptive models thus seem applicable also to a large manoeuvre, like the stall recovery in this thesis, but fall short with regard to the effect of motion and exact control behaviour.

Chapter 12

Recommendations

The work in this thesis suggests several areas of interest for further research. The observed discrete control behaviour is a distinct property of the pilot control behaviour, that is not replicated by the model. A new cognitive element in the pilot model is probably necessary to fully reproduce this effect. However, to further investigate this, a better model of the pilot neuromuscular system, control column and the interaction of these is most likely necessary.

The experiment results also showed other possible situations of interest. The observed effect of g-load during the centrifuge motion condition was relatively small from an operational point of view. A scenario where a g-load closer to the aircraft limit load of 2.5 g is necessary might result in more significant effects. Especially considering that fact that the subjective experience of 2.5 g was reported by pilots to be significantly higher than expected in past experiments.
The speed tape was also found to be an important indication for pilots in the surveys, but the effect was difficult to determine from the experiment data. The most important indication on the speed tape, the barber pole, was usually not a limiting factor in the experiment. A scenario, where the barber pole is a more important factor, might yield more insight into the pilot response to this indication.

Bibliography

AIRBUS (2014). *Commercial Aviation Accidents 1958-2013, A Statistical Analysis*. AIRBUS. URL: http://www.airbus.com/company/aircraft-manufacture/quality-and-safety-first/?eID=maglisting_push&tx_maglisting_pi1%5BdocID%5D=39258

Barton, J. (2004). *Dynamic Estimation of Oncoming Vehicle Range and Range Rate: An Assessment of the Human Visual System's Capabilities and Performance*. University of California, Berkeley.

Beardmore, R. (2013). *Coefficients of Friction*. www.roymech.co.uk. URL: http://www.roymech.co.uk/Useful_Tables/Tribology/co_of_frict.htm Retrieved: 02-12-2013

Boeing (2011). *Statistical Summary of Commercial Jet Airplane Accidents, Worldwide Operations 1959-2010*. Boeing Commercial Airplanes.

Boeing Company (1998). *Airplane Upset Recovery: Training Aid*. Boeing.

EASA (2012). *Annual General Report 2012*. EASA. URL: http://easa.europa.eu/communications/docs/annual-report/EASA-Annual_General_Report_2012.pdf

FAA (2012). *Advisory Circular 120-109: Stall and Stick Pusher Training*. FAA. URL: http://www.faa.gov/documentLibrary/media/Advisory_Circular/AC%20120-109.pdf

Fucke, L., Groen, E., Goman, M. M. G., Abramov, N., Wentink, M., Nooij, S., & Zaichik, L. (2012). Final results of the supra project: Improved simulation of upset recovery. *28th Congress of the International Council of the Aeronautical Sciences*, (pp. 4607–4616).

Grant, P. R., & Schroeder, J. A. (2010). Modelling Pilot Control Behaviour for Flight Simulator Design and Assessment. In M. Silvestro (Ed.) *Proceedings of the AIAA Guidance, Navigation, and Control Conference, Toronto, Canada, Aug. 2-5*, AIAA-2010-8356. American Institute for Aeronautics and Astronautics.

Groen, E., Ledegang, W., Field, J., Smaili, H., Roza, M., Fucke, L., Nooij, S., Goman, M., Mayrhofer, M., Zaichik, L., Grigoryev, M., & Biryukov, V. (2012). Supra - enhanced upset recovery simulation.

Groen E., F. L. (2011). Supra simulation of upset recovery in aviation: Project overview and status. EASA Safety Conference. SUPRA.

Hess, R. (1977). *A dual-loop model of the human controller in single-axis tracking tasks*. National Aeronautics and Space Administration.

Hess, R. A. (1979). A Rationale for Human Operator Pulsive Control Behavior. *Journal of Guidance Control and Dynamics*, *2*, 221–227.

Hess, R. A. (1981). Pursuit Tracking and Higher Levels of Skill Development in the Human Pilot. *IEEE Transactions on Systems, Man, and Cybernetics*, *SMC-11*(4), 262–273.

Hess, R. A. (1997a). Unified Theory for Aircraft Handling Qualities and Adverse Aircraft-Pilot Coupling. *Journal of Guidance, Control, and Dynamics*, *20*(6), 1141–1148.

Hess, R. A. (1997b). Unified Theory for Aircraft Handling Qualities and Adverse Aircraft-Pilot Coupling, Journal of Guidance, Control and Dynamics. *20*(6), 1141–1148.

Hosman, R., Schuring, J., & van der Geest, P. (2005). Pilot model development for the manual balked landing maneuvre.

Hosman, R. J. A. W. (1996). *Pilot's Perception and Control of Aircraft Motions*. Ph.D. thesis, Delft University of Technology, Faculty of Aerospace Engineering.

Hosman, R. J. A. W., Belyavin, A. J., Hörmann, H. J., Robel, G., Schuring, J., Van der Geest, P., & Towler, J. M. (2009). The pilot model balked landing simulation project: A government, industry and national research cooperation. *The Aeronautical Journal*, *113*(1149), 715–725. Paper No. 3053.

Kleinman, D., Baron, S., & Levison, W. (1970). An optimal control model of human response part i: Theory and validation. *Automatica*, *6*(3), 357 – 369.

Ledegang, W. D., Groen, E. L., & Wentink, M. (2012). Pilot performance in centrifuge-based simulation of unusual attitude recovery. *Journal of Aircraft*, *49*(4), 1161–1167. URL: www.scopus.com

McRuer, D. T., Graham, D., Krendel, E. S., & Reisener, W. J. (1965). Human Pilot Dynamics in Compensatory Systems, Theory Models and Experiments with Controlled Element and Forcing Function Variations. Tech. Rep. AFFDL-TR-65-15, Air Force Flight Dynamics Laboratory, Wright-Patterson Air Force Base (OH).

McRuer, D. T., & Krendel, E. S. (1974). Mathematical Models of Human Pilot Behavior. AGARDograph AGARD-AG-188, Advisory Group for Aerospace Research and Development.

Mulder, J., van Staveren, W., van der Vaart, J., & de Weerdt, E. (2007). *Flight Dynamics Lecture Notes AE3-302*. TU Delft.

Nieuwenhuizen, F., Zaal, P., Mulder, M., & Van Paassen, M. (2006). A new multi-channel pilot model identification method for use in assessment of simulator fidelity. vol. 2, (pp. 958–966). Cited By (since 1996) 1.

Oxford Aviation Academy (2011). *Human Performance Limitations*. Oxford Aviation Academy.

SUPRA (2012). Public supra website live. URL: http://www.supra.aero Retrieved: 02-12-2013

van Paassen, M. M., & Mulder, M. (1998). Identification of Human Operator Control Behaviour in Multiple-Loop Tracking Tasks. In *Proceedings of the Seventh IFAC/IFIP/IFORS/IEA Symposium on Analysis, Design and Evaluation of Man-Machine Systems, Kyoto Japan*, (pp. 515–520). Pergamon.

Wentink, M. (2012). *Afstudeeropdracht Martijn Rambonnet*.

Appendix A

SUPRA Project: Background Information

A-1 Project history and context

The SUPRA project is a European Seventh Framework Programme (FP-7) project focused on the Transport Theme. The main objectives set forward by the European Union for these projects is to decrease the accident rate and to improve the elimination and recovery of human error (SUPRA, 2012). To achieve these objectives three innovations were put forward by the SUPRA project:

- Extended aerodynamic modelling of aircraft behaviour
- Special motion cueing for upset manoeuvres
- Improved perception modelling

The extended aerodynamic model extends on the normally available validated flight envelope in commercial Level-D simulators to provide representative behaviour of a generic aircraft outside the normal flight envelope. This mathematical model was for a large part developed by De Montfort University (DMU) based on simulations, wind tunnel data and flight test data. It features an angle of attack, α, envelope of -20 to 90 degrees and a sideslip angle, β, range of -30 to 30 degrees (Groen E., 2011).

One of the research facilities participating in this project was Desdemona B.v. in The Netherlands. The Desdemona simulator, short for Desorientation Demonstrator AMST, features a fully gimbaled cabin with a separate heave and linear axis on top of a centrifuge platform. Desdemona was one of the simulators used for the validation experiments and motion cueing development work.

During January 2012 the model was tuned and the implementation was validated by the Gromov Flight Research Institute (GFRI). The flight tests were done by the test pilot Vladimir Biryukov, who has experience with a wide range of aircraft and is considered an expert on stalls and other types of upsets (SUPRA, 2012). During these tests and from the experience gained while developing the motion cueing and test scenarios, it became apparent that after a short learning curve a lot of pilots displayed a similar behaviour with relatively small differences. By recommendation of supervisor Mark Wentink all data of the two experiments was extensively logged and pilots were given a short survey to gain a better understanding of their behaviour during a stall recovery for possible use during a thesis.

A-2 SUPRA aerodynamic model

The aerodynamic model consists of a compiled MATLAB function which incorporates a large number of look-up tables to calculate the aerodynamic response of the aircraft. This function is included in a SIMULINK

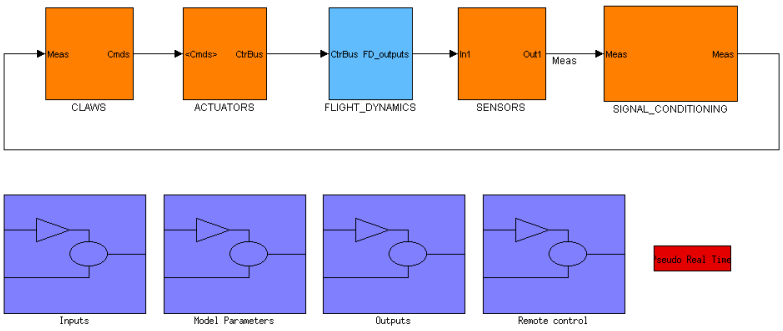

Figure A-1: Overview of the SUPRA aircraft model structure

model which adds the control system, actuator dynamics, engine dynamics, weather and other system models (see Figure A-1). The internal behaviour of the model can be changed via parameters to change the simulated aircraft configuration and resulting behaviour. This allows the model to be used to show behaviour characteristic for different types of aircraft. Parameters that can be changed are for example: anti-damping in roll at low speeds, roll-off components, buffet onset and engine/tail configuration.
Additionally several features have been added specifically for use in the Desdemona simulator including a high speed buffet, basic autopilot, flight data computations for the displays and extended engine indications.

A-3 Upset scenarios

In cooperation with the team from GFRI and the Dutch National Aerospace Laboratory (NLR) a wide variety of upsets and scenarios were created for the SUPRA model, ranging from nose low upsets to high pitch, high roll-off stalls and deep stall t-tail configurations. Based on this and the scenarios from the Airplane Upset Recovery Training Aid (Boeing Company, 1998) the most important scenarios were selected for use in further experiments.

Appendix B

SUPRA Experiment 1: Post-Experiment Survey

See next page

Questionnaire about indications and motion cues during upset and stall recoveries.

The goal of this questionnaire is to find the most important visual indications and motion cues during a stall or upset recovery of an airliner. For the aerodynamic model the SUPRA generic airliner model with enhanced validity outside the normal operating envelope is used.

For reference the following initial conditions are used:

- 30 degrees pitch up, stalled (alpha > 14)
- Flight level 130
- Trimmed for normal flight range
- Symmetric stall
- 737-800 PFD indications

This situation is comparable to upset scenario C3 and will result in an initial unloading phase where Nz will be smaller than 1. Once the lowest pitch attitude has been reached and velocity has been recovered a loading phase with Nz >1 will be necessary.

Question 1: Rank the 5 most important indications and or motion cues during the unloading phase (Nz < 1)

Importance	Visual indications	Importance	Visual indications	Importance	Motion Cues
	Pitch ladder		FPV		G-Load
	Horizon		PLI		Pitch
	Speed		Outside view		Pitch rate
	Speed tape		Yoke deflection		
	Altimeter		Yoke forces		
	Altitude tape				
	VSI				

Question 2: Rank the 5 most important indications and or motion cues during the loading phase (Nz > 1)

Importance	Visual indications	Importance	Visual indications	Importance	Motion Cues
	Pitch ladder		FPV		G-Load
	Horizon		PLI		Pitch
	Speed		Outside view		Pitch rate
	Speed tape		Yoke deflection		
	Altimeter		Yoke forces		
	Altitude tape				
	VSI				

Question 3: Would you use other indications/cues or indications/cues differently in real life with respect to the centrifuge simulation in Desdemona?

- No
- Yes, _____

Question 4: Are you able to recognize the generic 2.5g load limit by seats of the pants or do/would you use any other indication/cues:

- Yes
- No, _____

Appendix C

SUPRA Experiment 2: Post-Experiment Survey

See next page

Questionnaire about indications and motion cues during upset and stall recoveries.

To better understand what visual indications and motion cues you used during the experiment, we would like you to rank the 5 most important indications and/or motion cues for you during the unloading phase and loading phase in the recovery of a stall. For this consider the stalls in centrifuge mode as you flew them in Desdemona:

unloading phase (Nz < 1)		**loading phase (Nz > 1)**	
Importance	**indications**	**Importance**	**Indications**
	Pitch ladder		Pitch ladder
	Horizon		Horizon
	Speed		Speed
	Speed tape		Speed tape
	Altimeter		Altimeter
	Altitude tape		Altitude tape
	VSI		VSI
	Outside view		Outside view
	Yoke deflection		Yoke deflection
	Yoke forces		Yoke forces
	G-Load (motion cue)		G-Load (motion cue)
	Pitch (motion cue)		Pitch (motion cue)
	Pitch rate (motion cue)		Pitch rate (motion cue)
	Other:		Other: .....
	….		….
	….		….

Number the 5 most important indications and cues where number 1 is the most important.

Appendix D

Experiment: Briefing

See next page

Experiment briefing: Pilot behaviour in upsets, Desdemona January 2013

Experiment introduction
Thank you for participating in this scientific experiment about pilot behaviour in stall upsets. In this experiment you will be asked to recover the aircraft (short- to medium-range airliner) from an artificially induced stall. We use a modified autopilot to fly the aircraft into a sudden upset and you will be asked to recover the aircraft to a safe flying condition. These stalls will occur at two different altitudes (FL200 and FL350) and in some scenario's speed or pitch will hidden from the PFD.

The results from the experiment will be used in an attempt to mathematically model pilot behaviour in these types of situations and to predict the effects of removing cockpit indications on pilot behaviour.

Aircraft model and cockpit
The flight simulator you will be flying is the Desdemona simulator. The simulator features a motion base capable of fully rotating the cabin around all axis and using a centrifuge to simulate constant g-forces larger than 1g.

The simulated aircraft is based on a generic aircraft model validated for upset manoeuvres (valid for angles of attack ranging from -20 to 90 degrees and sideslip angles of up to 30 degrees). The aircraft itself is comparable to a 2 engines under the wing medium-range airliner (MTOW ~100 tons) and has a control system with some basic control augmentation systems, e.g. a roll damper and pitch control system.

The cockpit for this experiment consists of half a 737NG-type cockpit providing you with the basic flight displays and controls of the captains side. For control inputs a yoke with electric trim switches is used, rudder pedals and a throttle quadrant with 2 thrust levers.

Motion conditions
Besides the effects of missing indications on the PFD the experiment will also be used to investigate the effects of simulated motion on pilot behaviour. There will be three different motion conditions:

1. **No-motion** The simulator will not move during the manoeuvre and the motion is comparable to a fixed base simulator.
2. **Hexapod** The simulator motion cueing will be similar to the motion cueing used on Level-D training simulators and provide basic pitch and roll motion cues
3. **G-Cueing** By moving the cabin in a circular orbit it is possible to use centrifugal force to simulate increased g-forces during flight. In this motion condition we will start with the centrifuge when you enter the stall. At the end of the stall recovery when you level off the aircraft the autopilot will automatically take over control of the aircraft and start a right turn. This is because the deceleration of the centrifuge to 1g is not correlated with the aircraft model and will cause some false cues. **During g-cueing it is very important to not move your head.**

Experiment conditions
In the experiment there will be 4 scenario's:

1. Normal flight deck indications
2. Speed tape missing from PFD, indicated by the orange indication 'SPD' on the PFD
3. Pitch information missing from the PFD, indicated by a missing pitch ladder and the orange indication 'PITCH' on the PFD
4. Yoke spring force constant. Normally yoke force will change with speed, in this scenario yoke force has been set to be independent of speed.

Recovery procedure for the stall scenario's
For the aircraft you are flying the recovery procedure for a high pitch stall is as follows:

- Pitch down to -20 degrees
- Add thrust
- Wait for speed to increase to manoeuvre speed indicated by the yellow hook on the speed tape. This gives you +0.3 g margin from the 1g stickshaker speed.
- Start raising the nose of the aircraft at a pitch rate of approximately 2 degrees per second.
- Stabilize the aircraft for level flight

Remarks:

- Try not to overstress the aircraft (-1g +2.5g)
- Try to recover the aircraft attitude as soon as possible after accelerating to sufficient speed, but avoid a secondary stall
- Do not use rudder in the stall

Experiment setup
The experiment will take about two hours total or four hours when taking turns with a second pilot.

The order of the experiment will be as follows (the scenario and motion conditions will be randomized):

- Familiarization with aircraft, cockpit and controls
- One manual flight into stall for training
- Motion condition 1: 4 scenario's
- Motion condition 2: 4 scenario's
- Motion condition 3: 4 scenario's
- Break/switch with second pilot
- Motion condition 1: 4 scenario's
- Motion condition 2: 4 scenario's
- Motion condition 3: 4 scenario's
- Short questionnaire

In case of any motion sickness or simulator sickness (or any other reason) during the experiment please tell us and we will have a short break or end the experiment (at your discretion).

Appendix E

Experiment: Post-Experiment Survey

See next page

Pilot Name ##-01-2013

Experiment survey: Pilot behaviour in upsets, Desdemona January 2013

Pilot experience:

Flying hours: _____

Current type ratings: _____

Experiment:

Was the procedure in any way unrealistic in your opinion?:

_____

_____

Did you experience any problems/false cues which caused you to behave differently from how you would react in an aircraft?:

_____

_____

_____

_____

_____

List the most important cockpit indications and motion cues for you during the different recovery phases. List no more than 5 in total per phase:

Some examples of the different indications and motion cues are:

- *Pitch ladder*
- *Speed*
- *Barber pole*
- *Speed trend*
- *Altimeter*
- *VSI*
- *Outside horizon*
- *Yoke deflection*
- *Yoke force*
- *Pitching (motion)*
- *Pitch rate (motion)*
- *G-load from (centrifuge)*
- *Timing*
- *Stickshaker*

Scenario 1: Normal flight indications

	Pitch down to -20deg	**Wait for sufficient speed**	**Pitch up for level flight**
Cockpit indications			
Motion cues (when available)			

Pilot Name ##-01-2013

In the other scenario's some indications where obviously missing, if you used any **additional** indications or motion cues with respect to the scenario 1 list them in the next few boxes for each scenario's.

Scenario 2: Speed information missing from PFD

	Pitch down to -20deg	**Wait for sufficient speed**	**Pitch up for level flight**
Cockpit indications			
Motion cues (when available)			

Scenario 3: Pitch information missing from PFD

	Pitch down to -20deg	**Wait for sufficient speed**	**Pitch up for level flight**
Cockpit indications			
Motion cues (when available)			

Scenario 4: Yoke force independent from speed

	Pitch down to -20deg	**Wait for sufficient speed**	**Pitch up for level flight**
Cockpit indications			
Motion cues (when available)			

How useful would these types of motion simulations be in addition to current pilot training?

Very useless 0 ——————————— 10 Very useful Rating: ____

_____

_____

_____

That completes the experiment, thank you!

Appendix F

Statistical Analysis of the Effect of Control Loading on Control Behaviour

Scenario 4 makes it possible to further investigate the effects of control loading on the control inputs. Assuming that static friction causes the stepped profile it would be expected that a higher control force gradient would decrease the effect of static friction. To quantify and compare the effect of static friction a comparison has been made between scenario 1 and scenario 4 for the timespan where the CAS is larger than 200kt (200kt is equal to the constant spring force of scenario 4). In this comparison the control loading spring constant in scenario 1 is equal or larger than in scenario 4. A step was defined as minimally 0.5s of virtually constant position (control deflection speed lower than 0.02% of full scale deflection per second). The results with regard to the number of steps and control input dead time (combined length of all steps) have been summarized in Table F.

Table F-1: Change in longitudinal input steps and control deadtime between scenario 1 and 4

	Number of steps [-]	**Control dead time [s]**
Scenario 1	$\mu = 5.78, \sigma = 2.320$	$\mu = 12.18, \sigma = 2.96$
Scenario 4	$\mu = 5.65, \sigma = 2.21$	$\mu = 12.67, \sigma = 3.39$
Anova	$p = 0.83$	$p = 0.15$

The results are not statistically significant and the differences are relatively small. This suggests that there is not a relation between control force and the stepped profile. However, the difference in control force gradient between the two scenarios was relatively small (on average 21% higher in scenario 1).

Appendix G

Simulink Implementation of the Pilot Model

See next page

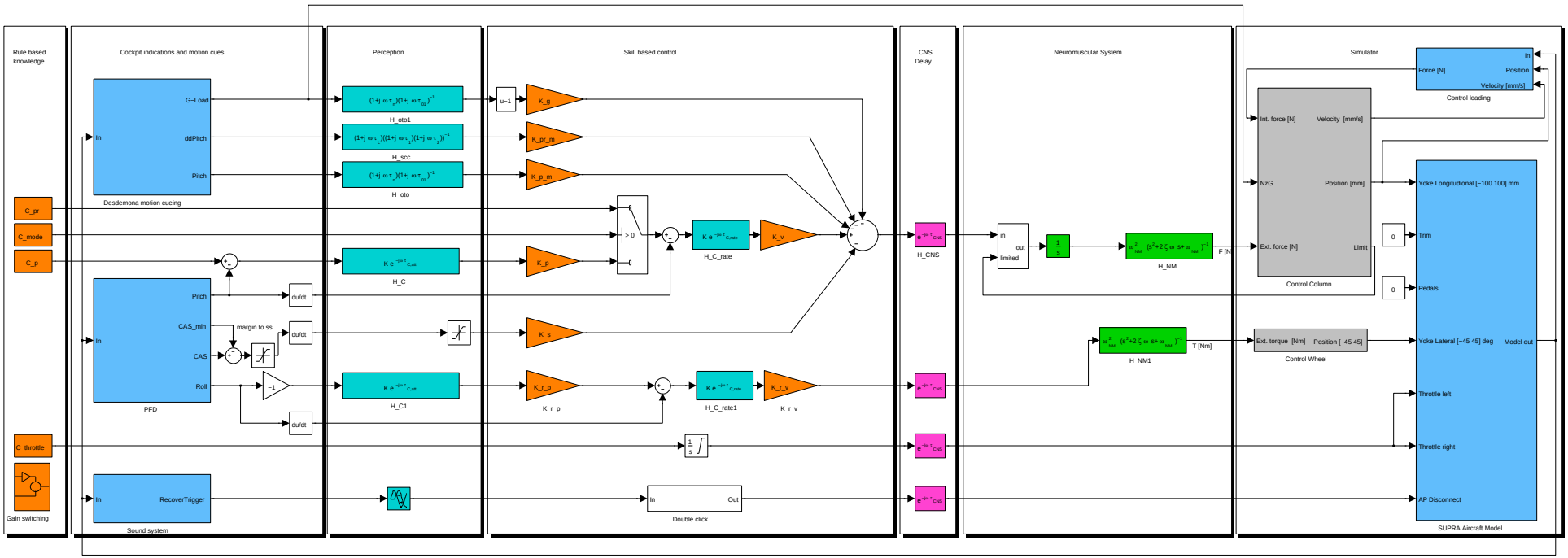
Rule based knowledge
Cockpit indications and motion cues
Perception
Skill based control
CNS Delay
Neuromuscular System
Simulator
C_pr
C_mode
C_p
C_throttle
Gain switching
Desdemona motion cueing
G–Load
ddPitch
Pitch
PFD
CAS_min
CAS
Roll
margin to ss
Sound system
RecoverTrigger
H_oto1
H_scc
H_oto
H_C
H_C1
K_g
K_pr_m
K_p_m
K_p
K_s
K_r_p
K_C_rate
K_v
K_C_rate1
K_r_v
Double click
H_CNS
H_NM
H_NM1
F [N]
T [Nm]
Control loading
Force [N]
Position
Velocity [mm/s]
Int. force [N]
Velocity [mm/s]
NzG
Position [mm]
Ext. force [N]
Limit
Control Column
Ext. torque [Nm]
Position [–45 45]
Control Wheel
Yoke Longitudional [–100 100] mm
Trim
Pedals
Yoke Lateral [–45 45] deg
Throttle left
Throttle right
AP Disconnect
Model out
SUPRA Aircraft Model